GENERAL CIRCULATION MODEL SIMULATIONS OF SOUTHERN AFRICAN REGIONAL CLIMATE

Alec Michael Joubert

Degree awarded with distinction on 30 June 1994.

Dissertation submitted to the Faculty of Science,
University of the Witwatersrand, Johannesburg
for the Degree of Master of Science.

ABSTRACT

Six general circulation model simulations of present-day southern African climate are assessed. Each of these models are early-generation equilibrium climate models linked to simple mixed-slab oceans. Simulations of surface air temperature over the subcontinent are sensitive to the grid-scale parameterisation of convection in summer. At high latitudes, large simulation errors are caused by errors in the specification of sea-ice albedo feedbacks. Increased spatial resolution and the inclusion of a gravity wave drag term in the momentum equations results in a markedly-improved simulated mean sea level pressure distribution. The models successfully simulate the pattern of rainfall seasonality over the subcontinent, although grid-point simulation of precipitation is unreliable. Treatment of convection, cloud radiative feedbacks and the oceans by this generation of models is simplistic, and consequently there is a large degree of uncertainty associated with predictions of future climate under doubled-carbon dioxide conditions. For this reason, more reliable estimates of future conditions will be achieved using only those models which reproduce present climate most accurately. Early-generation general circulation models suggest a warming of 4°C to 5°C for the southern African region as a whole throughout the year. Over the subcontinent, warming is expected to be least in the tropics, and greatest in the dry subtropical regions in winter. Estimated changes in mean sea level pressure indicate a southward shift of all pressure systems, with a weakening of the subtropical high pressure belt and mid-latitude westerlies. Little agreement exists between the models concerning predictions of regional precipitation change. However, broad scale changes in precipitation patterns are in accordance with predicted circulation changes over the subcontinent. Generally wetter conditions may be expected in the tropics throughout the year and over the summer rainfall region during summer. Decreased winter rainfall may be expected over the winter rainfall region of the south-western Cape. However, estimated precipitation changes are grid-point specific and therefore must not be over-interpreted. The present climate validation has resulted in more reliable estimates of future conditions for the southern African region. This approach should be extended to recent simulations which include more comprehensive treatment of important physical processes.

I declare that this dissertation is my own, unaided work,
and that it has not been submitted previously
as a dissertation or thesis for any degree
at any other University.

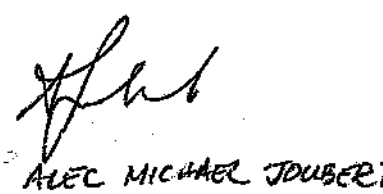

University of the Witwatersrand, 1994

To Fiona

and the Lurgy

PREFACE

Naturally-occurring greenhouse gases serve to keep the Earth warm enough to be habitable. The atmospheric concentration of these gases is increasing as a result of human activities and will lead to an enhanced greenhouse effect. The consequence will be to alter the radiative forcing of the Earth's climate, possibly resulting in global climatic change. General circulation models represent the most sophisticated attempt to understand and infer climatic changes as a result of an enhanced greenhouse effect.

General circulation models resolve the full three-dimensional structure of the overall climate system, based on the numerical solution of the basic physical laws governing the dynamical and physical processes of the atmosphere. However, due to their coarse spatial resolution, several physical processes which occur at sub-grid-scales are incorporated into the models in simplified physical terms, or parameterisations. Considerable uncertainty in their predictions of climatic change are introduced as a result. One method of providing confidence in models' predictions of future climatic change is to validate their simulations of present climate against the observed climate of the real atmosphere and ocean.

Global-scale simulation of present climate and its variability by several current models has been shown to be broadly realistic. For this reason, predictions of global patterns of climatic change by these models are therefore considered reliable. Considerable uncertainty exists, however, concerning possible regional climatic change. To date, it has not been possible to interpret predictions of climatic change for the southern African region with confidence. To do this the present-day performance of models needs to be assessed for the region. On the basis of their performance, informed statements can be made regarding simulations of possible future conditions that may occur as a consequence of global warming.

The general aim of this dissertation is to assess the present-day simulation of southern African regional climate using general circulation models and, as a result of this, to evaluate scenarios for future regional climate change. In particular, the objectives of this study are:

(i) to assess and compare the present-day simulations of southern African regional climate given by several different early-generation general circulation models,

(ii) to determine which models best represent the present-day climate for the region,

(iii) to identify particular parameterisations of regionally-important physical processes which allow for accurate simulations of present conditions,

(iv) to compare simulations of future climates resulting from doubling of carbon dioxide in different general circulation models.

The dissertation is divided into five chapters. **Chapter 1** provides an overview of previous relevant work. A brief description of southern African climate is given. The concept of climate modelling and the major features of general circulation models are introduced. In **Chapter 2** data and statistical methods are described. Validation and comparison of general circulation model simulations of present-day surface air temperature, mean sea level pressure and land surface precipitation in the southern African region is considered in **Chapter 3.** In **Chapter 4** those models for which present-day climate simulations are shown to be most accurate are used for doubled carbon dioxide predictions of future conditions. Finally, the results of the study as a whole are summarised in **Chapter 5.**

Part of Chapter 2 has been submitted to the South African Society of Atmospheric Sciences Tenth Anniversary Issue of the *South African Journal of Science.* Parts of Chapters 3 and 4 are being considered for publication in the *South African Journal of Science* and *Water SA.* Parts

of Chapter 3 were presented at the *Fourth International Conference on Southern Hemisphere Meteorology and Oceanography*, held in Hobart, Tasmania during 1993, and appear in the Preprints volume of that conference. Parts of Chapter 4 were presented at the 1993 Tenth Anniversary Annual Conference of the South African Society for Atmospheric Sciences.

Observational data were obtained from the *World Monthly Surface Station* data set from the National Centre for Atmospheric Research (NCAR). Marine air temperatures were taken from the United Kingdom Meteorological Office Sea Surface Temperature data set. Mean sea level pressure data were obtained from the Southern Hemisphere Mean Sea Level Pressure data set kindly supplied by Dr P.D. Jones of the Climatic Research Unit of the University of East Anglia. Land surface precipitation data were obtained from the Global Land Precipitation data set supplied by Dr M. Hulme of the same institution. General circulation model data were mainly obtained from NCAR. Dr P. Whetton and Dr. I. Watterson of the the Commonwealth Scientific and Industrial Research Organisation (CSIRO) supplied data for both the 4-level and 9-level CSIRO general circulation models. The cartographic work of Mrs W. Job is acknowledged. Special thanks are extended to Simon Mason, Sue van den Heever, Graham Cook, Jackie Galpin, Bruce Hewitson and Franz Meixner. The co-supervision of Dr Janette Lindesay and Prof P.D. Tyson is acknowledged with gratitude. The research was funded by the Foundation for Research Development and forms part of the special programme on Southern African Climatic Change: Analysis, Interpretation and Modelling (SACCAIM).

CONTENTS

CHAPTER 1

BACKGROUND

Introduction

The projected increases in the concentration of atmospheric carbon dioxide (CO_2) and other greenhouse gases are expected to have significant impacts on global climate (Cess *et al.*, 1990; Watson *et al.*, 1990). General circulation models (GCMs) provide a sophisticated treatment of the full three-dimensional structure of the earth-atmosphere system and have been widely used to infer such climatic change (Hansen *et al.*, 1983, 1984; Manabe and Wetherald, 1987; Schlesinger and Zhao, 1989; Washington and Meehl, 1984, 1989; Wilson and Mitchell, 1987). The degree of confidence that can be placed in these simulated changes is largely dependent on the accuracy with which the models simulate present-day (control) climates (Mitchell *et al.*, 1987). Most GCMs simulate the broad-scale features of present climate adequately (Boer *et al.*, 1991; Cess *et al.*, 1990; Gates *et al.*, 1990, 1992), but their ability to reproduce present-day regional climate is considerably weaker (Grotch and MacCracken, 1991; Portman *et al.*, 1992). Accurate regional simulations of present climates are essential prerequisites for predicting future climatic change and for the implementation of planning and policy decisions based on GCM predictions (Shine and Henderson-Sellers, 1983). Assessment of the regional climate performance by GCMs is thus an essential part of model validation (Giorgi *et al.*, 1990; Grotch and MacCracken, 1991; Hewitson and Crane, 1992; Portman *et al.*, 1992). While validation studies of the present-climate performance of GCMs have been undertaken for other parts of the southern hemisphere (Whetton and Pittock, 1991), an assessment of the

climate simulation by GCMs over the southern African region has not been undertaken previously.

The climate of South and southern Africa has been well documented by, among others, Taljaard (1953, 1958, 1972, 1982) and Tyson (1986). The major features of the region's climate are described below.

Southern African Climate

The location of the southern African subcontinent between the South Atlantic and Indian oceans and within the subtropical high pressure belt, together with its pronounced topography, are important determinants of the climate of the southern African region. A major part of the subcontinental interior lies above 1000 m while the south-eastern escarpment extends above 3000 m (Fig. 1.1). Two semi-permanent oceanic anticyclones to the west and east of the subcontinent and the circumpolar westerlies to the south dominate the atmospheric circulation. The warm Mozambique and Agulhas currents off the east coast and the cold Benguela upwelling region along the southwest coast, as well as the interaction between the Agulhas and Benguela systems in the Agulhas Retroflection Zone influence the temperature, moisture characteristics and behaviour of rainfall-producing systems advected over the subcontinent.

Pressure Systems

The southern African subcontinent extends from the tropics to approximately 35°S (Fig. 1.1) and is therefore influenced by pressure systems of tropical, subtropical and mid-latitude origin. Within the tropics, airflow converges along the Inter-Tropical Convergence (ITC) over the eastern parts and along the Zaïre Air Boundary (ZAB) over the western parts of the subcontinent (Fig. 1.2). Atmospheric circulation within the subtropical latitudes is dominated by two semi-permanent anticyclones situated east and west of the subcontinent over the Indian and Atlantic oceans respectively (Taljaard *et al.*, 1969; Taljaard, 1972; van Loon, 1972). The southern limit of the subtropical high pressure belt

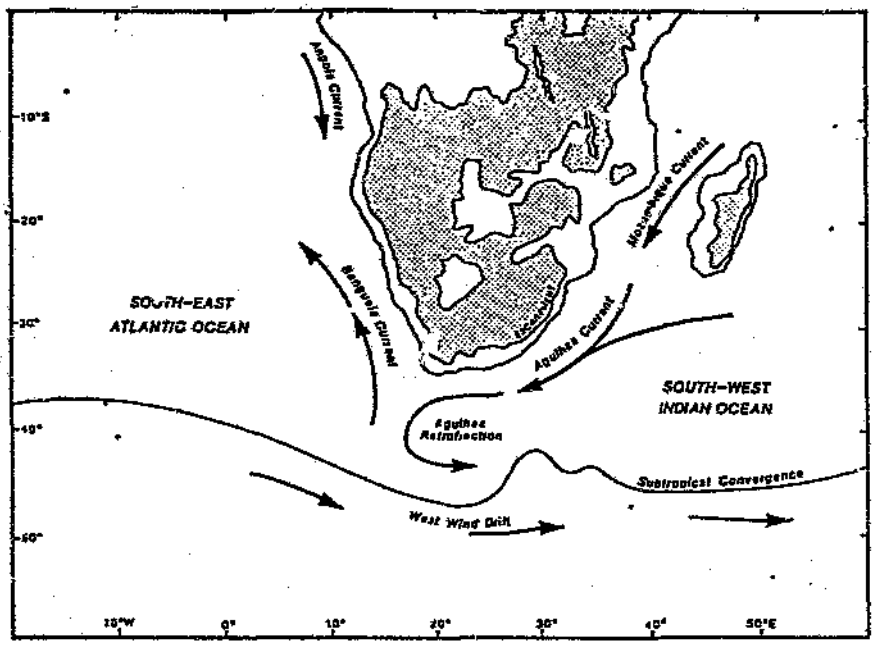

Figure 1.1: Shows location of southern Africa indicating the topography (shaded over 1000 m), oceans and currents (after Lindesay, 1994).

marks the transition to the mean circumpolar westerly circulation characterised by transient low pressure systems.

Both the ITC and ZAB form regions for the preferential development of low pressure systems, pronounced convective activity and major latent heat release over southern Africa in summer (D'Abreton, 1992; Hastenrath, 1985; Jackson, 1989; Taljaard, 1972; Webster, 1983). The ITC migrates with the seasons (Fig. 1.2), displaced as far as 20°S in the (austral) summer and north of the equator in (austral) winter (Taljaard, 1972). The broad seasonality of southern African rainfall is associated with this seasonal migration of the ITC and ZAB. Both the South Atlantic and South Indian anticyclones undergo positional shifts during the year (Fig. 1.3) and are important determinants of rainfall variability over the subcontinent (Tyson, 1981; 1984). The South Atlantic Anticyclone shifts latitudinally from 25°S in May to 31°S in February and longitudinally from 16°W in August to 2°W in December (McGee and Hastenrath, 1966) (Fig. 1.3 left, top and bottom). The Indian Ocean Anticyclone

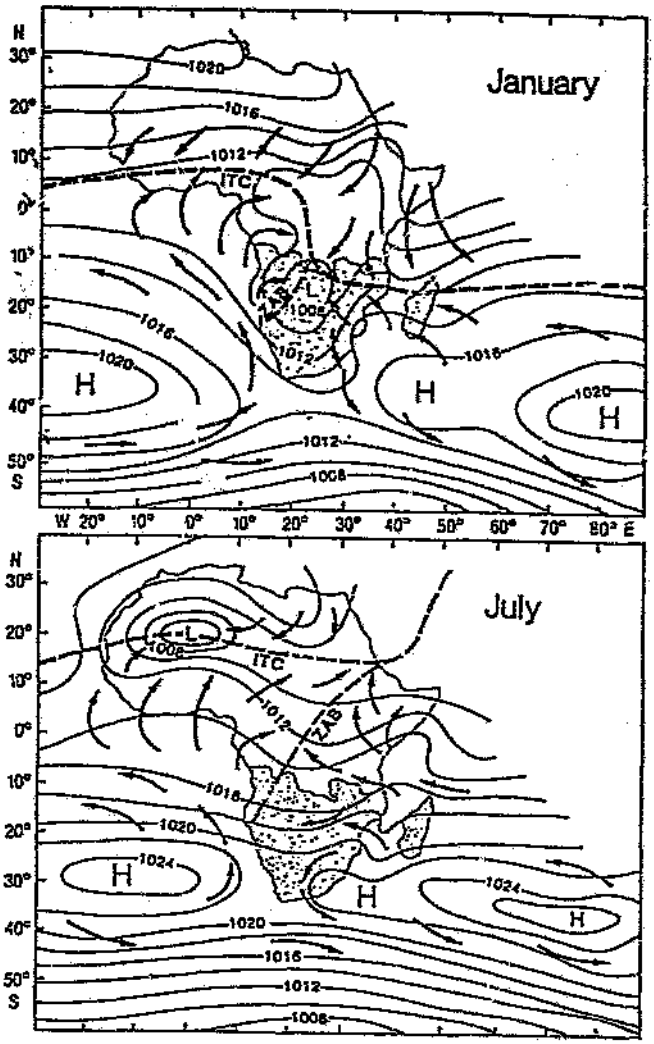

Figure 1.2: Schematic illustration of the mean wind convergence and positions of the Inter-Tropical Convergence (ITC) and Zaïre Air Boundary (ZAB) over Africa and adjacent oceans in January and July (after Taljaard, 1972).

shifts southward from 29°S in June and October to 33°S in February. A larger westward longitudinal shift of 24° occurs from 88°E in December to 64°E in June (van Loon, 1972; Tyson, 1986) (Fig. 1.3 right, top and bottom). Anticyclonic conditions over the central subcontinent in winter (Fig. 1.2) have been attributed to an independent cell of high pressure (Streten, 1980)

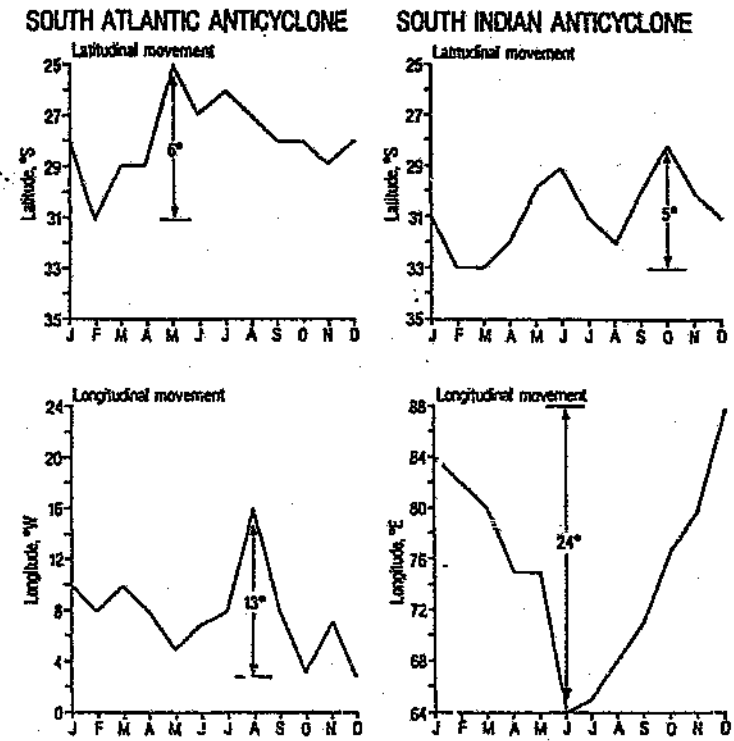

Figure 1.3: Annual variation of latitude and longitude of the South Atlantic and Indian anticyclones (after Tyson, 1986, modified after Vowinckel, 1956, McGee and Hastenrath, 1966).

resulting from subsiding air originating in the Asian monsoon (Harrison, 1986a; Harrison, 1993). Variations in the mean mid-latitude storm track (Taljaard, 1967; van Loon, 1972; Trenberth, 1981) are characterised by a 5° to 10° northward shift in winter as the circumpolar circulation expands northward. This is in keeping with the northward movement of both the westerly jet stream at 200hPa over Marion Island (van Loon *et al.*, 1971) and the ITC. These seasonal changes in the location and intensity of surface oceanic anticyclones and concomitant changes in the frequency, intensity and tracks of the westerly disturbances to the south, together with changes in tropical easterly disturbances, are the main controls on both intra- and inter-annual rainfall variability over the southern African region.

Surface Air Temperature

Surface air temperatures throughout the region display a well-defined poleward temperature gradient (Fig. 1.4). The tropics are characterised by a high degree of thermal uniformity, both seasonally and spatially (Riehl, 1979). In the subtropics and mid-latitudes, temperatures are more variable in response to a large annual cycle of insolation and the effects of seasonally varying air masses and winds (Lindesay, 1994). Over much of the subcontinent, therefore, temperature variations in both space and time are largely dependent on topography and continentality. In the tropics, intra-annual temperature ranges are small (approximately 5°C), owing to the ameliorating effect of increased cloudiness. Outside of the tropics, large diurnal temperature ranges exist (often exceeding the annual range), resulting in monthly mean temperatures which are susceptible to extremes, particularly of minimum temperature (Fig. 1.5a). The effect of continentality is apparent in the large summer to winter range (Fig. 1.5b) of 15°C over the arid regions of Namibia and South Africa which are influenced by seasonal air mass changes resulting from perturbations in the westerlies (Lindesay, 1994).

Rainfall

Mean annual rainfall within the tropics exceeds 800 mm, with the east-west arrangement of the isohyets reflecting the latitudinal movements of the ITC (Fig. 1.6a). The pattern is made more complex by the effects of high moisture input and convergent airflow from the equatorial Atlantic ocean to the west, the marked topography and large lakes of tropical East Africa, as well as the effects of divergent airflow from the north-west monsoon and lower annual totals to the east. South of 20°S there is a marked longitudinal gradient in annual rainfall totals (Tyson, 1986), ranging from more than 800 mm along the south-east coast to less than 100 mm along the west coast (Fig. 1.6a). The effects of orography, with higher rainfall totals to the windward side of mountains, is evident in the higher rainfall totals to the east of the escarpment, as well as in Madagascar. The influence of sea surface temperatures and their control of moisture characteristics and convective potential in the moist

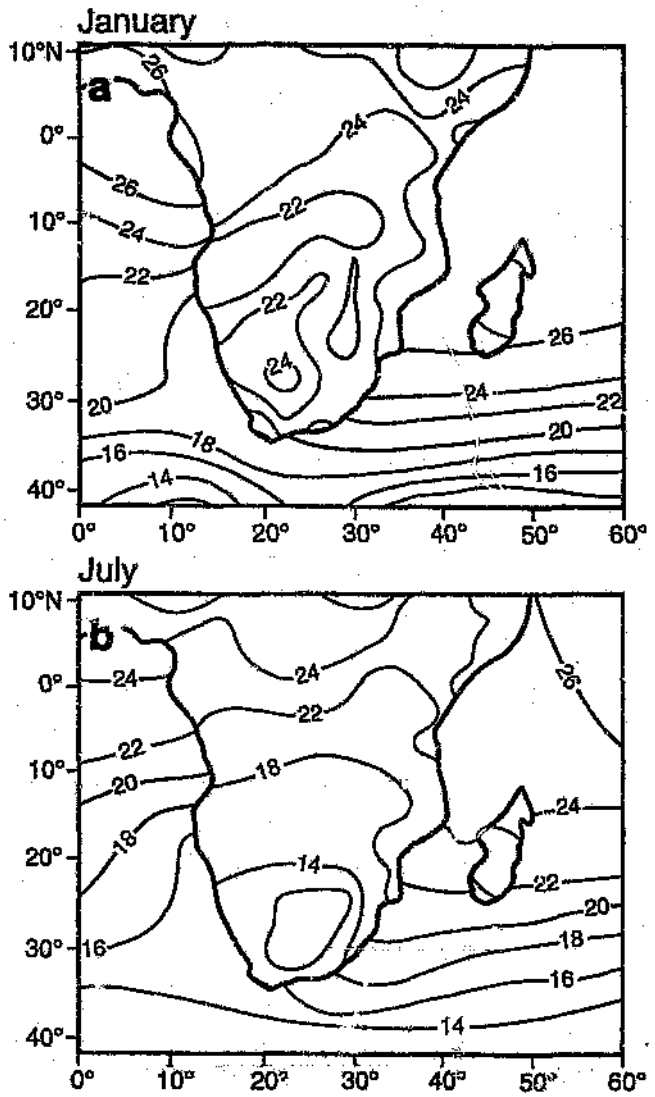

Figure 1.4: a) Mean January and b) July surface land and marine air temperatures for the southern African region (sources: *Monthly Climatic Data for the World* and *Meteorological Office Historical Sea Surface Temperature* data set).

convergent air advected onto the east coast is largely responsible for the marked east-west rainfall gradient across the subcontinent south of 20°S (Fig. 1.6a).

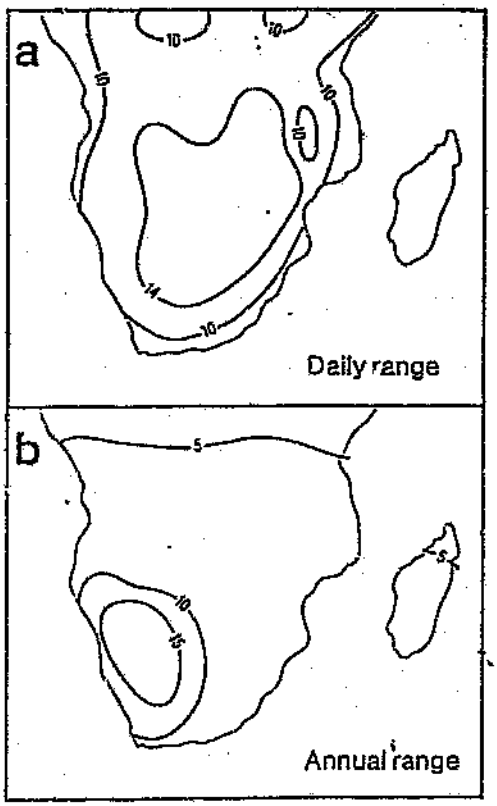

Figure 1.5: a) The diurnal range of temperature over southern Africa, and b) the annual temperature range, in °C (after Nieuwolt, 1977).

Rainfall over much of the subcontinent is strongly seasonal (Hsu and Wallace, 1976; Tyson, 1986; Lindesay, 1994) with a strong summer (October-March) maximum (Nicholson *et al.*, 1988; Lindesay, 1994) (Fig. 1.6b). Only the south-west Cape (with a winter rainfall maximum) and the southern Cape coast (year-round rainfall) do not experience a summer rainfall maximum (Keen and Tyson, 1973; McGee and Hastenrath, 1966). Rainfall variability has been the focus of considerable research at both temporal (Harrison, 1984b, 1986b; Tyson, 1981, 1986; Tyson *et al.*, 1975; Tyson and Dyer, 1978, 1980) and spatial scales (Lindesay, 1988a, 1988b; Miron and Tyson, 1984; Tyson, 1981, 1984). The effects of systematic circulation changes on rainfall have been described (Harangozo and Harrison, 1983, Harrison, 1983, 1986a; Lindesay and Jury, 1991; Tyson, 1984), of which the tropical-temperate interaction identified in tropical-temperate-troughs (Harangozo, 1989; Harrison, 1984a, 1986a; Lindesay and Jury, 1991) has been shown to be an important control of summer rainfall variability over the subcontinent.

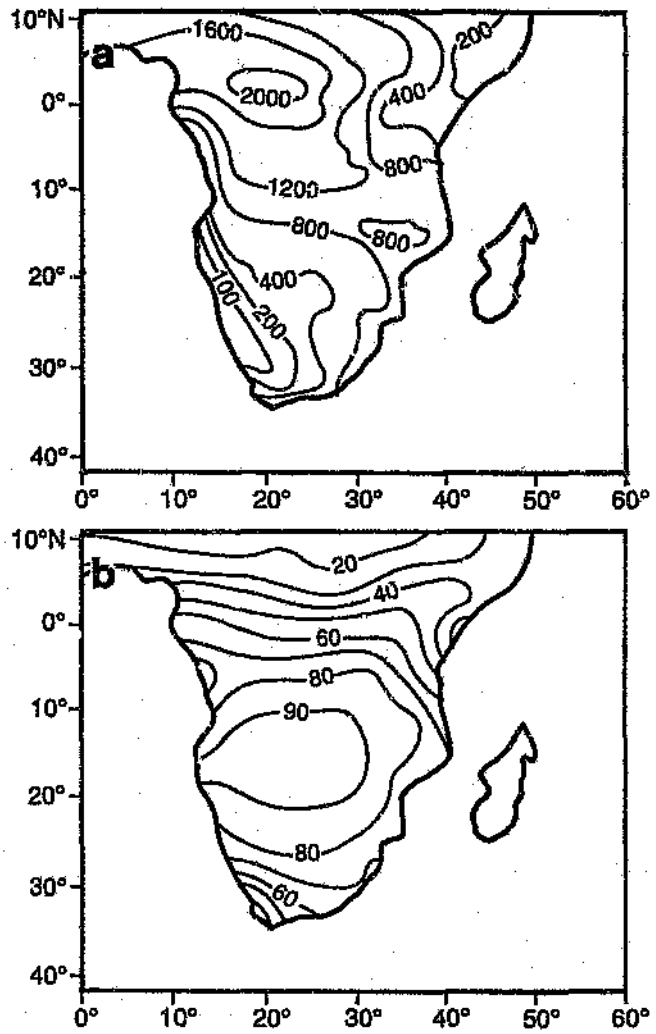

Figure 1.6: (a) Mean annual rainfall over Africa south of the equator, in mm (modified after Nicholson *et al.*, 1988) and (b) contribution of the summer season (October-March) to annual rainfall totals, expressed as a percentage (source: Hulme, 1992).

Climate Modelling

All climate models attempt to simulate and understand the many processes that produce climate. The aim is to predict the effects of changes and interactions which may affect the climate system (Henderson-Sellers and McGuffie, 1987). This is done by describing the climate system in terms of its basic physical laws. The nature of climate models may be described in terms of a hierarchy based on the sophistication with which four key components are

parameterised. These are radiation, dynamics, surface processes and time and space resolution (Shine and Henderson-Sellers, 1983). Four types of models have been developed.

1. *Energy balance models* (Budyko, 1969; Sellers, 1969, 1973, 1976; Warren and Schneider, 1979). These are one-dimensional models in which the zonally-averaged variation of surface temperature is described. Simplified relationships are used to calculate each of the terms contributing to the energy balance at a particular latitude.

2. *One-dimensional radiative-convective models* (Manabe and Möller, 1961; Manabe and Strickler, 1964, Manabe and Wetherald, 1967) compute the vertical temperature structure of the atmosphere from the balance between radiative heating or cooling and the vertical heat-flux, generally incorporating radiative transfer models.

3. *Two-dimensional zonally-averaged dynamical models* represent the atmosphere on a latitude-altitude grid. The dynamical and physical processes are calculated in terms of zonally-averaged variables.

4. *General circulation models* resolve the full three-dimensional structure of the atmosphere and ocean so that synoptic-scale processes are explicitly modelled. All physical processes believed to be important are represented (Fig. 1.7). These are the most sophisticated form of climate models and provide a powerful tool for inferring future climatic change associated with perturbations to the earth's radiative forcing (Henderson-Sellers and McGuffie, 1987).

General Circulation Models

General circulation models (GCMs) provide a sophisticated treatment of the full three-dimensional structure of the earth-atmosphere system based on the physical conservation laws which describe the redistribution of momentum, heat and water vapour by atmospheric motions (Cubasch and Cess, 1990). The atmosphere is divided into vertically discrete layers, and predicted

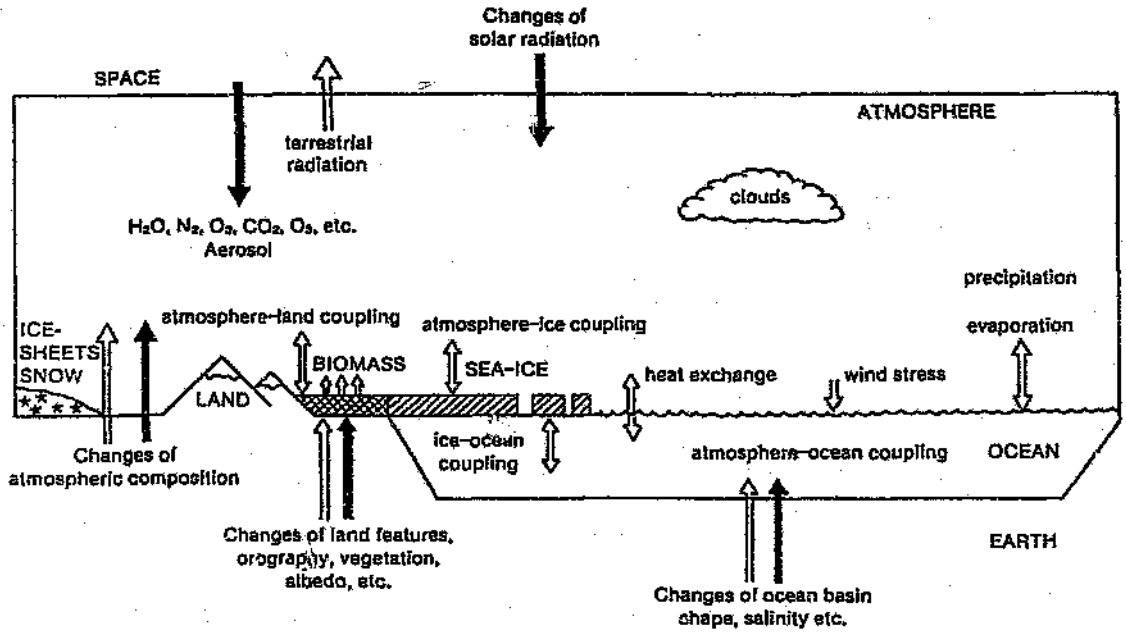

Figure 1.7: Schematic illustration of the components of the climate system which are incorporated directly or indirectly (using parameterisations) in GCM structure (after Henderson-Sellers and McGuffie, 1987).

variables (wind, temperature, humidity, surface pressure, rainfall) are determined either at individual grid points (finite difference models) or by a finite number of prescribed mathematical functions (spectral models). The value of the predicted variables is determined by advancing the model in discrete time steps from an initial condition. The spatial resolution of GCMs is constrained by the need for computational efficiency and is therefore usually fairly coarse, being of the order of 300 to 1000 km (Cubasch and Cess, 1990). More recent simulations have demonstrated a general reduction in model errors as a result of increased resolution, changes in the parameterisation of convection, cloudiness and surface processes and the parameterisation of gravity wave drag (Boer *et al.*, 1991; Gates *et al.*, 1990, 1992). The computational cost of such high resolution models must, however, be weighed against the consistently low confidence in GCM regional-scale simulations (Grotch and MacCracken, 1991). Several strategies aimed at improving

regional simulations have been identified (Gates *et al.*, 1992) and will be discussed further below.

Processes which are not resolved at GCM grid scales are incorporated into the models using parameterisations. A key atmospheric process to be parameterised is that of radiation, because it is through this process that greenhouse gases affect the general circulation. The radiative effects of clouds have been parameterised in several schemes, either by prescription (Manabe and Stouffer, 1980; Wetherald and Manabe, 1986; 1988), estimation from the relative humidity (Hansen *et al.*, 1984; Gordon and Hunt, 1987; Stouffer *et al.*, 1989; Washington and Meehl, 1984, 1989; Wetherald and Manabe, 1988; Wilson and Mitchell, 1987) or by calculation of the variation of cloud optical properties from the cloud water content (Mitchell *et al.*, 1989).

Cumulus convection is another important sub grid-scale process which is parameterised by different methods in GCMs. The moist convective adjustment adjusts the vertical temperature and water vapour profile of the atmosphere to a conditionally stable state (Manabe *et al.*, 1965). The penetrative convection scheme mixes moist conditionally unstable air from lower layers with dryer air aloft (Hansen *et al.*, 1984; Mitchell *et al.*, 1989; Schlesinger and Zhao, 1989; Wilson and Mitchell, 1987). Both schemes ascribe the moisture characteristics of an air mass to an entire grid-cell. In terms of particular convective events, which occur at much finer spatial resolutions, it becomes impossible to capture the complexity of individual events in terms of their size, frequency and intensity (Gordon *et al.*, 1992). The result is a mis-matching of scale between observed and simulated convective precipitation events (Whetton *et al.*, 1993). The simplistic treatment of cloud feedback processes is known to be problematic in GCMs (Harrison *et al.*, 1990). Cloud optical properties are fixed in both present-day and future climate simulations in many early-generation models (for example, Gordon *et al.*, 1992; Hansen *et al.*, 1984; Manabe and Wetherald, 1987; Wilson and Mitchell, 1987). The effect of cloud radiative forcing of temperature and possible changes to this forcing are thus poorly represented in these models.

Other physical processes relating to land surface processes, such as the determination of heat and water transfer within the soil, are also parameterised. Upper and lower boundary conditions are specified for each model. These include the input of solar radiation at the top of the atmosphere, orography and land-sea distribution, albedo, surface roughness and vegetation characteristics which are needed to establish solutions to the model equations.

GCM treatment of oceans is generally simplistic. In each of the models considered here, an atmospheric model is linked to a simple mixed-layer slab-ocean in which a simple slab of fixed depth, with relatively uniform temperature and a prescribed heat storage, is used (Hansen *et al.*, 1983; Manabe and Wetherald, 1987; Schlesinger and Zhao, 1989; Wilson and Mitchell, 1987). The mixed-layer slab-oceans do not include a deep ocean or ocean currents and sea surface temperatures are specified from climatology. The absence of currents may be accounted for using a Q-flux correction which calculates the additional heat flux at the ocean surface required to simulate present-day sea surface temperature patterns and their seasonal variation.

In estimating future conditions, equilibrium climate models simulate a perturbation of the radiative forcing of climate by establishing an equilibrium at present climate CO_2 levels and then (usually) doubling that concentration and allowing a new equilibrium to re-establish (Hansen *et al.*, 1983; Manabe and Wetherald, 1987; Mitchell *et al.*, 1989; Schlesinger and Zhao, 1989; Washington and Meehl, 1984, 1989; Wetherald and Manabe, 1988; Wilson and Mitchell, 1987).

Equilibrium models are less computationally intensive than fully coupled ocean-atmosphere models or transient model simulations (which allow CO_2 levels to increase slowly instead of instantaneously doubling their concentration). Intercomparisons between equilibrium models are facilitated by the similarity in experimental design. These models can also be brought to statistical equilibrium relatively easily and provide a benchmark for model sensitivity experiments. Most recent equilibrium climate runs tend to conform to the Intergovernmental Panel on Climate Change (IPCC) 1990 'Business as

Usual' scenario of a globally-averaged mean temperature increase ranging from 1.5°C to 4.5°C (Gates *et al.*, 1992). More recent equilibrium climate models have included higher spatial resolution, more sophisticated treatments of cloud radiative feedbacks in the tropics (see e.g. the interactive cloudiness parameterisation of McFarlane *et al.*, 1992), and have highlighted the inadequacy of using carbon dioxide as a proxy for the radiative effects of all the greenhouse (trace) gases. The inclusion of several trace gases as demonstrated by Wang *et al.* (1991) should produce a warmer atmosphere, thereby reducing the systematic error of a cold bias noted by Boer *et al.* (1991, 1992) in most surface air temperature simulations. The simplistic treatment of oceans and ocean circulation in mixed-layer slab-ocean models is reflected in an asymmetry in warming at higher latitudes during winter common to all such models. This is the result of several physical processes and sea-ice albedo feedbacks (Hansen *et al.*, 1984; Manabe and Stouffer, 1980; Mitchell, 1989).

The dominant importance of ocean-atmosphere interactions in influencing and controlling global climate has lead to the coupling of oceanic and atmospheric GCMs. A basic problem in the construction of coupled models is the wide range of time scales (ranging from about one day for the atmosphere to 1000 years for the deep ocean) at which the system must operate. Synchronous coupling of ocean-atmosphere models is extremely time-consuming, and limited computer resources often prohibit equilibrium being reached. A secondary problem to such coupling is that of model drift in which coupled models tend to drift toward a state that reflects the systematic errors of the respective model components because each model is no longer constrained by prescribed fluxes at the atmosphere-ocean interface.

Transient studies using fully coupled ocean-atmosphere models represent a significant recent advance in GCM modelling, offering a higher sophisticated simulation of the real climate system. Encouraging similarities exist between the few transient experiments which have been published (Cubasch *et al.*, 1993; Hansen *et al.*, 1988; Manabe *et al.*, 1991, 1992; Meehl *et al.*, 1993; Stouffer *et al.*, 1989; Washington and Meehl, 1989). Most notable of these is that warming at any given time is less than the corresponding equilibrium value for

an instantaneous forcing (CO_2 doubling), with a globally-averaged mean temperature rise at effective CO_2 doubling in the range of 1.3° to 2.3°C. Whilst this range confirms the results for the simpler models reported by Gates *et al.* (1990), the values are approximately 60% of the equilibrium warming under doubled CO_2 conditions (Gates *et al.*, 1992). This is partly due to the fact that these models account for the thermal inertia of the oceans and therefore are not at equilibrium at the time of effective CO_2 doubling. After an initial period of little warming (the so-called 'cold start' attributed to faults in experimental design), all models show a near-constant temperature increase of 0.3°C per decade, which is again comparable to the IPCC 1990 'Business as Usual' scenario. There is also broad agreement between the models as to the large-scale patterns of change and these are again comparable to those of the equilibrium climate models. However, the transient GCMs show none of the asymmetrical warming at southern high latitudes of the equilibrium models (Washington and Meehl, 1989), due to the formation of deep water in the oceans.

Model Validation

The sensitivity of GCM climates to perturbations of their radiative forcing (by doubling CO_2) is known to be dependent on their simulation of unperturbed climate (Mitchell *et al.*, 1987). The inability of GCMs to represent regional climate accurately (Gates *et al.*, 1990; 1992; Grotch and MacCracken, 1991; Schlesinger and Mitchell, 1987) is strongly related to uncertainties present in the parameterisation of climate feedback mechanisms such as cloud feedback processes (Cess *et al.*, 1990; Cubasch and Cess, 1990). As there can be no guarantee that processes which produce present climate do not undergo change themselves in a perturbed climate, accurate representation of present climate is not *sufficient* to guarantee that a particular sensitivity to change is correct (Mitchell *et al.*, 1987). Neither can it be assumed that an accurate representation of the present climate is confirmation that the processes responsible for the accurate distribution are necessarily being simulated correctly. Comparison of the present climates of several models which include similar processes can, however, identify sensitivity errors between models which do not produce similar errors in their control simulations. Such

validations of present day climate GCM simulations against observed data (Boer *et al.*, 1992; Grotch and MacCracken, 1991; Portman *et al.*, 1992) are thus used as a means of establishing confidence in the regional climatic change scenarios of individual models.

Validation at Regional Scales

In the 1992 IPCC Supplementary Report, Gates *et al.* (1992) identify two approaches to the problem of regional scale climate simulation. Firstly, using a one-way nested approach, Giorgi *et al.* (1990) have shown that a mesoscale model embedded within a GCM and driven with boundary conditions set by the GCM can significantly improve the regional-scale climate distribution. A second statistical approach involves the development of empirically-derived relationships between the regional climate and the large-scale flow (Hewitson and Crane, 1992; Karl *et al.*, 1990; Wigley and Santer, 1990; Wigley *et al.*, 1990). Both approaches are however dependent on the accuracy of the large-scale flow generated by the GCM, and therefore do not avoid the need for improvement in GCM simulations (Gates *et al.*, 1992).

Considerable uncertainties remain in the simulation of regional climates and regional climatic change by GCMs (Grotch and MacCracken; 1991; Portman *et al.*, 1992). A valuable strategy for developing reliable regional climate simulations is the validation and intercomparison of GCM climates for various regions of the globe. Establishing the facility with which regional climate is currently simulated by several GCMs will identify errors within such simulations and hence allow improved parameterisation of the processes responsible for climate at this scale. In the southern hemisphere, such an analysis has been undertaken for the Australian region (Whetton and Pittock, 1991) but as yet not for the southern African region. The reviews by Tyson (1990, 1991, 1993) identified only the broadest features of predicted climatic changes over southern Africa. There is a need to validate present-day climate simulations before changes predicted by GCMs for this region become reliable. The present-day climate simulations for the southern African region by several GCMs are thus validated against observations and intercompared. Confidence in selected climatic change scenarios will be established on the

basis of the facility with which individual models simulate the observed patterns of particular climate variables over the southern African region.

Hypotheses

In this dissertation, the relative performance of six early-generation general circulation models will be assessed over the southern African region. As most model simulations produce long-term mean climates, the assessment will focus on the ability of the GCMs to simulate the intra-annual variability of the region's climate. Three key climatic parameters, namely surface air temperature, mean sea level pressure and land surface precipitation, will be considered for this analysis.

The hypotheses to be tested are:

a) that the spatial patterns and magnitudes of particular climatic variables for the southern African region are simulated accurately by the general circulation models;

b) that the intra-annual variability of southern African climate is accurately simulated by the general circulation models;

c) that physical processes occurring at sub-grid-scales are adequately parameterised by the models;

d) that the regional climate simulations described above are simulated equally well by all general circulation models; and

e) that the validation of present climate simulations will allow the development of more reliable predictions of future climate under doubled CO_2 conditions for the southern African region.

****

The climate of the southern African region has been outlined. The concept of climate modelling has been introduced and the important features of general circulation modelling have been described. The validation and intercomparison of the present-day climate simulations of six early-generation general circulation models for the southern African region will allow the development of reliable predictions of future climate under doubled CO_2 conditions. The methodology to be used is discussed in *Chapter 2*.

CHAPTER 2

DATA AND STATISTICAL METHODS

Introduction

The southern African region considered here extends from 10°N to 60°S and from 20°W to 100°E. As model resolutions differ and are not aligned with the equator, the northern boundary of the region is defined as one grid-point north of the equator.

Data

Observational Data

Land surface air temperatures have been taken from the National Centre for Atmospheric Research (NCAR) *World Monthly Surface Station* data set. Due to poor data-availability for the thirty-year period between 1951 and 1980, means have been calculated for the forty-year period 1945-1985 in order to improve data-coverage. Marine air temperatures for 1951-1980 have been determined from the *United Kingdom Meteorological Office Historical Sea Surface Temperature* (MOHSST) 5° x 5° mean sea surface temperature and air-sea temperature difference data sets. Mean sea level pressures for 1951-1985 have been extracted from the *Southern Hemisphere Mean Sea Level Pressure* data set (Jones, 1991). The data are available for latitudes 15°S to 60°S on 5° x 5° grid resolution. Land surface precipitation for 1951-80 has been extracted from the *Global Land Surface Precipitation* data set (Hulme, 1992) on a 5° x 5° grid.

These data sets originate from independent sources. As far as is possible, means have been calculated for the thirty-year period between 1951 and 1980. As each data set has a unique application, no spatial domains overlap. Each variable is thus considered independently in the model validation procedure. The use of observational data sets unique to the southern African region further complicates the assessment of the overall performance of the models for several different regions of the globe.

Simulated Data from General Circulation Models

The general circulation models used in this study are early-generation equilibrium climate models, with most simulations completed before 1989. Although the configuration and parameterisation of processes is unique to each of these models, they have been chosen because they all include similar physical processes. Comparison of their present-day climate simulations allows for the identification of sensitivity errors between models which do not produce similar errors in their control simulations (Boer *et al.*, 1991; Grotch and MacCracken, 1991; Portman *et al.*, 1992).

Simulated data for the 1 x CO_2 and 2 x CO_2 equilibrium runs from the following GCMs were obtained from the Data Support Section of NCAR. The models are the 1984 GISS model of the Goddard Institute for Space Studies (Hansen *et al.*, 1983, 1984), the 1987 and 1988 GFDL models of the Geophysical Fluid Dynamics Laboratory (Manabe and Wetherald, 1987; Wetherald and Manabe, 1988) and the 1987 UKMO model of the United Kingdom Meteorological Office (Wilson and Mitchell, 1987). Two different versions of the GFDL model, one excluding and one including a Q-flux procedure, were available. For the purposes of this study, these have been named the GFDL and GFDLQ simulations, respectively. No version of the NCAR Community Climate Model was available. Two more recent simulations (completed after 1989) were obtained from the Commonwealth Scientific and Industrial Research Organisation (CSIRO). These are the 1990 4-level (CSIRO4) simulation (Gordon and Hunt, 1991; Gordon *et al.*, 1992) and the 1992 9-level (CSIRO9) simulation (McGregor *et al.*, 1993; Whetton *et al.*, 1993).

Details of the various GCM experiments are provided in Table 2.1. All experiments include the full annual cycle of radiation. Only the GFDL simulations do not include a diurnal cycle. Clouds are represented diagnostically as a function of relative humidity and cloud optical properties are fixed. There is considerable range in the horizontal and vertical resolutions of the models. The UKMO has the highest vertical resolution (11 levels) and the CSIRO4 and CSIRO9 simulations have finest horizontal resolution (approximately 3.2° x 5.6°). Control climate CO_2 levels vary from 300 to 330 ppm. The monthly mean 1 x CO_2 fields are constructed from data for 10 model years, except for the UKMO model, where 15 years has been used. One of two convection parameterisation schemes is used. The GISS and UKMO simulations use the penetrative convection scheme, whereas the GFDL and CSIRO simulations use a moist convective adjustment. In the case of the CSIRO simulation, the moist convective adjustment also generates a mass flux (Arakawa, 1972). Only the CSIRO simulations make use of a gravity wave drag term in their momentum equations although this has subsequently been included in several more recent versions of the models considered here (for example, the UKMO model, Mitchell *et al.*, 1989).

Each model interacts with a simple mixed-layer slab ocean. Temperatures are relatively uniform with depth and heat storage is prescribed. No ocean currents exist and sea surface temperatures are specified from climatology. All models (except for the GFDL simulation) include a Q-flux correction. Models which include a Q-flux correction are favoured in an intercomparison study as sea surface temperatures are constrained to reflect climatological values. However, this correction also prevents ocean temperature and sea ice from responding in climatic change sensitivity (doubled CO_2) experiments and thus a crucial feedback mechanism is excluded (Washington and Meehl, 1991).

Observed and simulated topography for the southern African region are compared in Figure 2.1. Poorly-resolved topography is recognised as a significant limitation on the veracity of the model output at regional and local scales (Whetton and Pittock, 1991). This problem will be exacerbated in regions of pronounced topographic gradients such as in southern Africa. The effect of the representation of topography in spectral models is generally to

Table 2.1: Specifications of the GCM experiments used in this intercomparison. Model resolution is given in degrees (finite difference models) or wave number of truncation (spectral models). Convection schemes adopted by these models include the penetrative convection (PC) and moist convective adjustment (MCA). Clouds are diagnosed from relative humidity (RH). All models have fixed cloud radiative properties (F). Equilibrium carbon dioxide concentrations are given in ppm. Predicted globally-averaged warming as a result of equilibrium surface temperature change is given in °C (after Cubasch and Cess, 1990 and McGregor *et al.*, 1993).

	GISS (1984)	GFDL (1987)	GFDLQ (1988)	UKMO (1987)	CSIRO4 (1990)	CSIRO9 (1992)
Horizontal resolution	7.8x10.0	R15	R15	5.0x7.5	R21	R21
model levels	9	9	9	11	4	9
seasonal cycle	yes	yes	yes	yes	yes	yes
diurnal cycle	yes	no	no	yes	yes	yes
cloud scheme	RH	RH	RH	RH	RH	RH
cloud properties	F	F	F	F	F	F
convection scheme	PC	MCA	MCA	PC	MCA	MCA
oceanic Q-flux	yes	no	yes	yes	yes	yes
number of model years	10	10	10	15	10	10
$1xCO_2$ concentration	315	300	300	323	326	330
warming °C	4.2	4.0	4.0	5.2	4.0	4.8

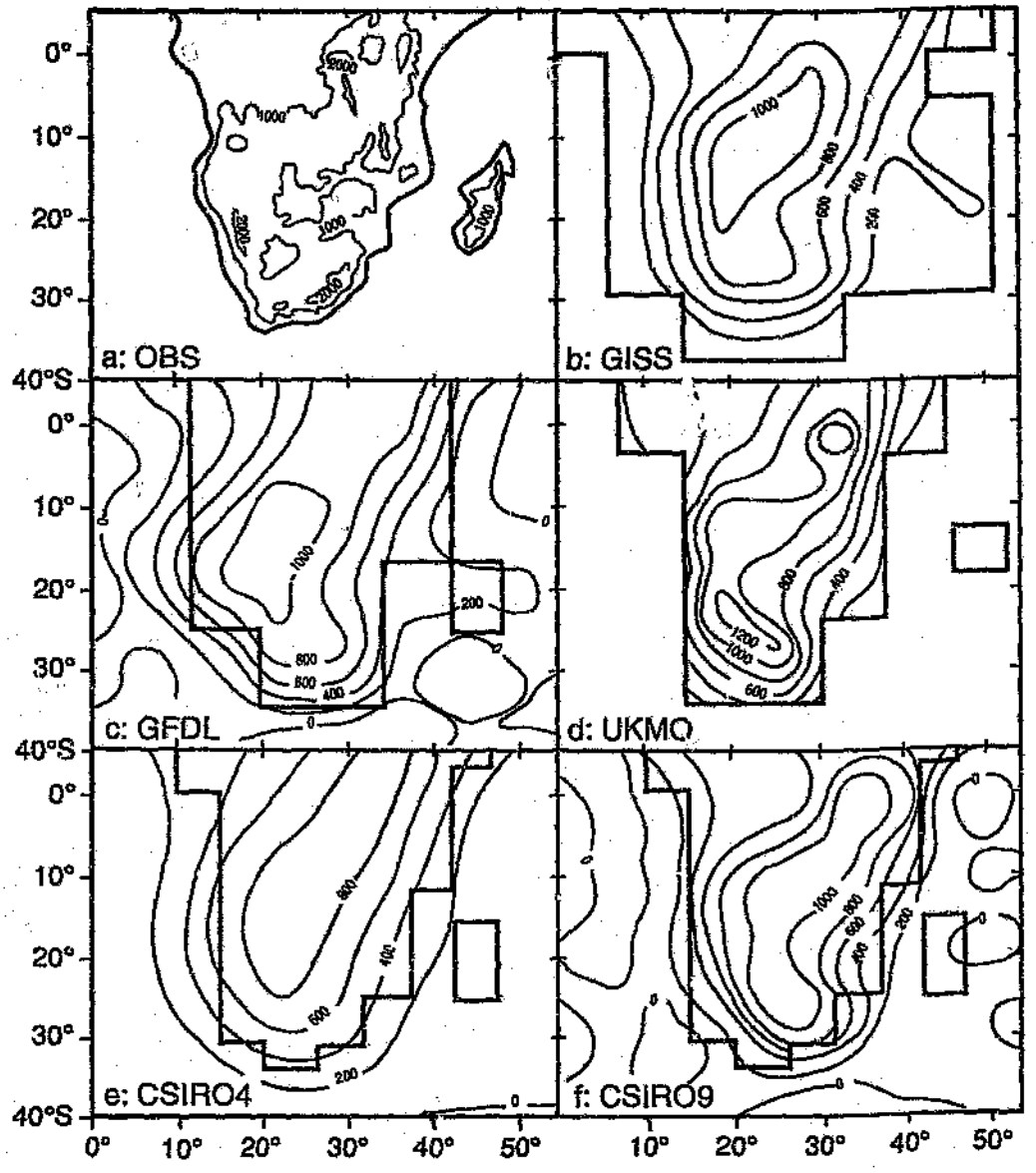

Figure 2.1: Observed (a) and simulated topography for GISS (b), GFDL (c), UKMO (d), CSIRO4 (e) and CSIRO9 (f) models (in metres).

smooth topographical features and under-estimate maximum heights. Both the GFDL and CSIRO4 spectral models suffer from this problem (Fig. 2.1). The improved vertical resolution of the CSIRO9 spectral model has included a more realistic geography and hence better representation of topographic features over the subcontinent (McGregor *et al.*, 1993). Generally, coarse horizontal resolution will have the effect of misrepresenting all regions of

exaggerated topography, such as the eastern escarpment. Poor representation of southern African topography must be allowed for in the assessment of the spatial patterns of model output, particularly in the case of precipitation.

Statistical Methodology

The present-day climate analysis focuses on the simulation of the pattern and magnitude of the observed distributions. January and July conditions are compared in order to assess the simulation of seasonality over the southern African region. The comparison of control and perturbed (2 x CO_2) simulations aims to identify the nature and extent of simulated changes.

A wide range of resolutions exist amongst both GCM-simulated and observed fields. In order to assess the degree of similarity between simulated and observed fields, observed data were interpolated onto each model grid.

For each model, grid-point differences between simulated and observed values were calculated (the simulation error). A root mean square (rms) error (the simulation error throughout the region) has been calculated from

$$rms = \frac{\sqrt{\sum_{i=1}^{n}(x_i - y_i)^2}}{n} \qquad (2.1)$$

where x_i and y_i are the ith observations of independent variables x and y respectively and n defines the total number of grid points across the field.

The similarity between simulated and observed patterns for a particular variable were calculated using a pattern correlation coefficient from

$$r_{xy} = \frac{\sum_{i=1}^{n}(x_i - \bar{x})(y_i - \bar{y})}{\sigma_x \sigma_y} \qquad (2.2)$$

where $\bar{x}$ and $\bar{y}$ are the area averages and σ_x and σ_y are the standard deviations of x and y respectively.

The rms error provides an overall measure of the error in simulating the absolute value of a variable over the region as a whole. Secondly, the pattern correlation coefficient gives a measure of the similarity of the pattern structure of the observed and simulated fields. For an intercomparison of several models, both quantities are needed because two models which have similar rms errors may differ greatly in their ability to represent the pattern structure of the observed field, and *vice versa*. Furthermore, it is also possible that the absolute value of a given variable may be over- or under-estimated across a field, while simultaneously, the spatial variability and hence the pattern structure of the given field may be well-captured.

Testing for the significance of differences between simulated and observed fields is problematic (Wigley and Santer, 1990). The degree of spatial autocorrelation present in both simulated and observed fields for a particular variable is often high, rendering invalid the assumption made in standard significance testing that individual observations are independent of each other. If the degree of spatial autocorrelation present in the field is high, the number of independent observations will be reduced and hence result in an over-estimate of the significance of the whole field. This problem is usually overcome by using Monte Carlo techniques to account for field significance (Livezey and Chen, 1983). However, where only long-term means are available, it is not possible to utilise such techniques because no information about the variability in the simulated field is available. It is therefore impossible to calculate the field significance of differences between simulated and observed long-term mean fields.

The Wilcoxon matched pairs signed ranks test investigates the median difference between pairs of scores from two matched samples of size n. Using this test it is possible to ascertain whether the medians of the two matched samples are significantly different from each other, thus providing an estimate of the significance of differences between the two fields. This test treats a matched pair

$$\{x_i, y_i\} \text{ for } i = 1,2 \ldots n \tag{2.3}$$

as a single sample by considering the signed difference

$$d_i = x_i - y_i \tag{2.4}$$

of each pair (if $d_i = 0$, that particular pair is ignored). The matched pair may then be thought of as a single observation on a bivariate random variable (Siegel, 1956; Conover, 1980).

The absolute differences $|d_i|$ (without regard to sign) are ranked, tied ranks being assigned the average of tied ranks, and the sign of d_i is reassigned to each rank. The Wilcoxon matched pairs signed ranks test thus accounts for both the magnitude and sign of the score differences. The null hypothesis (H_0) that the medians are the same is tested against an appropriate alternative hypothesis (H_1). The probability p for the corresponding test statistic W can be tested for the significance of the median differences against a suitable significance level α (here $\alpha = 0.05$) using the following H_1,

$$H_1 : \text{median of } x > y. \; H_0 \text{ is rejected if } 1 - p < \alpha \tag{2.5}$$

$$H_1 : \text{median of } x < y. \; H_0 \text{ is rejected if } p < \alpha \tag{2.6}$$

For the two CSIRO models, ten years of simulated data were available for each of the control and perturbed runs. A more rigorous statistical comparison of spatial means, patterns and variances, using a suite of nine statistics developed by Wigley and Santer (1990) has thus been implemented.

In all cases, significance levels are assessed using a pooled permutation procedure (Preisendorfer and Barnett, 1983). The pooled permutation procedure combines two ten-year samples (the control and perturbed runs) and then divides this new subset of twenty years randomly into two new ten-year samples. Test statistics are then re-calculated in a series of randomisations and a null sampling distribution is calculated against which the original test statistic can be compared. This procedure overcomes problems arising from spatial autocorrelation, unknown sampling distributions and multiplicity in the case of univariate statistics. A full summary of the statistics used by Wigley and Santer (1990), as well as a complete description of the pooled permutation procedure is given in Appendix A.

****

The observational and simulated data required to undertake an assessment of the present-day climate performance of six early-generation general circulation models for the southern African region have been described. The statistical procedures used to assess differences between simulated and observed fields and to assign significance to such differences have been discussed. These techniques will be applied to a validation of the control climate simulation of observed surface air temperature, mean sea level pressure and precipitation for the southern African region in *Chapter 3*.

CHAPTER 3

SIMULATIONS OF PRESENT CLIMATE

Introduction

Predictions of future climatic change by general circulation models (for doubled CO_2 conditions) are considered reliable if the models perform well under present-climate conditions (Mitchell *et al.*, 1987). As general circulation models demonstrate broad-scale agreement on the features of present-day climate for the globe as a whole, predictions of *global* climatic change are considered reliable (Gates, *et al.*, 1990, 1992). Equally, understanding how well the models reproduce regional and local climates will lead to an improvement in the representation of physical mechanisms which determine regional climate, and hence in the predictive capabilities of the models (Grotch and MacCracken, 1991; Portman, *et al.*, 1992). Simulated future conditions from a range of general circulation models have been presented before for the southern African region (Tyson, 1990, 1991, 1993). The predictions were not, however, based on an assessment of the present-climate performance of the models.

In this chapter, an assessment of the present-climate performance of six early-generation general circulation models for the southern African region will be presented. The assessment focuses on the simulation of surface air temperature, mean sea level pressure and precipitation for the southern African region.

Results

Surface Air Temperature

The models do not simulate the January surface air temperature distribution well over the land (Fig. 3.1). Their failure to capture the [illegible] summer convective processes fully is demonstrated by a patchiness in the pattern of simulation errors within the tropics (Fig. 3.2) and a consistently poor simulated pattern of surface air temperature over the subcontinent (Table 3.1). Both the 1987 GFDL and 1988 GFDLQ models simulate the pattern of present-day surface air temperature poorly, producing large overall (Table 3.1) and grid-point simulation errors (Fig. 3.2b,c). The 1984 GISS and 1987 UKMO models appear to capture the strong mid-summer convection more accurately than the GFDL models, with an improved simulation of the pattern of January surface air temperature (Fig. 3.1a,d). The improved vertical resolution of the 1992 CSIRO9 model (Fig. 3.1f) over its 1990 4-level predecessor (CSIRO4) (Fig. 3.1e) also results in a more accurate simulation.

Table 3.1: Statistical intercomparison for surface air temperature over the land. The pattern correlation coefficient (r) and root mean square (rms) error (in °C) are calculated for model land grid-points only. Significance of median differences between observed and simulated fields is calculated using the Wilcoxon matched pairs signed ranks test.

	JANUARY			JULY		
	r	rms error	signifi-cance	r	rms error	signifi-cance
GISS	0.52	2.77	95	0.85	2.70	95
GFDL	0.26	4.76	99	0.61	5.03	99
GFDLQ	0.11	3.91	95	0.65	4.50	99
UKMO	0.48	2.73	21	0.79	3.61	67
CSIRO4	0.42	2.96	99	0.74	3.72	99
CSIRO9	0.35	2.67	99	0.86	3.56	99

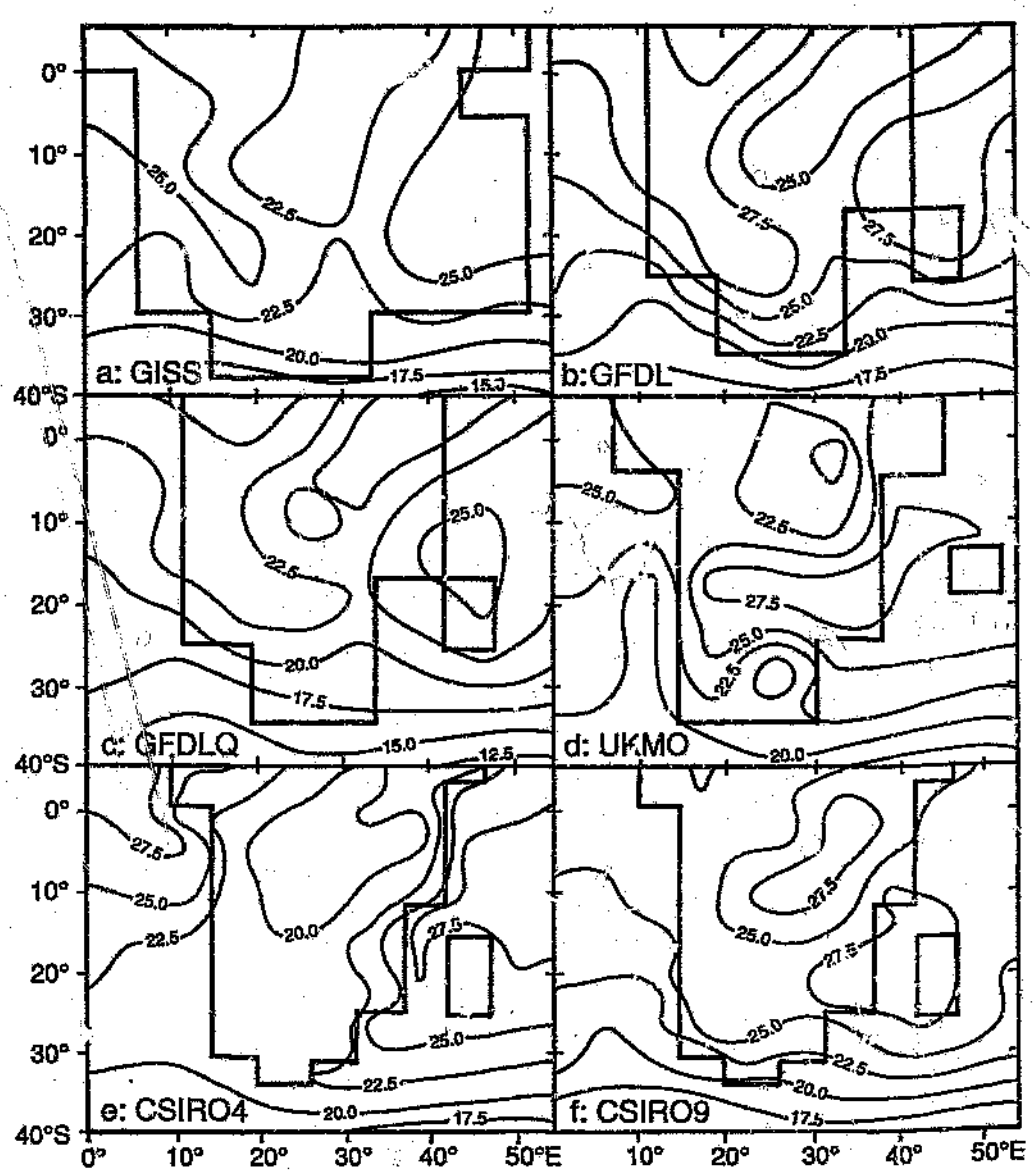

Figure 3.1: Simulated 1 x CO_2 January surface air temperatures for the GISS (a), GFDL (b), GFDLQ (c), UKMO (d), CSIRO4 (e) and CSIRO9 (f) models (in °C). The present-day January surface land and marine air temperature distribution is shown in Figure 1.4 (a).

The GISS, UKMO and CSIRO9 models all produce relatively low root mean square errors ranging between 2°C and 3°C (Table 3.1).

The January marine air temperature simulations are generally more acceptable than the simulations of surface air temperature over the land (Fig.

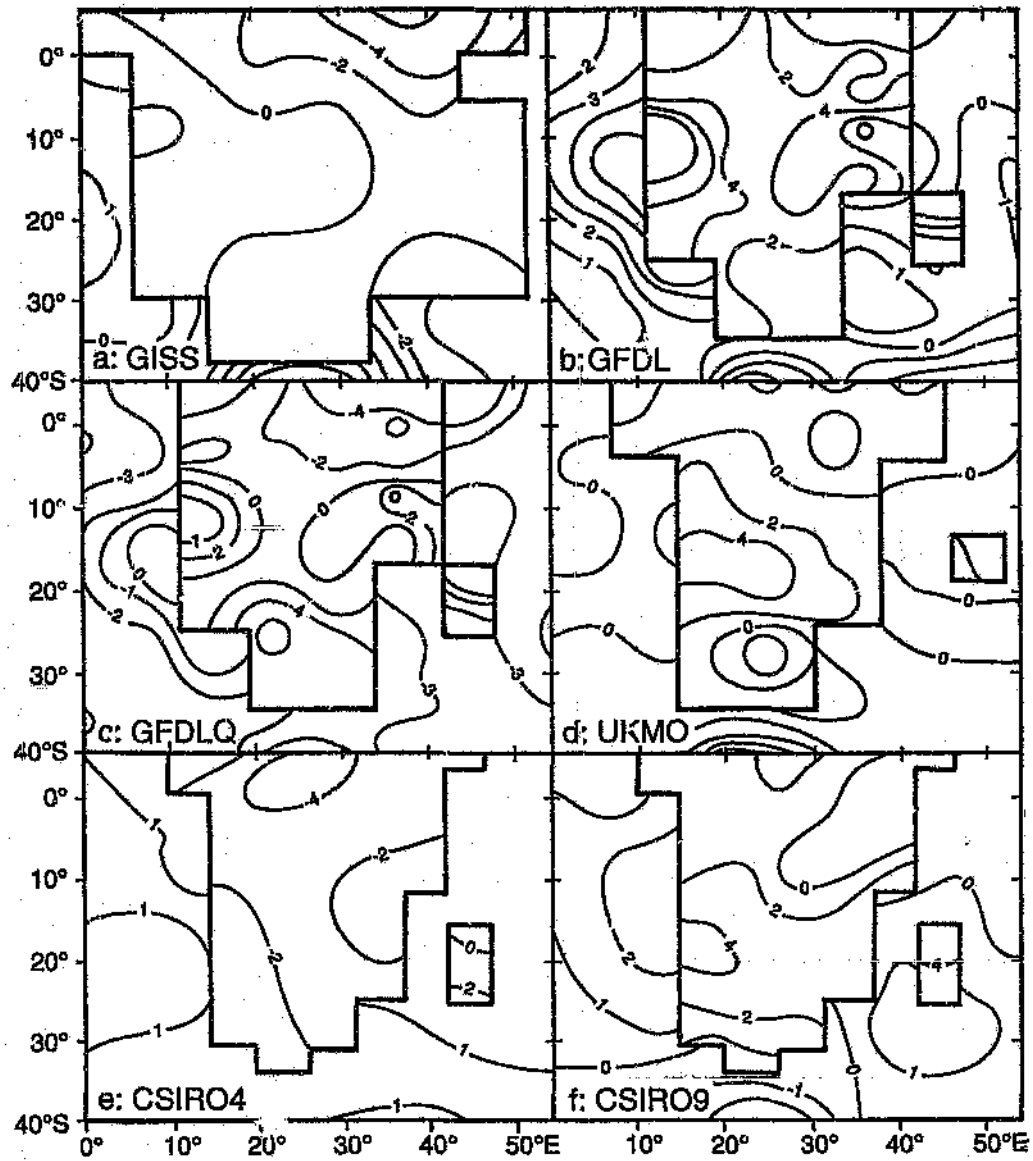

Figure 3.2: Calculated differences (simulation minus observed) for January surface land and marine air temperatures for the GISS (a), GFDL (b), GFDLQ (c), UKMO (d), CSIRO4 (e) and CSIRO9 (f) models (in °C).

3.1). The effect of the Q-flux procedure used in all but the GFDL simulation results in an accurate simulation of the pattern and magnitude of present-day marine air temperatures (Table 3.2). For the GFDLQ model, however, the incorporation of a Q-flux procedure has over-compensated for higher than observed GFDL temperatures, producing significantly cooler conditions (Fig. 3.2c) and a larger root mean square error (Table 3.2). Simulation errors are

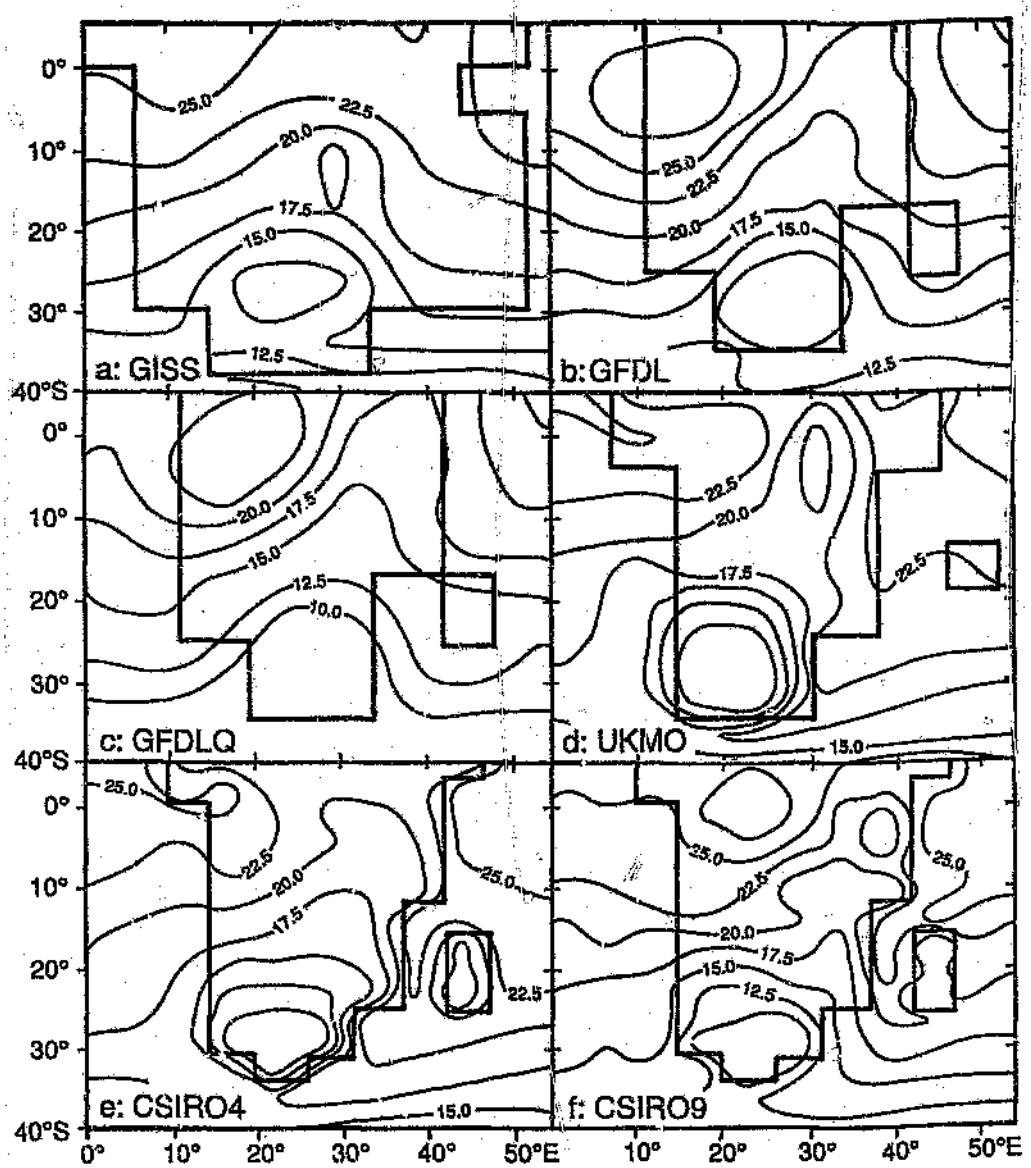

Figure 3.3: Simulated 1 x CO_2 July surface air temperatures for the GISS (a), GFDL (b), GFDLQ (c), UKMO (d), CSIRO4 (e) and CSIRO9 (f) models (in °C). The present-day July surface land and marine air temperature distribution is shown in Figure 1.4 (b).

large at higher latitudes (Fig. 3.2) and may exceed 6°C below 60°S (not shown).

The July surface air temperature distribution over the land improves markedly over January simulations in all models (Fig 3.3). The improvement

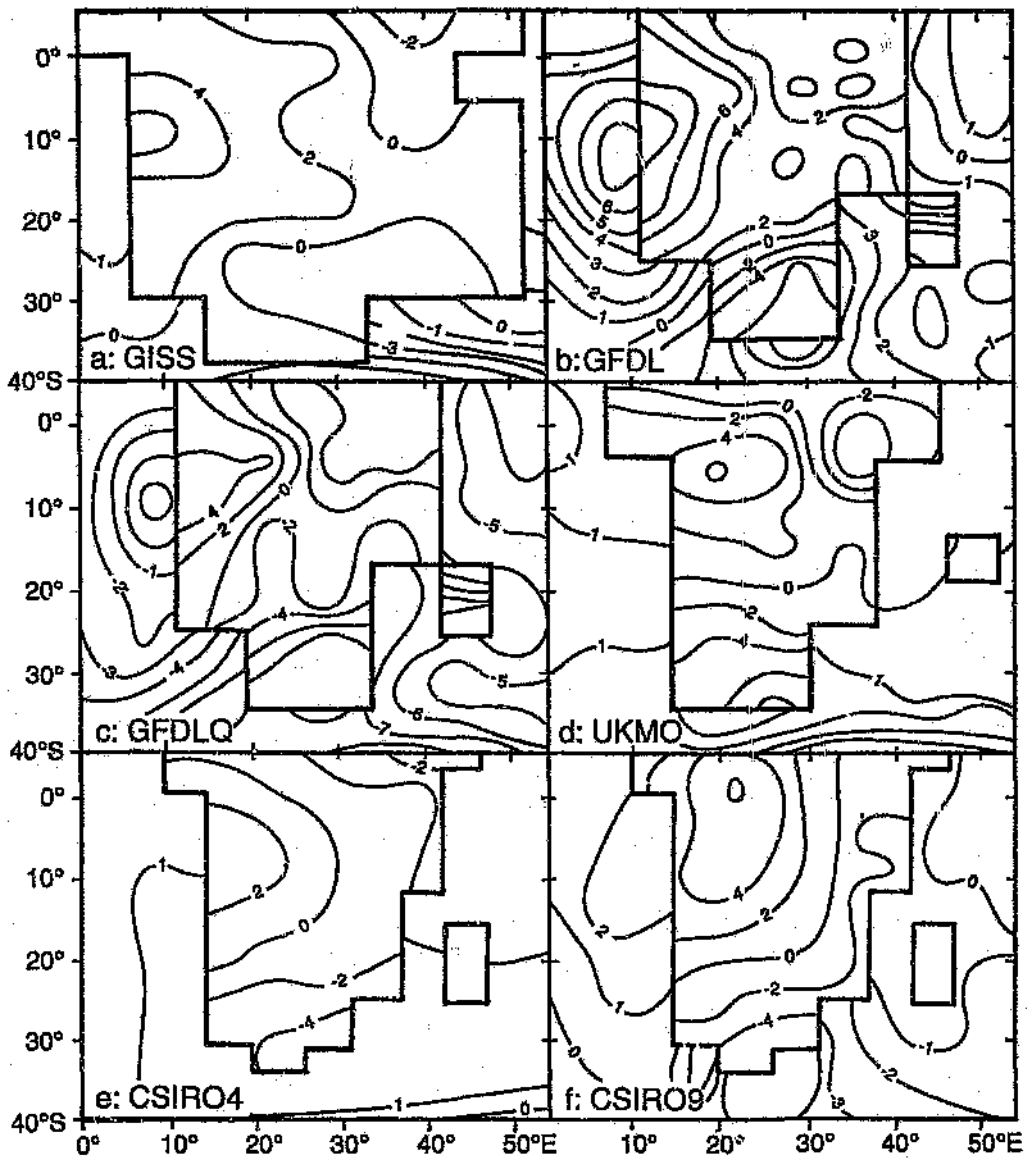

Figure 3.4: Calculated differences (simulation minus observed) for July surface land and marine air temperatures for the GISS (a), GFDL (b), GFDLQ (c), UKMO (d), CSIRO4 (e) and CSIRO9 (f) models (in °C).

in the simulated pattern of surface air temperatures over much of the subcontinent in the middle of the dry season indicates that in the absence of clouds the models are more successful in simulating the observed temperature distribution (Table 3.1). However this improvement is not reflected in an improved simulation of the magnitude of July temperatures (Table 3.1). Grid-point simulation errors show that the models simulate lower

Table 3.2: Statistical intercomparison for marine air temperature. The pattern correlation coefficient (r) and root mean square (rms) error (in °C) are calculated for model sea grid-points only. Significance of median differences between observed and simulated fields is calculated using the Wilcoxon matched pairs signed ranks test.

	JANUARY			JULY		
	r	rms error	signifi-cance	r	rms error	signifi-cance
GISS	0.95	1.83	53	0.94	2.61	15
GFDL	0.93	1.95	99	0.93	2.19	23
GFDLQ	0.96	3.18	99	0.96	4.88	99
UKMO	0.97	1.14	99	0.96	1.52	99
CSIRO4	0.98	1.31	99	0.97	1.51	99
CSIRO9	0.96	1.32	99	0.96	1.98	99

than observed temperatures over the southern subcontinent and higher than observed temperatures in the western and central regions (Fig. 3.4). The July marine air temperature simulation again closely resembles the pattern and magnitude of the present-day distribution (Table 3.2). At higher latitudes, grid-point errors south of 40°S are larger than in January (Fig. 3.4).

Mean Sea Level Pressure

The January mean sea level pressure simulations by the GISS, GFDL, GFDLQ and UKMO models demonstrate a characteristic failure to simulate pressures at high latitudes accurately (Fig. 3.5a to d). Grid-point errors in excess of 14 hPa are apparent (Fig 3.6a-d). Such errors are most noticeable in the coarse horizontal resolution simulations such as the GISS and UKMO models (where simulation errors south of 60°S exceed 20 hPa) and result in a poor representation of both the pattern structure and magnitude of the present-day mean sea level pressure distribution (Table 3.3). Simulated pressures over the subcontinental interior are generally lower than observed (Fig. 3.6). The

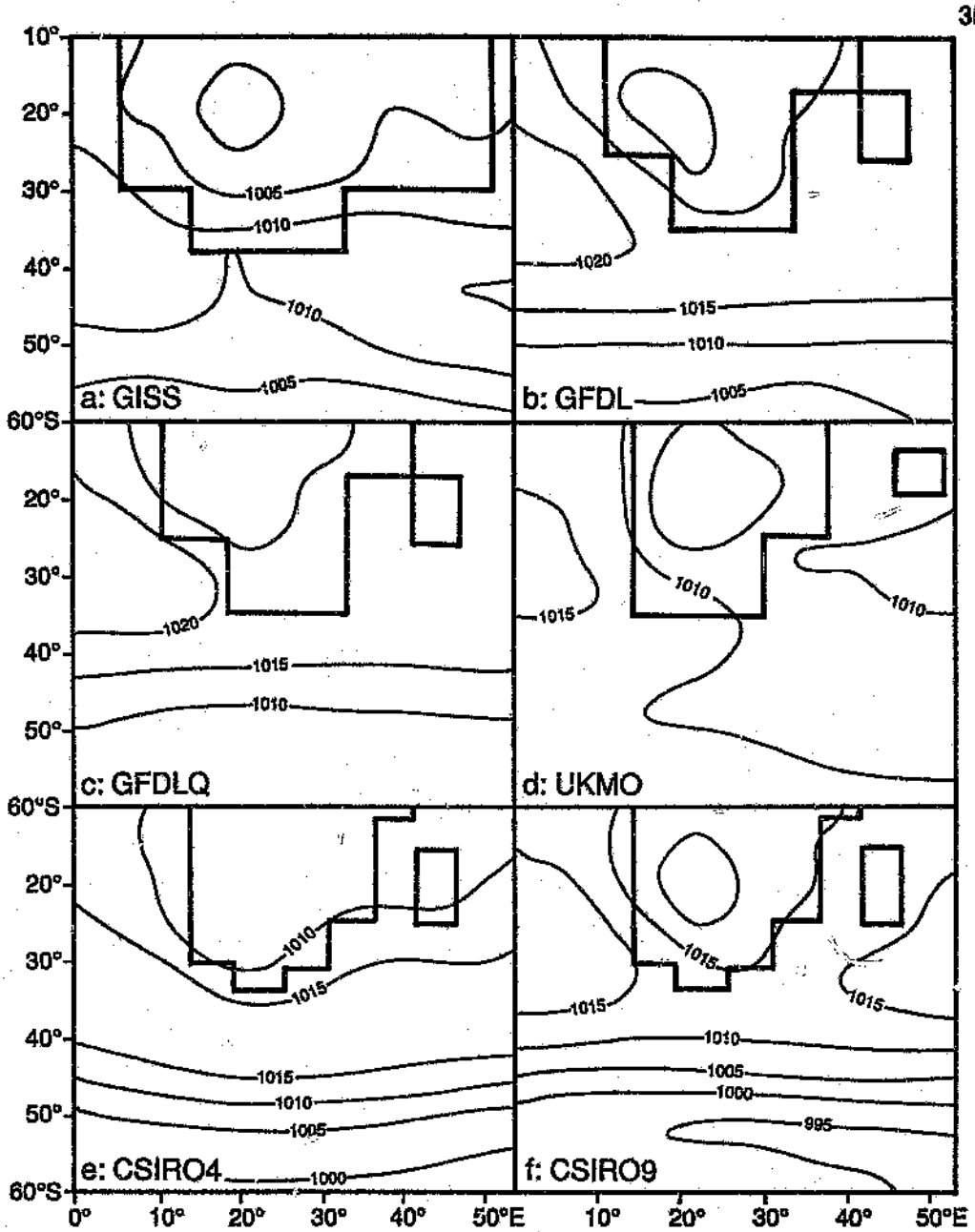

Figure 3.5: Simulated 1 x CO_2 January mean sea level pressure for the GISS (a), GFDL (b), GFDLQ (c), UKMO (d), CSIRO4 (e) and CSIRO9 (f) models (in hPa). The present-day January mean sea level pressure distribution is shown in Figure 1.2.

subtropical high pressure cells are generally displaced southward in response to the weaker meridional pressure and temperature gradients.

In contrast to each of these models, the two higher-resolution CSIRO simulations (Fig. 3.5e,f) achieve a better simulation of the pattern and

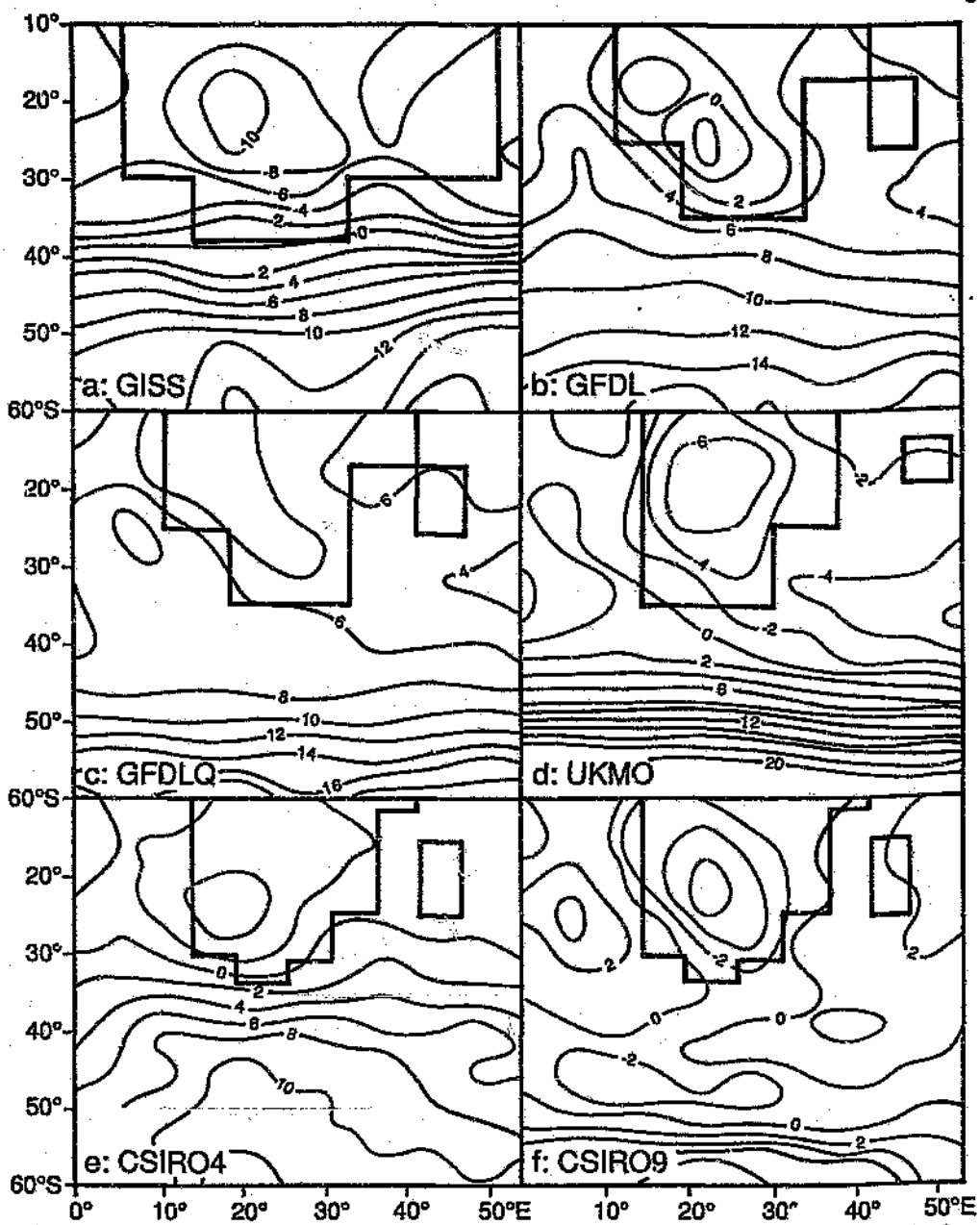

Figure 3.6: Calculated differences (simulation minus observed) for January mean sea level pressure for the GISS (a), GFDL (b), GFDLQ (c), UKMO (d), CSIRO4 (e) and CSIRO9 (f) models (in hPa).

magnitude of the observed distribution, simulating an improved poleward pressure gradient with lower overall (rms) errors (Table 3.3). Only the CSIRO models include a gravity wave drag term in the momentum equations. Of the two, the higher vertical resolution CSIRO9 model produces smaller high latitude (Fig. 3.6f) and overall (rms) errors (Table 3.3). Like the other models, both CSIRO models simulate lower than observed pressures over the

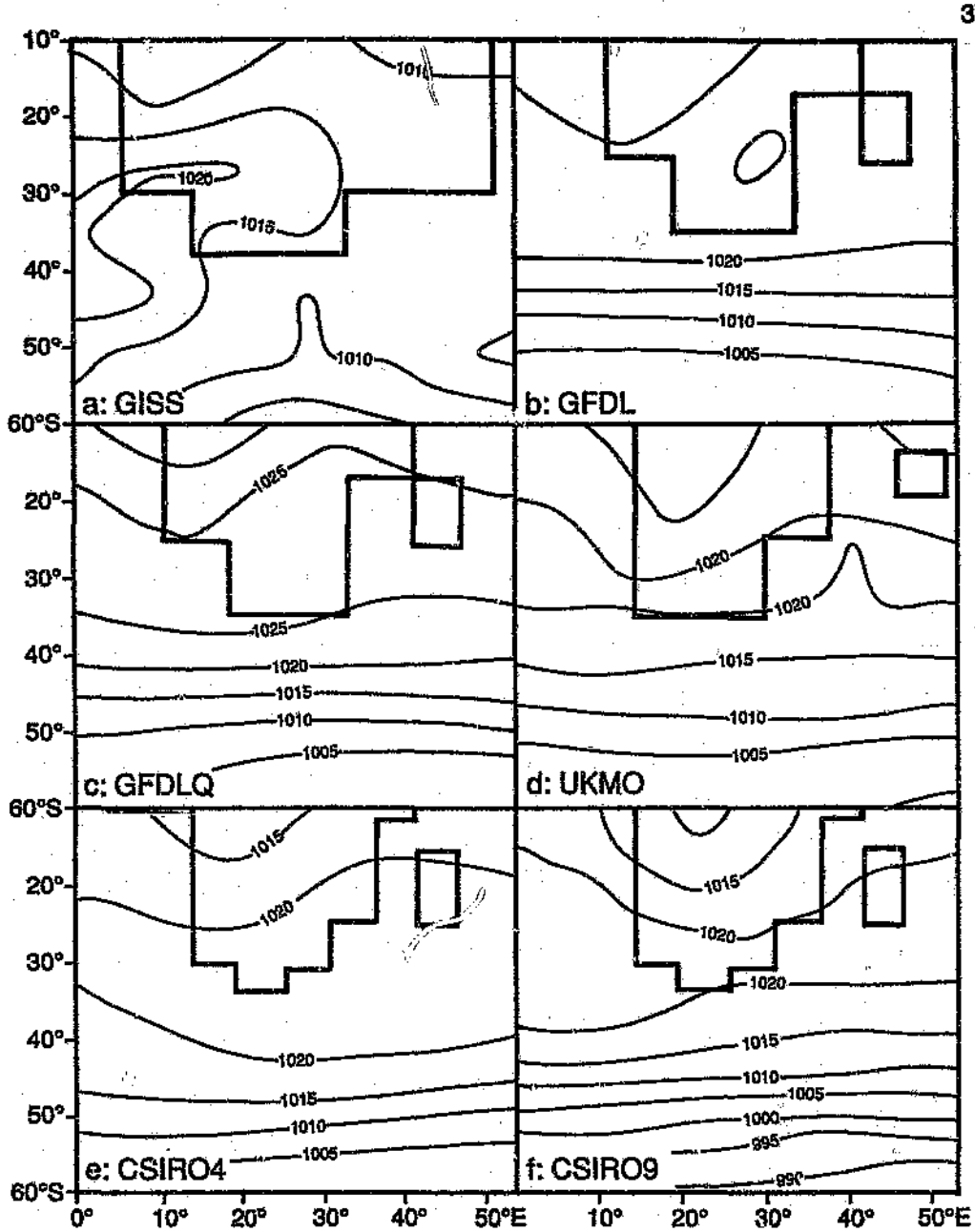

Figure 3.7: Simulated 1 x CO_2 July mean sea level pressure for the GISS (a), GFDL (b), GFDLQ (c), UKMO (d), CSIRO4 (e) and CSIRO9 (f) models (in hPa). The present-day January mean sea level pressure distribution is shown in Figure 1.2.

subcontinent, over-estimating the strength of the heat-low. The stronger heat low may be expected in association with the warmer than observed temperatures simulated by all models over the central and western subcontinent (see Fig. 3.2).

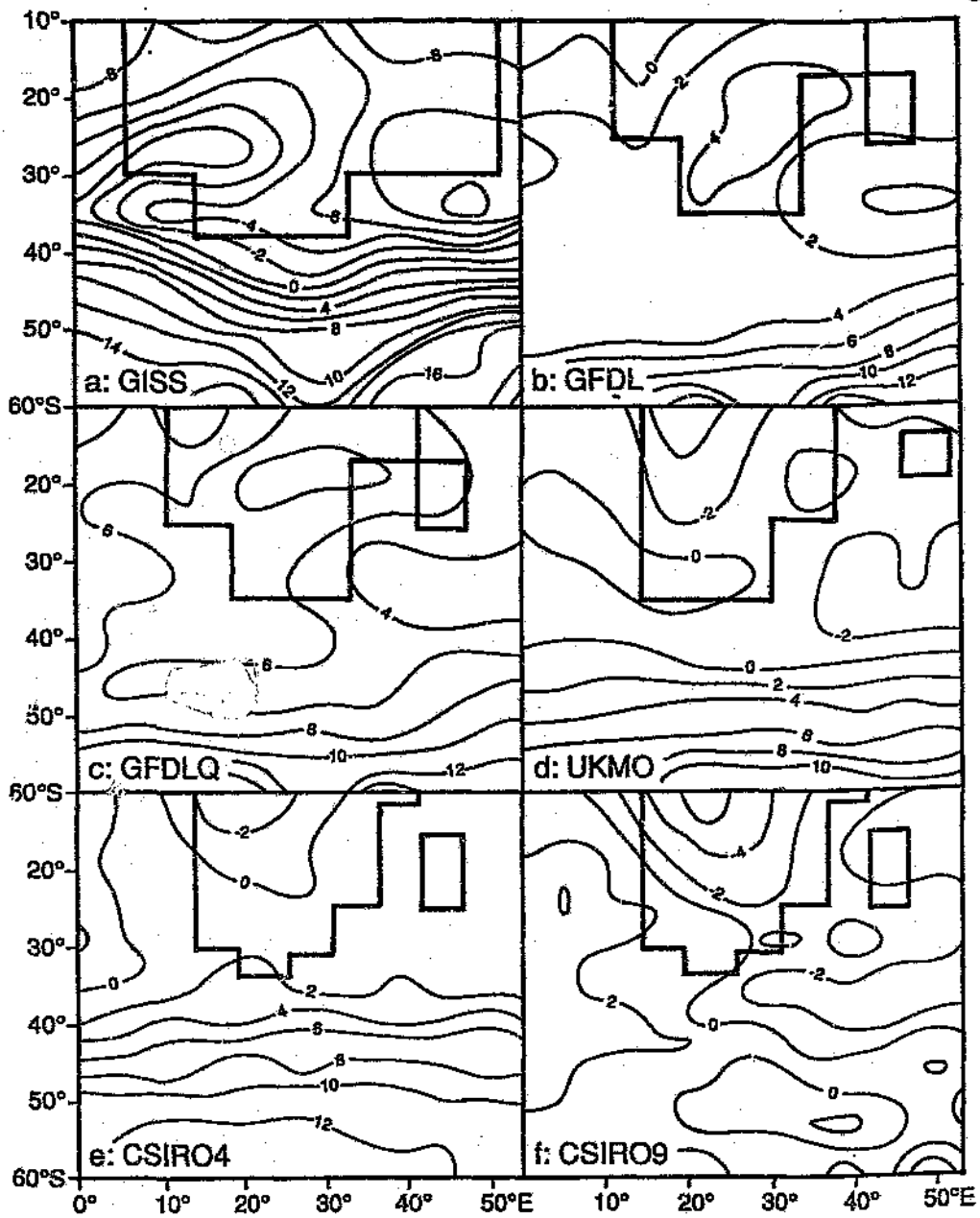

Figure 3.8: Calculated differences (simulation minus observed) for July mean sea level pressure for the GISS (a), GFDL (b), GFDLQ (c), UKMO (d), CSIRO4 (e) and CSIRO9 (f) models (in hPa).

In July, the GISS, GFDL and GFDLQ simulations remain poor, although the UKMO simulation improves markedly (Fig. 3.7a-c). The accurate simulation of pressures during July as opposed to January suggests that the UKMO model fails to simulate the mean sea level pressure distribution accurately in both hemispheres simultaneously (Boer *et al.*, 1991). Both CSIRO models simulate the observed pattern and magnitude of mean sea level pressures

Table 3.3: Pattern correlation coefficient (r) and root mean square (rms) error (in hPa) statistical intercomparison of observed and simulated mean sea level pressure. Significance of median differences between observed and simulated fields is calculated using the Wilcoxon matched pairs signed ranks test.

	JANUARY			JULY		
	r	rms error	signifi-cance	r	rms error	signifi-cance
GISS	0.20	9.85	30	0.32	11.32	7
GFDL	0.94	9.16	99	0.97	9.72	99
GFDLQ	0.95	6.62	99	0.97	8.73	99
UKMO	0.12	9.65	31	0.97	4.30	17
CSIRO4	0.90	5.33	99	0.96	6.64	99
CSIRO9	0.95	3.23	99	0.97	2.94	99

accurately (Table 3.3). The higher resolution CSIRO9 model simulates lower overall errors (Table 3.3) with smaller errors at higher latitudes than the CSIRO4 model (Fig. 3.8e,f).

Precipitation

The ability of the models to simulate the broad-scale features of rainfall seasonality over the subcontinent will be examined. Given that grid-point simulation of precipitation generally is known to be poor (Gates *et al.*, 1990, 1992), this approach represents a more reliable test of the models' ability to simulate regional precipitation patterns (Whetton and Pittock, 1991) than the approach adopted for surface air temperature and mean sea level pressure above.

Rainfall seasonality has been calculated as the October-March (summer) contribution to the annual rainfall total, expressed as a percentage (Fig. 3.9).

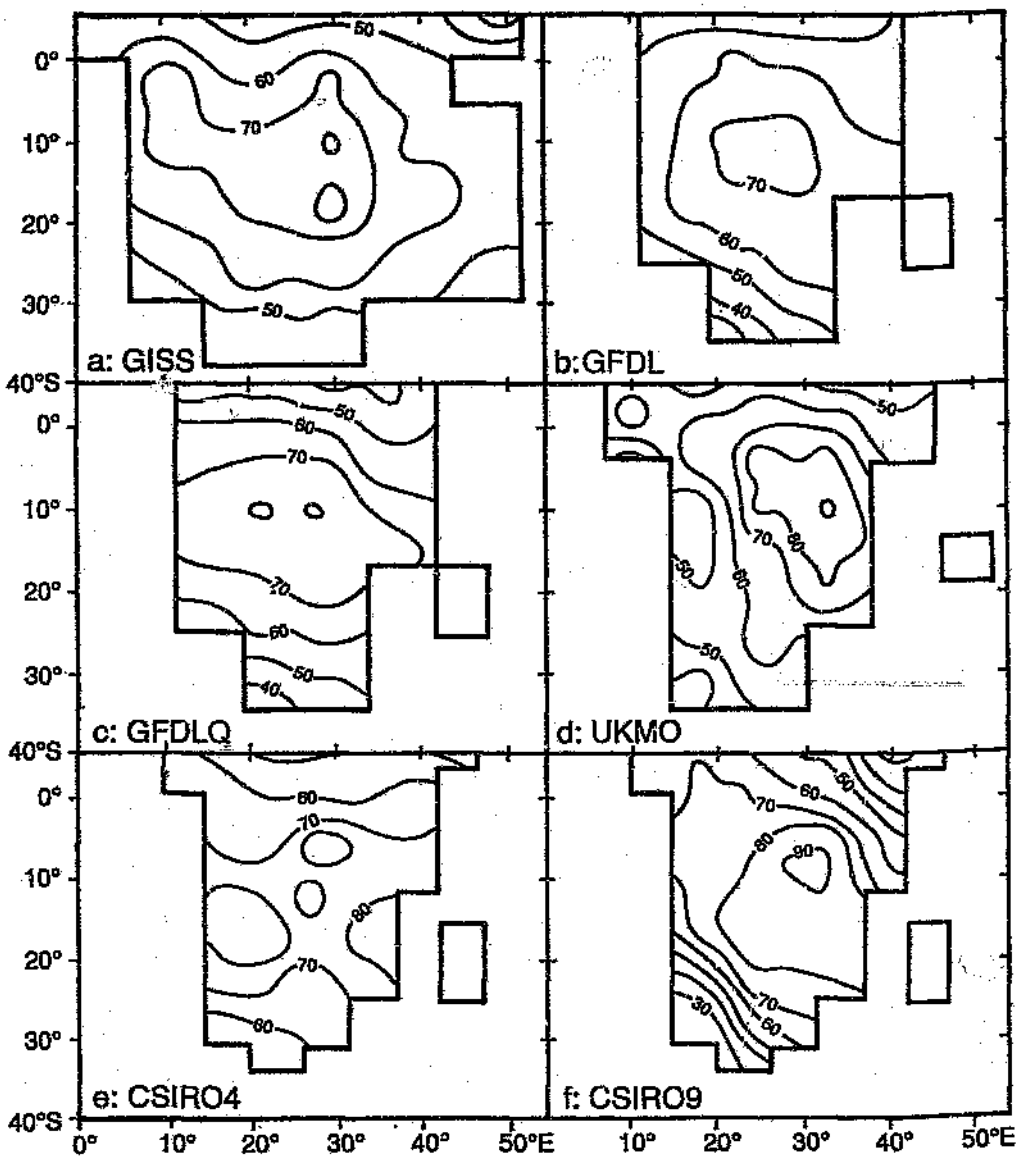

Figure 3.9: 1 x CO_2 simulations of the percentage contribution of summer season (October-March) to the annual rainfall total for the GISS (a), GFDL (b), GFDLQ (c), UKMO (d), CSIRO4 (e) and CSIRO9 (f) simulations. The present-day distribution is shown in Figure 1.6 (b).

Much of the central southern African subcontinent receives in excess of 70% of its rainfall in the summer half year (Fig. 1.6b). Only the south-western Cape region displays a winter rainfall maximum, receiving less than 40% of its rainfall during summer. Each of the GISS, GFDL, UKMO and CSIRO9 models (Fig. 3.9a,b,d,f) simulate the summer season rainfall maximum over the central

subcontinent adequately. The GFDLQ and CSIRO4 simulations (Fig 3.9c,e) of the summer maximum over the central subcontinent are less accurate than those of the other four models. The summer rainfall maximum simulated by the UKMO model over the western parts of subtropical Africa is smaller than observed (Fig. 3.9d). Summer season rainfall contributions within the tropics approximate observations well. The models also appear to simulate the sharp seasonal rainfall gradient between the summer and winter rainfall regions despite their coarse horizontal resolution.

To examine the simulation of precipitation for specific regions of the subcontinent, regional rainfall averages for three regions have been calculated. The regions have been defined on the basis of their annual rainfall regime, using land-based grid points only (Fig. 3.10). The first region is defined here as the *tropical rainfall region*, but includes only grid points north of 10°S. Rainfall in this region exhibits a semi-annual cycle (Tyson, 1986). The second region, referred to here as the *summer rainfall region*, includes most of the rest of the subcontinent and is characterised by an annual rainfall cycle with a well-defined summer rainfall maximum (Tyson, 1986, Fig. 1.6b). The third region is the *winter rainfall region* of the south-western Cape. Averages calculated for the winter rainfall region involve no more than two grid points in all cases and must therefore be interpreted with caution.

Monthly precipitation averages for the *tropical rainfall region* indicate that the models successfully simulate the semi-annual rainfall cycle (Fig. 3.11a). However, both daily precipitation rates and the amplitude of this semi-annual cycle are generally not well reproduced. The amplitude of the semi-annual cycle simulated by both the UKMO and CSIRO4 models is considerably larger than observed. The GISS, GFDL and CSIRO4 models simulate daily precipitation rates which exceed the observed rate throughout the year. The simulated precipitation rates for GFDLQ, UKMO and CSIRO9 models exceed observations during the summer months but are lower than observed during winter. In addition, the CSIRO9 semi-annual cycle is out of phase with observations, reaching its maxima a month earlier in both March and October.

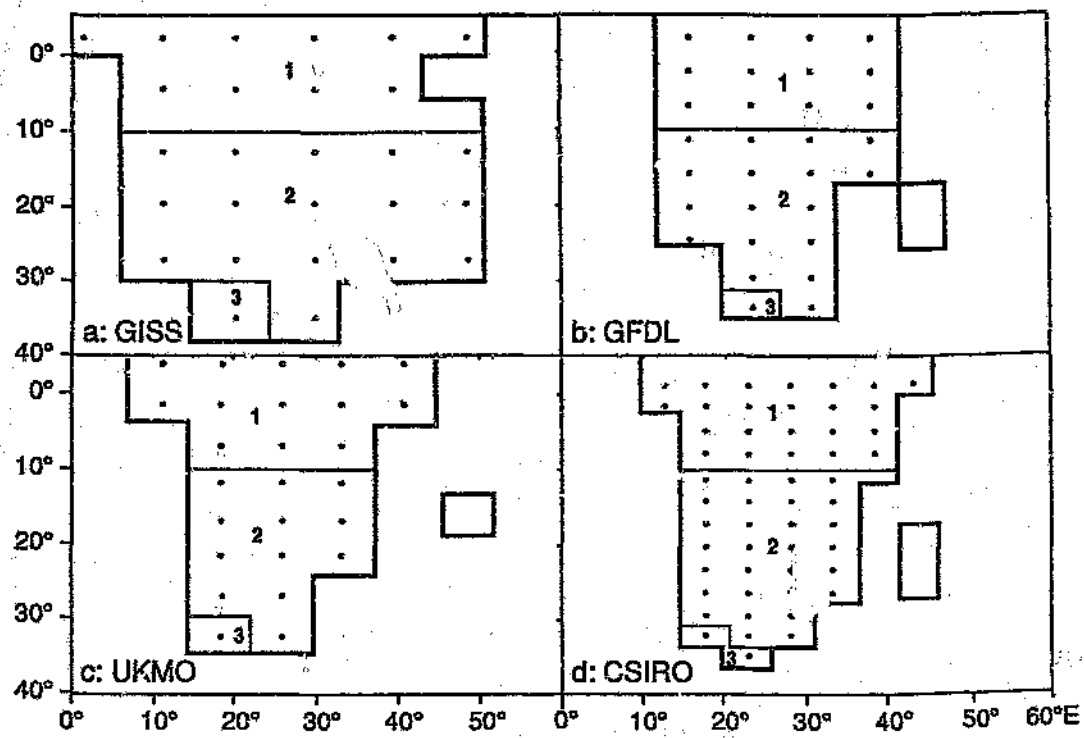

Figure 3.10: Map showing the division of model grid points into tropical (1), summer rainfall (2) and winter rainfall (3) regions for the GISS (a), GFDL (b), UKMO (c) and CSIRO9 (d) models. As model resolution does not change in either of the two GFDL and CSIRO models, only one map for each is shown.

Each of the models accurately simulates an annual rainfall cycle with a strong summer maximum for the *summer rainfall region* (Fig. 3.11b). the GISS and GFDL simulations under-estimate the amplitude of the annual cycle but simulate precipitation rates which exceed observations. Precipitation rates simulated by the CSIRO4 model exceed observations but the amplitude of the annual cycle is also over-estimated. The annual cycles simulated by the GFDLQ, UKMO and CSIRO9 models closely resemble observations, with a well-defined summer maximum. Of the models, the CSIRO9 simulation is closest to observations throughout the year.

The GISS, GFDL and GFDLQ models simulate higher than observed precipitation rates for the *winter rainfall region* with winter maxima three to six times that of the observations (Fig. 3.11c). By contrast, the UKMO, CSIRO4 and CSIRO9 models tend to under-estimate precipitation rates for this region. The annual cycle for this region is generally poorly simulated.

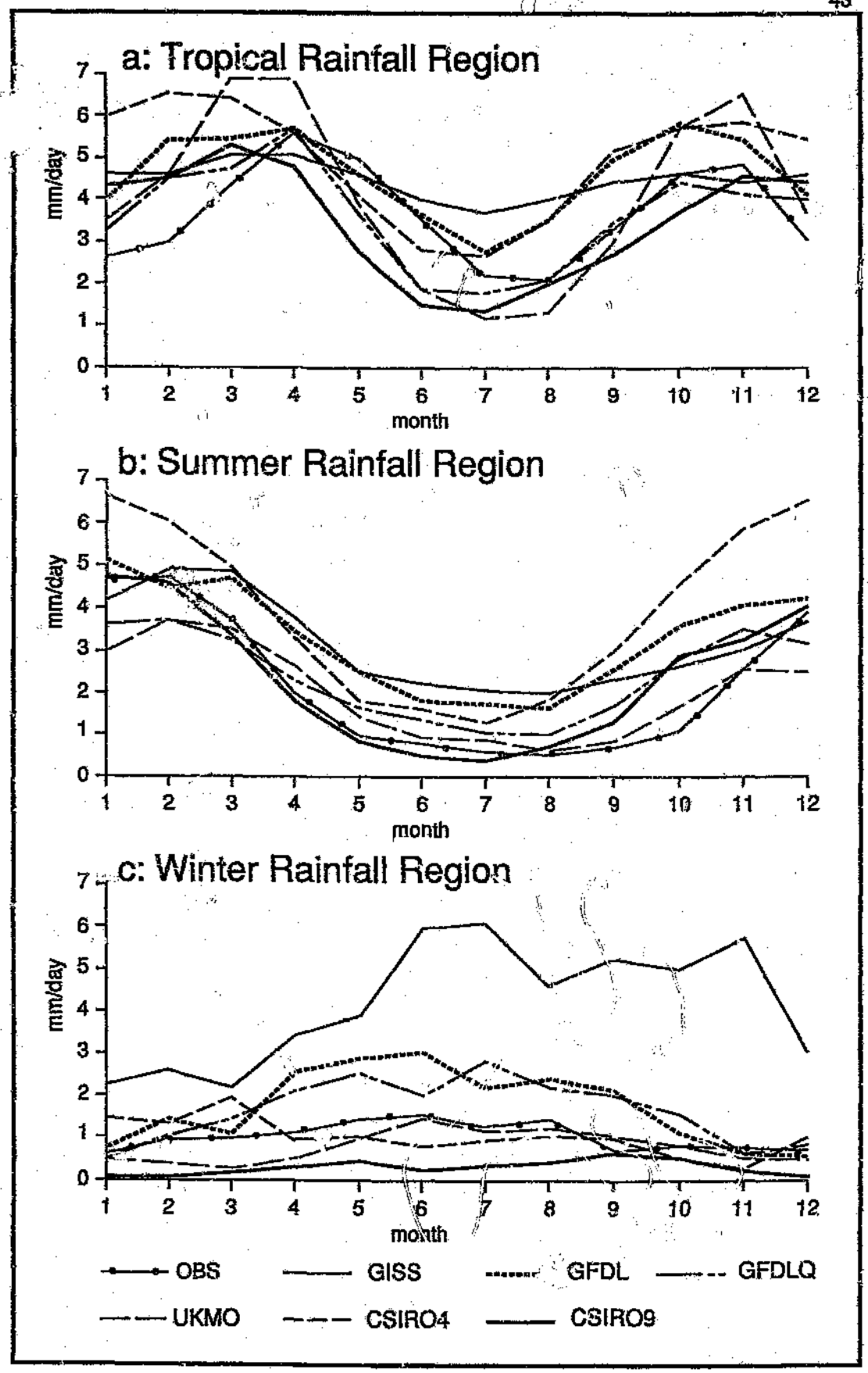

Figure 3.11: Comparison of observed and simulated monthly average precipitation rates for the tropical (*a*), summer (*b*) and winter (*c*) rainfall regions (defined in Fig. 3.10), in mm/day. Precipitation rates for the GISS,

Discussion

Regional climate simulations by the six early-generation general circulation models considered in this chapter are sensitive to the coarse spatial resolution and parameterisations of physical processes used in the models. Calculated errors in the simulation of southern African climate are generally characteristic of those reported elsewhere for this generation of mixed-slab ocean equilibrium climate models (Gates *et al.*, 1990; 1992).

The simulation of southern African surface air temperatures is in good agreement with simulations by the same models for the Australian region (Whetton and Pittock, 1991). The Australian study (completed prior to the 1992 release of the CSIRO9 model) also demonstrated large errors in both the 1987 GFDL and 1988 GFDLQ simulations and concluded that the 1984 GISS, 1987 UKMO and 1990 CSIRO4 simulations were more reliable for that region. Over southern Africa the GISS, UKMO and CSIRO9 models simulate the surface air temperature distribution over the subcontinent most accurately. The increased vertical resolution of the 9-level CSIRO model over its 4-level predecessor results in a markedly improved simulation. All three models combine relatively fine vertical resolution with parameterisations of convection appropriate to the strong vertical uplift and latent heat release associated with cumulus convection in the region. The penetrative convection scheme used by the GISS and UKMO simulations and the moist convective adjustment modified to generate a mass flux (Arakawa, 1972) used by the CSIRO9 model result in more accurate surface air temperature simulations than the simpler moist convective adjustment (Manabe *et al.*, 1965) used in the GFDL and GFDLQ models.

During January, however, when summer convective activity is predominant over the subcontinent, the pattern and magnitude of surface air temperatures are poorly simulated by all the models. The cumulus parameterisation schemes used by each of the GISS, UKMO and CSIRO9 models are, however,

apparently more appropriate to the strong vertical uplift and latent heat release associated with cumulus convection in the southern African region. Although the models do not represent the surface air temperature distribution precisely, they do capture the net effect of radiative forcing of temperature by cumulus clouds more accurately than the GFDL and GFDLQ models. The poor simulation of surface air temperature during summer is strongly contrasted against the marked improvement during winter (in the absence of convective cloud formation) observed for all models. There is no corresponding improvement in the magnitude of temperatures during winter, possibly related to errors in the specification of the annual cycle in solar radiation in the models.

The failure of the 1987 GFDL and 1988 GFDLQ models is more notable due to the fact that 0.99 sigma level temperatures, and not surface temperatures were used here. The formulation of the GFDL models is such that model surface temperature poorly reflects surface air temperatures over land (following Whetton and Pittock, 1991). The large simulation errors calculated for the 0.99 sigma level may be expected to be even larger if values for the surface were used. The models also do not incorporate a diurnal cycle. Diurnal temperature ranges over the subcontinent may exceed annual ranges (Lindesay, 1994) and therefore the absence of a diurnal cycle represents an important shortcoming in the GFDL model over the southern African region.

Marine air temperatures are generally well simulated in both January and July by all models. The Q-flux procedure incorporated in all except the GFDL simulations successfully constrains sea surface temperatures, and hence the marine air temperature distribution, to observed values. Characteristic errors at high latitudes are related to errors in the simulation of sea-ice albedo feedbacks (Mitchell, 1989). More recent fully coupled ocean-atmosphere models (Cubasch *et al.*, 1993; Manabe *et al.*, 1991, 1992; Meehl *et al.*, 1993; Stouffer *et al.*, 1989; Washington and Meehl, 1989) have demonstrated reduced high latitude warming due to the formation of oceanic deep water in these simulations.

As a general criticism of surface air temperature simulations by this generation of models, the treatment of cloud feedback processes in this generation of models represents a major area of uncertainty in regional surface air temperature simulations (Cess *et al.*, 1990; Harrison *et al.*, 1990). By diagnosing the presence of cloud directly from the relative humidity, and fixing cloud optical properties, the radiative forcing of temperature by clouds is simplistically treated (Harrison *et al.*, 1990). More recent mixed-layer slab-ocean models have incorporated cloud feedback processes based on variable cloud water content (for example, Mitchell *et al.*, 1989) and therefore explicitly simulate cloud microphysical processes more realistically (Mitchell *et al.*, 1990).

The simulated mean sea level pressure distribution is a powerful test of a model's ability to simulate the atmospheric circulation near the earth's surface (Gates *et al.*, 1990). Characteristically, atmospheric GCMs linked to mixed-layer slab oceans fail to simulate the equator-to-pole pressure gradient accurately. An error common to several models is an inability to simulate the deep Antarctic trough (Boer *et al.*, 1991). This is related to the coarse spatial resolution of most models and the inaccurate simulation of surface stress needed to balance the large-scale momentum flux from the source regions associated with tropical easterlies to the sink regions in the extratropical westerlies (Boer *et al.*, 1991). Surface stress is parameterised by means of a drag coefficient in the momentum equations. The models considered here generate additional drag in order to balance momentum over the continental landmasses of the northern hemisphere. In the southern hemisphere, the much reduced percentage of landmass in comparison to the northern hemisphere has the effect of reducing the meridional pressure gradient and hence near-surface wind and pressure fields, resulting in the poor simulation of the Antarctic trough. Inclusion of a gravity wave drag term in the momentum equations improves the parameterisation of surface stress and leads to a more accurate simulated pressure distribution (Boer *et al.*, 1991). More recent equilibrium climate simulations also using mixed-layer slab-ocean models, which include both increased horizontal resolution and a gravity wave drag parameterisation, estimate present conditions which are similar to those simulated by the CSIRO9 model (see for example, Mitchell,

et al., 1989). More realistic simulations of the Antarctic trough may, however, be accompanied by poor simulations of tropical and extratropical pressure distributions. Models which simulate the pressure distribution in particular hemispheres accurately often fail to simulate an accurate mean sea level pressure distribution in both hemispheres simultaneously (Boer *et al.*, 1991), as is apparently the case for the UKMO model. Simulated pressures over the subcontinental interior are generally lower than observed, indicating a stronger than observed simulated heat low. The error occurs as a result of the higher than observed temperatures simulated in the same region.

The coarse-resolution GISS, GFDL, GFDLQ and UKMO models all fail to reproduce the poleward pressure gradient and deep Antarctic trough accurately. None of these models includes a gravity wave drag term. Both the CSIRO4 and CSIRO9 models have the finest horizontal resolution of the models considered here and include a gravity wave drag term. Of these, the higher vertical resolution CSIRO9 simulation is more accurate than the earlier 4-level model and produces the only simulation of mean sea level pressure which may be considered adequate for the southern African region.

The simulation of precipitation represents a link between the moisture, thermodynamic and dynamic equations within a GCM (Boer *et al.*, 1991). The coarse horizontal and vertical resolution of these GCMs means that local convective events, which are limited in spatial extent and characterised by strong vertical uplift, must be parameterised at sub-grid-scales. The mis-matching of scales between GCM grid cells and individual convective events causes the finer details of observed precipitation means, frequencies and intensities to be lost (Gordon *et al.*, 1992; Whetton *et al.*, 1993).

The grid-point simulation of precipitation amount is generally known to be poor (Gates *et al.*, 1992). However, the failure of a model to simulate adequately the pattern of rainfall seasonality over the subcontinent represents a more serious shortcoming than errors in simulated precipitation amount (Whetton and Pittock, 1991). Errors in the simulation of precipitation amount may be related to the poor representation of topography by the model and the grid-point parameterisation of cumulus convection. However, the successful

simulation of the annual pattern of rainfall seasonality for a region indicates the ability of a model to reproduce accurately the response of rainfall patterns to large-scale circulation changes associated with the annual cycle of radiation. Accurate simulation of rainfall seasonality provides greater confidence in simulated rainfall changes caused by smaller changes in radiation associated with doubling of atmospheric CO_2 (Whetton and Pittock, 1991).

Each of the models considered here simulates the broad-scale pattern of rainfall seasonality over the subcontinent acceptably well, reproducing the annual summer rainfall maximum over the central and western regions. In the case of the UKMO simulation, where the summer rainfall maximum does not extend as far west as observed, the error is related to the weaker than observed simulation of the west African monsoon (Wilson and Mitchell, 1987). Average daily rainfall simulations for three regions over the subcontinent indicate that the models successfully simulate the semi-annual cycle over the tropics and annual cycles in both the summer and winter rainfall regions. However, all the models generally fail to simulate average monthly precipitation rates accurately and perform inconsistently over all three regions. For example, while the CSIRO9 model provides fairly accurate estimates of rainfall amounts over the summer rainfall region, this is not true over the winter rainfall region. In the tropics, the CSIRO9 model under-estimates precipitation and simulates a semi-annual rainfall cycle that is one month out of phase with observations.

The parameterisation of precipitation processes, particularly that of convection, is specific to each individual model. It is for this reason that the simulation of regional precipitation patterns differ significantly from model to model. As far as is possible therefore, the aim of developing reliable simulations of present-day precipitation and predictions of regional precipitation change is well served by considering a wide range of models (Whetton *et al.*, 1993). For this reason, four simulations of precipitation have been selected as being acceptable for southern Africa. The GISS, GFDL, UKMO and CSIRO9 simulations all reproduce the summer rainfall maximum over the central subcontinent and a winter rainfall region to the south-west.

Despite the failure of these models to simulate regional precipitation amounts reliably, they are considered acceptable due to their accurate simulation of the pattern of rainfall seasonality over the subcontinent.

The assumption is made in this dissertation that models which simulate the observed regional climate accurately will be more reliable in their simulations of future regional climate under doubled CO_2 conditions. It should be emphasised, however, that the results of this validation apply specifically to the particular early-generation GCM simulations available for this study. The procedure developed here may be extended in future to include a validation of the simulation of present-day inter-annual variability for the southern African region. In addition, this analysis should be extended in future to include simulations of present-day conditions for the region by more recent fully-coupled ocean-atmosphere and transient (as opposed to equilibrium) climate models.

Accurate simulations of particular variables by individual models have been identified. These simulations will be considered for future climatic change under doubled CO_2 conditions in Chapter 4. With respect to all three variables assessed, the CSIRO9 model gives the best overall simulation of present-day southern African climate of all the models. The model combines both fine spatial resolution and adequate parameterisation of key physical processes and consistently provides the most accurate simulation of present-day conditions over the southern African region.

****

The simulations of present-day surface air temperature, mean sea level pressure and precipitation using six early-generation general circulation models have been assessed for southern Africa. Accurate simulations of particular variables by individual models have been identified. The GISS, UKMO and CSIRO9 simulate present-day surface air temperatures accurately. Only the CSIRO9 simulation of mean sea level pressure is considered adequate. The simulated patterns of rainfall seasonality over the subcontinent by the GISS, GFDL, GFDLQ and CSIRO9 models are acceptable.

The CSIRO 9-level model combines relatively fine spatial resolution with adequate parameterisation of key physical processes and consistently provides the most accurate simulation of present-day conditions over the southern African region. These simulations will be considered for future climatic change under doubled CO_2 conditions in *Chapter 4*.

CHAPTER 4

FUTURE CLIMATIC CHANGE

Introduction

All the models that have been considered in this dissertation are early-generation equilibrium climate models. The models are initially run to a statistical equilibrium at current CO_2 levels. These levels are then instantaneously doubled to simulate a climatic perturbation due to increased levels of greenhouse gases, and the model is allowed to re-establish equilibrium. Climatic change is estimated as the difference between the equilibrium climates under present and doubled CO_2 concentrations. The models display considerable agreement concerning the broad-scale features of global climatic change. However, less agreement exists between models for predictions of future conditions for individual regions of the globe.

In the previous chapter, accurate simulations of present-day southern African climate by particular models were identified. Only those models shown in Chapter 3 to be reliable for southern Africa will be used in this chapter to estimate possible future conditions consequent upon a doubling of carbon dioxide. This procedure allows predictions of future conditions for this region to be interpreted with greater confidence. For surface air temperature changes, the 1984 GISS, 1987 UKMO and 1992 CSIRO9 models are appropriate. For mean sea level pressure, only the CSIRO9 model is adequate. For possible changes in precipitation, the GISS, 1987 GFDL, UKMO and CSIRO9 models will be used.

Results

Surface Air Temperature

Widespread temperature increases in both January and July under doubled CO_2 conditions are predicted for the southern African region (Fig. 4.1) by the GISS, UKMO and CSIRO9 models (temperature increases predicted by the GFDL, GFDLQ and CSIRO4 models are given in Appendix B). In both January and July, the consensus between the models is for a warming of between 4°C and 6°C for the region as a whole (Table 4.1). Estimated temperature increases for all models are highly significant (at the 99 percent confidence level). For the CSIRO9 model, grid point t-tests indicate that simulated temperature increases in both January (Fig. 4.1e) and July (Fig. 4.1f) are highly significant throughout the region, with field significance exceeding 99.9 percent (Table 4.1).

Table 4.1: Overall temperature change for the southern African region as a whole (under doubled CO_2 conditions) expressed as a root mean square error (in °C). Median differences between 1 x CO_2 and 2 x CO_2 simulations for the GISS and UKMO simulations is calculated using the Wilcoxon matched pairs signed ranks test. For the CSIRO9 simulation, statistical field significance is indicated.

	JANUARY		JULY	
	rms error	signifi-cance	rms error	signifi-cance
GISS	4.06	99	4.27	99
UKMO	5.35	99	5.75	99
CSIRO9	4.11	99	4.94	99

Within the tropics, warming may generally be expected to be lower than either the global or regional average, varying little with the season (Fig. 4.1). The

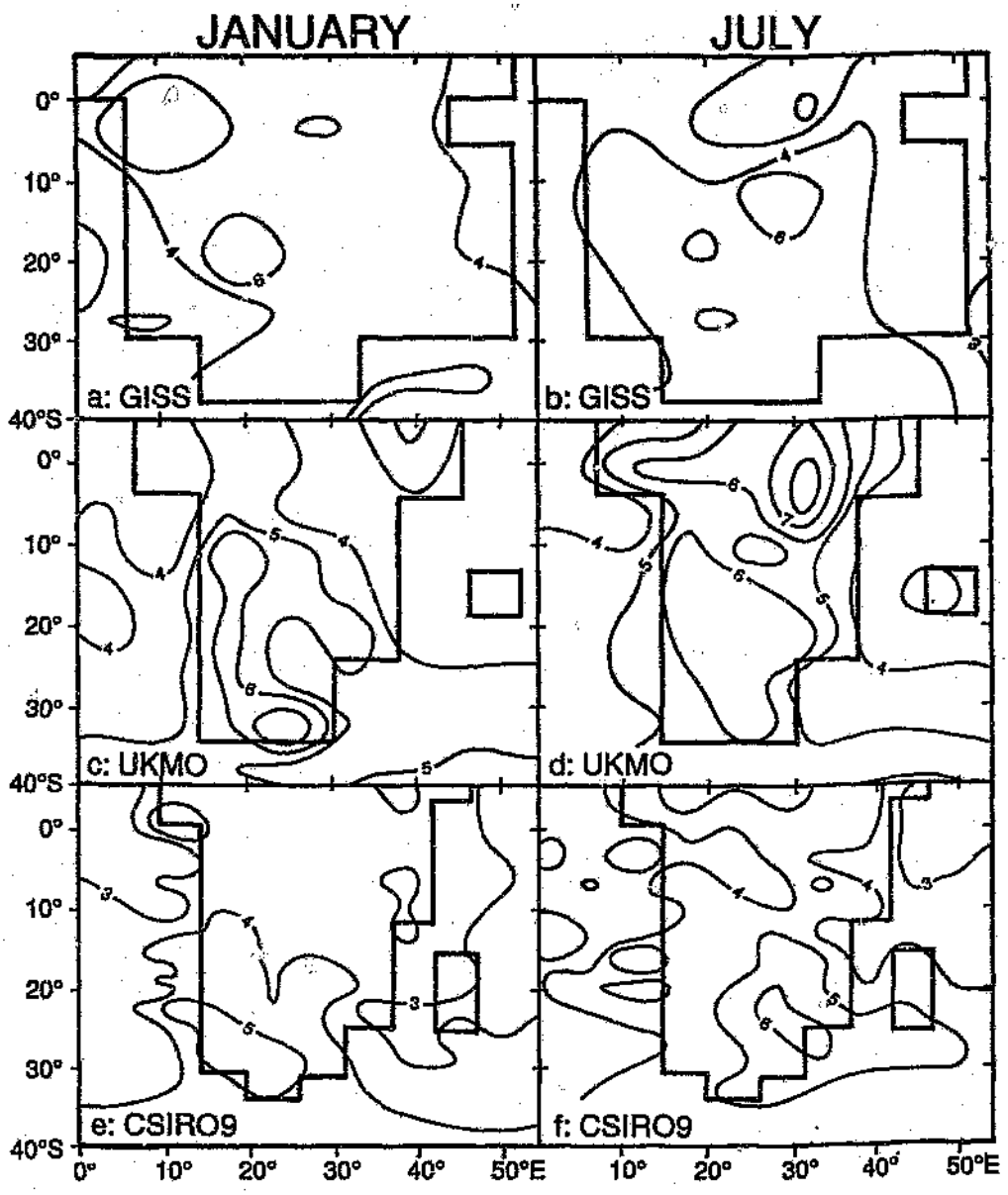

Figure 4.1: Calculated surface air temperature differences (2 x CO_2 minus 1 x CO_2) in January and July for the GISS (a,b), UKMO (c,d) and CSIRO9 (e,f) models, respectively (in °C). Temperatures differences for the CSIRO9 model are highly significant (above the 99 percent confidence level) throughout the region and are therefore not shaded.

GISS and CSIRO9 models suggest warming of 2°C to 4°C in both January (Fig. 4.1a,e) and July (Fig. 4.1b,f). In contrast, the UKMO model (Fig. 4.1c,d) predicts that warming may be as high as 4°C to 6°C. Over the drier areas of the central subcontinent predicted temperature increases are larger than within the

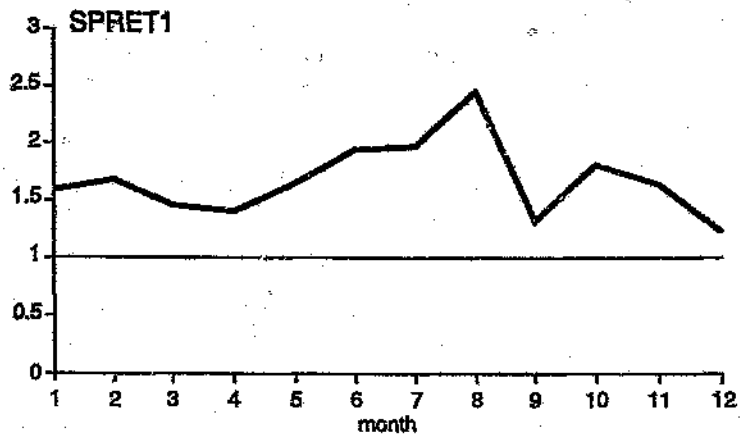

Figure 4.2: The ratio of spatially-averaged time variances for the CSIRO9 present-day and doubled CO_2 surface air temperature fields (SPRET1) over the full southern African region and for the full annual cycle.

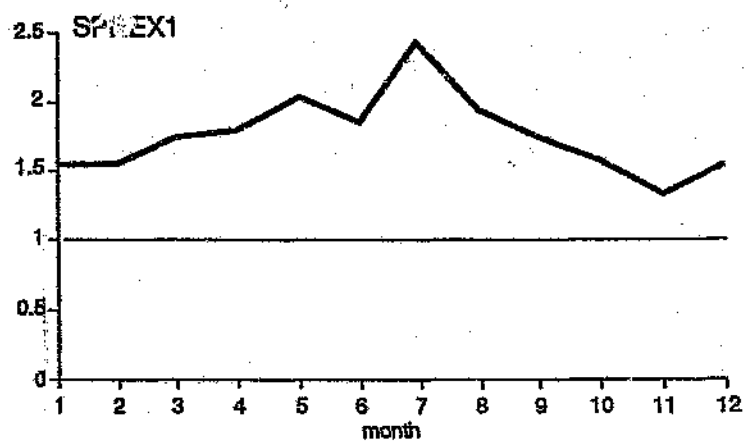

Figure 4.3: The ratio of time-averaged spatial variances for the CSIRO9 present-day and doubled CO_2 surface air temperature fields (SPREX1) over the full southern African region and for the full annual cycle.

tropics or the adjacent oceans. In January, the range of predicted temperature increase is 4°C to 5°C for the GISS and CSIRO9 models over the central subcontinent. Temperature increases in mid-winter are generally larger than in mid-summer over the central subcontinent, with estimates in July by all

three models exceeding 6°C. As in the tropics, temperature increases predicted by the UKMO model (in excess of 6°C in both January and July) are larger than predictions by either the GISS or CSIRO9 models.

Over the oceanic areas to the south of the subcontinent, all models simulate large temperature increases (in excess of 5°C) throughout the year (Fig. 4.1). As over the central subcontinent, predicted temperature increases are also larger in mid-winter than in mid-summer (Fig. 4.1). In July, predicted temperature increases south of 40°S by the UKMO and CSIRO9 models are greater than 7°C, exceeding 10°C south of 60°S.

Possible future changes in temporal and spatial *variability* of surface air temperature have been estimated using ten years of simulated data for both present-day and doubled CO_2 conditions for the CSIRO9 model. Changes in inter-annual variability of surface air temperature are estimated from the ratio of the spatially-averaged time variances of the present-day and doubled CO_2 fields (the SPRET1 statistic of Wigley and Santer, 1990, given in Appendix A). A ratio greater than unity represents lower temporal variability in the doubled CO_2 than in the present-day simulation (and *vice versa*). Changes estimated by the CSIRO9 model indicate that inter-annual surface air temperature variability may be expected to decrease over the southern African region under doubled CO_2 conditions (Fig. 4.2).

Changes in spatial variability are estimated using the ratio of the time-averaged spatial variances of the present-day and double CO_2 fields (the SPREX1 statistic of Wigley and Santer, 1990, given in Appendix A). A ratio greater than unity again indicates a decrease in spatial variability under doubled CO_2 conditions (and *vice versa*). As with changes in temporal variability, spatial variability of the surface air temperature field in the CSIRO9 model may be expected to decrease under doubled CO_2 conditions (Fig. 4.3). This is so throughout the year, with the decreases being strongest during the winter months.

Mean sea level pressure

Changes in mean sea level pressure during both January and July predicted by the CSIRO9 model (Fig. 4.4) indicate a decrease in pressure over the subcontinent and adjacent oceans, with a band of increased pressure over the southern oceans (estimated changes by the GISS, GFDL, GFDLQ, UKMO and CSIRO4 models are given in Appendix C). Estimated pressure changes indicate a weakening of both the subtropical anticyclones adjacent to the subcontinent and the mid-latitude westerly circulation to the south. Grid-point decreases in pressure in tropical and subtropical latitudes are generally significant at the 95 percent level in both January and July (Fig. 4.4a,b). However, pressure increases at higher latitudes are significant in January (Fig. 4.4a) but not in July (Fig. 4.4b). The pattern of mean sea level pressure change is field significant (above 95%) in January, but not in July.

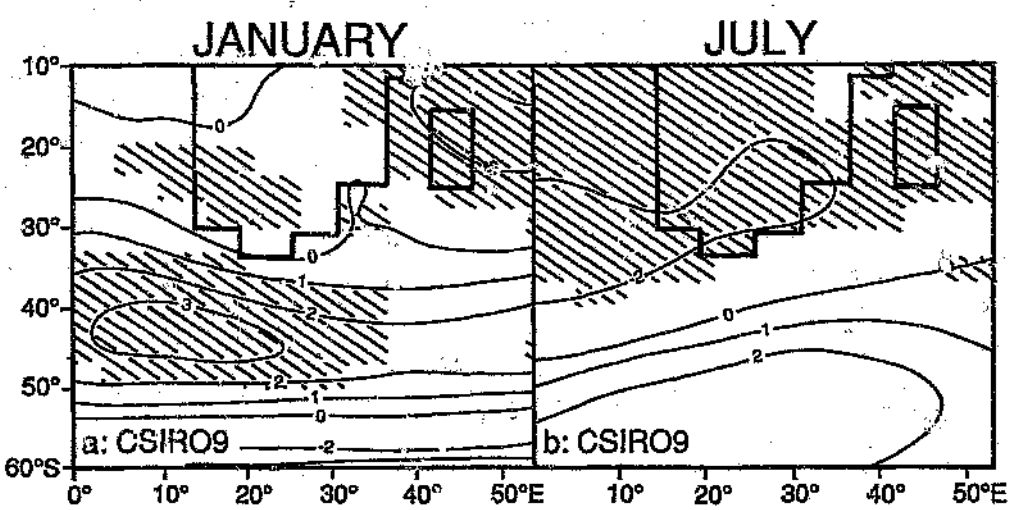

Figure 4.4: Changes in mean sea level pressure (2 x CO_2 minus 1 x CO_2) in January (a) and July (b) simulated by the CSIRO9 model. Changes significant at the 95% level (using a t-test) are shaded.

The CSIRO9 model does not indicate any large changes in temporal and spatial variability over southern Africa under doubled CO_2 conditions. Differences in temporal variability are expected to be small, with few locally-significant (grid-point) differences in temporal variance at either the 1% or 5% level (Fig. 4.5, calculated using the NF1 and NF5 statistics of Wigley and

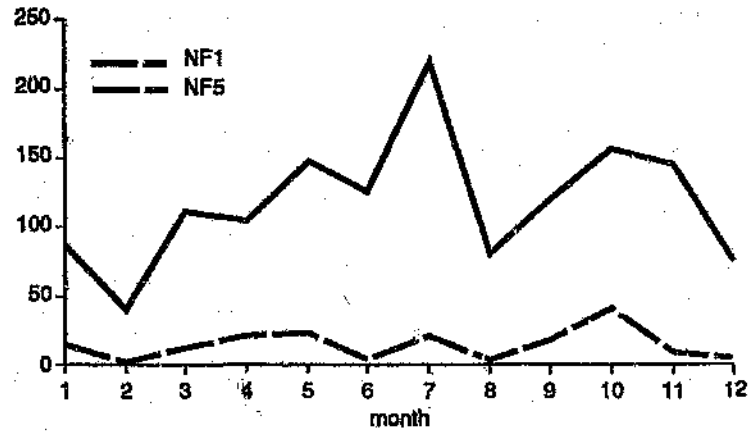

Figure 4.5: Changes in temporal variability, estimated using the number of locally significant two-tailed 1% (NF1) and 5% (NF5) F-tests (after Wigley and Santer, 1990), for future mean sea level pressure conditions simulated by the CSIRO9 model. The results indicate the number of successful tests at a given significance level out of a total of 1000 tests performed.

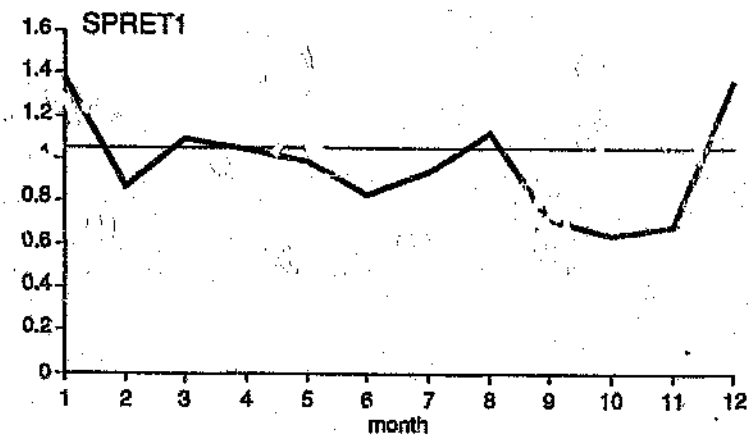

Figure 4.6: The ratio of spatially-averaged time variances for the CSIRO9 present-day and doubled CO_2 mean sea level pressure fields (SPRET1) over the full southern African region and for the full annual cycle.

Santer, 1990 and defined in Appendix A). The ratio of both spatially-averaged time variances (Fig. 4.6) and time-averaged spatial variances (Fig. 4.7) remain close to unity throughout the year. Both small increases and decreases in inter-annual and spatial mean sea level pressure variability may therefore be

expected throughout the year (Figs. 4.6 and 4.7). Such changes are not expected to be seasonally-dependent.

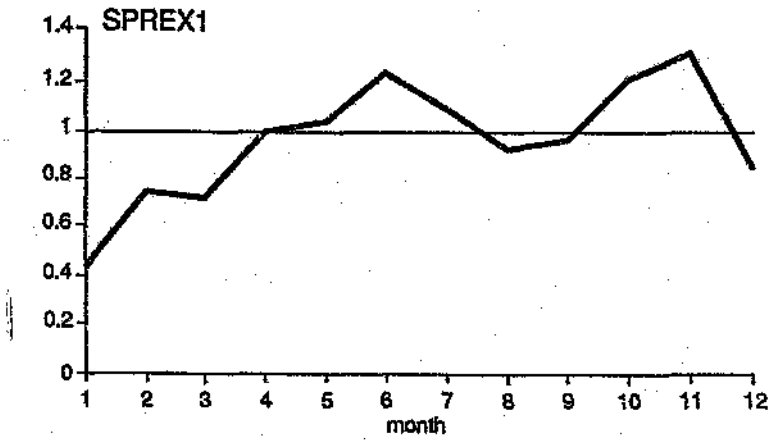

Figure 4.7: The ratio of time-averaged spatial variances for the CSIRO9 present-day and doubled CO_2 mean sea level pressure fields (SPREX1) over the full southern African region and for the full annual cycle.

Precipitation

Changes in seasonal precipitation during the January-March summer and July-September winter seasons indicate that none of the models predict spatially homogeneous changes over the subcontinent as a whole (Fig. 4.8). Furthermore, the GISS, GFDL, UKMO and CSIRO9 models display little inter-model agreement concerning predicted changes over all three of the *tropical*, *summer* and *winter* rainfall regions defined in Chapter 3 (predictions of regional precipitation change by the GFDLQ and CSIRO4 models are shown in Appendix D).

The *summer rainfall region* comprises most the southern African subcontinent. During both the January-March and July-September seasons, the pattern of precipitation change over much of the region is patchy. The GISS, GFDL, UKMO and CSIRO9 models all suggest locally-specific increases and decreases in precipitation across the region, but demonstrate little agreement concerning possible changes for the region as a whole. During the January to March season (Fig. 4.8a,c,e,g), precipitation may generally be

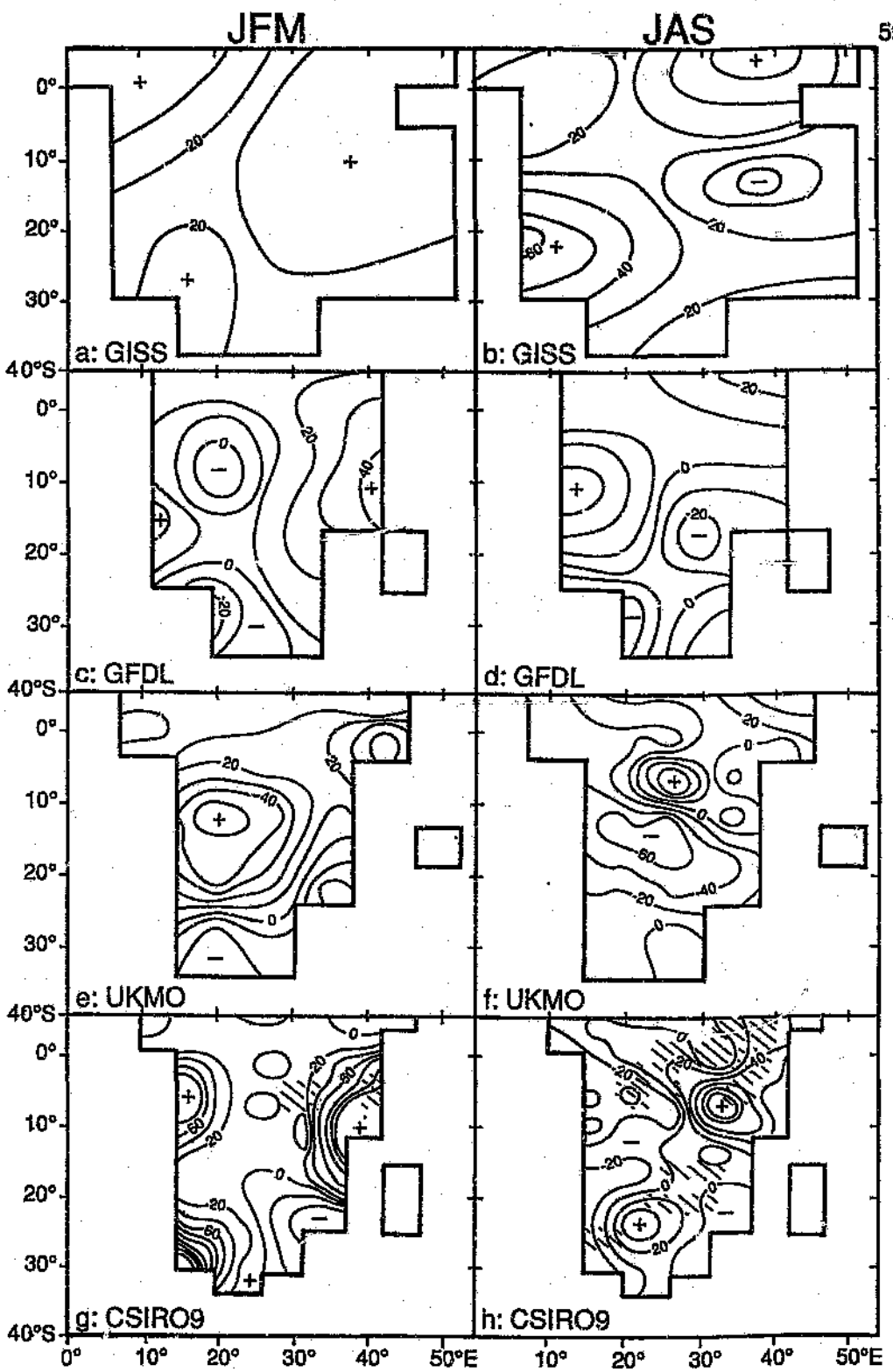

Figure 4.8: January-March (JFM) and July-September (JAS) seasonal changes in rainfall (doubled CO_2 minus present-day) for the GISS (a,b), GFDL (c,d), UKMO (e,f), and CSIRO9 (g,h) models, expressed as a percentage. For the CSIRO9 model, changes significant at the 95% confidence level are shaded.

expected to increase by 10 to 20 percent, with increases predicted by the UKMO and CSIRO9 models (Fig. 4.8e,g) exceeding 50 percent in certain areas. For the CSIRO9 model, changes in January-March rainfall are not field significant above the 95 percent confidence level, with only individual grid-point increases significant at this level (Fig. 4.8g). Precipitation averages for the region (Fig. 4.9) indicate that daily precipitation rates will increase throughout the summer months, with strongest increases in during the January-March period.

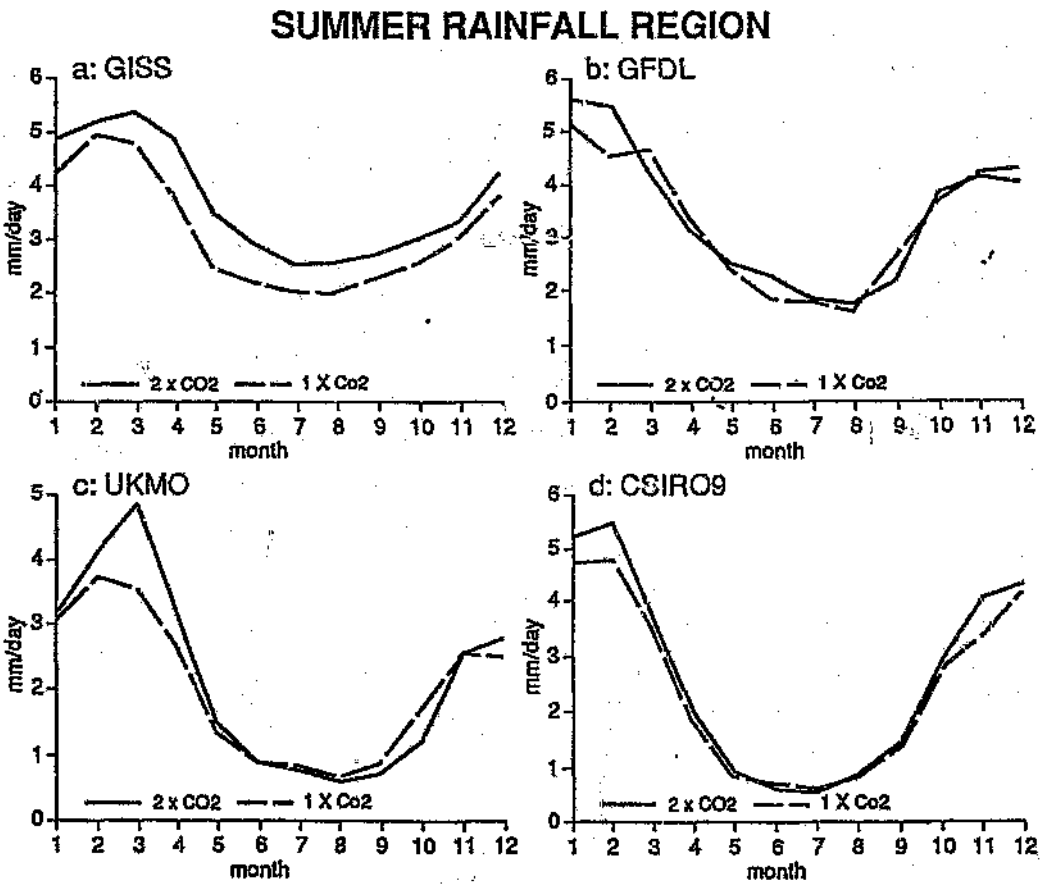

Figure 4.9: Simulated present-day and doubled CO_2 precipitation rates (in mm/day) for the GISS (a), GFDL (b), UKMO (c), and CSIRO9 (d) models over the summer rainfall region defined in Figure 3.10.

Locally-specific precipitation increases of approximately 20 percent are also predicted during the July-September season (Fig. 4.8b,d,f,h). As for January-March, few grid-point increases predicted by CSIRO9 model are significant (Fig. 4.8h), and precipitation changes are not field significant. The

increase predicted by the UKMO model (Fig. 4.8f) is again larger than for the other models. Regionally-averaged precipitation for the July-September period (Fig. 4.9) reflect the patchiness in the overall pattern of change over the summer rainfall region, indicating relatively small changes in average daily precipitation. Most models predict small decreases in average daily precipitation (less than 0.5 mm/day) during July-September but these changes are not expected to be significant as rainfall receipts remain low during winter and predicted changes do not represent a change in the strong summer rainfall maximum for the region.

The GISS, GFDL, UKMO and CSIRO9 models display greater consensus for predictions of precipitation change within the *tropical rainfall region* (north of 10°S). Predicted increases in precipitation of between 10 and 20 percent from all four models vary only slightly, both spatially and with the seasons (Fig. 4.8). Each of the models predicts regionally-averaged increases in daily precipitation in the order of 1 mm/day (Fig. 4.10). The GISS and GFDL models (Fig. 4.10a,b) predict increases throughout the year whilst the UKMO and CSIRO9 models (Fig. 4.10c,d) predict small decreases during the winter months. No change is expected in the semi-annual cycle of the tropical rainfall region, although the UKMO and CSIRO9 models predict that the amplitude of this cycle may increase.

Little consensus is achieved for estimates of change for the *winter rainfall region* of the south-western Cape (Fig. 4.8). As this region is represented by no more than 2 model grid points in any simulation, predicted changes are of necessity locally-specific and should be interpreted with circumspection. In the January-March season the GFDL and UKMO models (Fig. 4.8c,e) estimate decreases in precipitation of approximately 20 percent, while the GISS and CSIRO9 models (Fig. 4.8a,g) suggest that rainfall may increase (by in excess 100 percent in the CSIRO9 model). During July-September the GFDL, UKMO and CSIRO9 models (Fig. 4.8d,f,h) each predict decreases in rainfall of approximately 20 percent. In the case of the CSIRO9 model, this decrease is locally significant at the 95 % confidence level. In contrast, the GISS model (Fig. 4.8b) predicts an increase in seasonal rainfall of 20 to 30 percent. Regionally-averaged changes in daily precipitation for the region (Fig. 4.11)

are not well-defined, suggesting both small increases and decreases throughout the year. However, the UKMO and CSIRO9 models (Fig. 4.11c,d) both indicate daily precipitation increases in summer and decreases in winter. The predictions of precipitation increases in summer and decreases in winter by the UKMO and CSIRO9 models are in theoretical agreement with the southward shift in circulation systems predicted by these models, and, if correct, hold important implications for changes in rainfall seasonality over the south-western Cape.

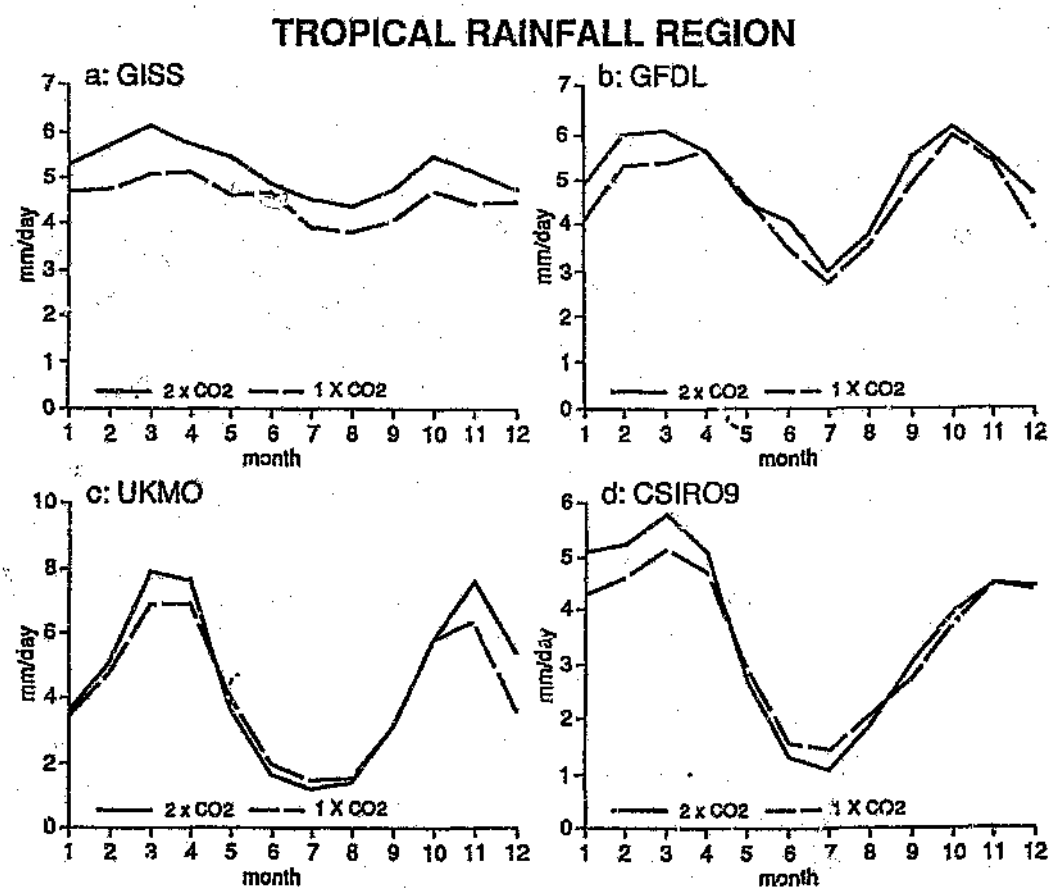

Figure 4.10: Simulated present-day and doubled CO_2 precipitation rates (in mm/day) for the GISS (a), GFDL (b), UKMO (c), and CSIRO9 (d) models over the tropical region defined in Figure 3.10.

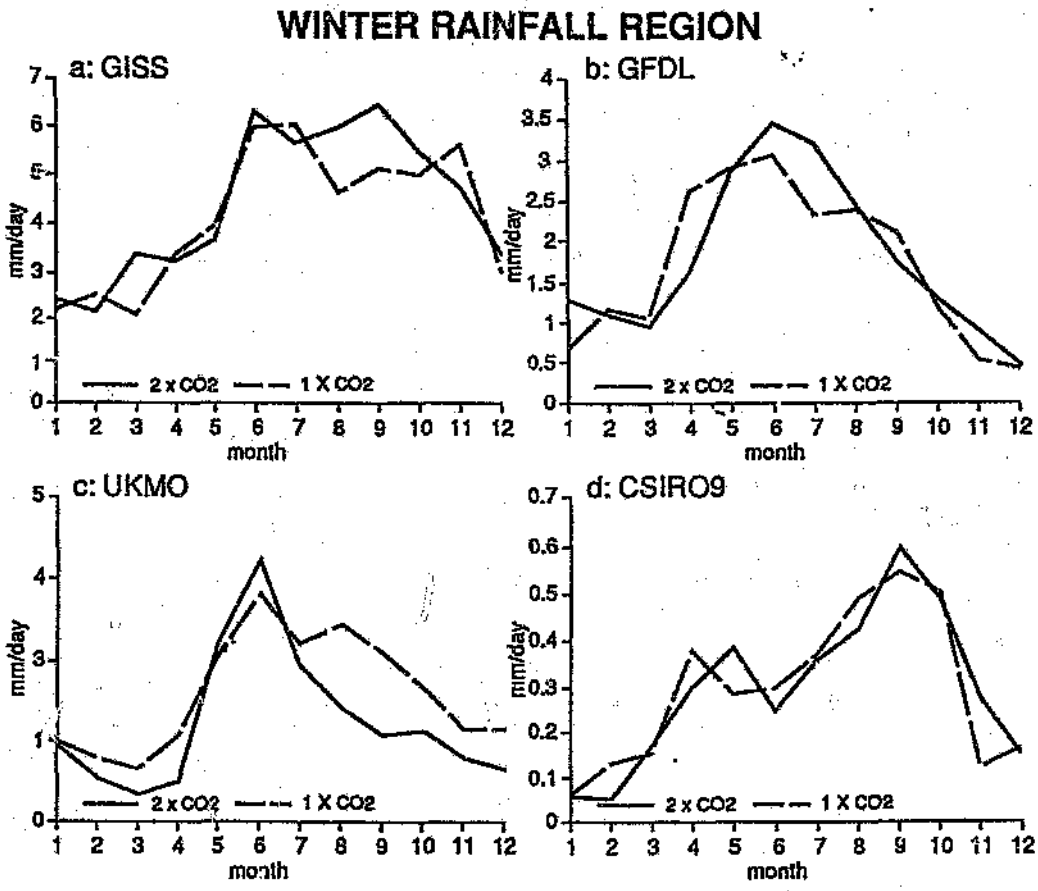

Figure 4.11: Simulated present-day and doubled CO_2 precipitation rates (in mm/day) for the GISS (a), GFDL (b), UKMO (c), and CSIRO9 (d) models over the winter rainfall region defined in Figure 3.10.

Discussion

The GISS, UKMO and CSIRO9 models agree on the general patterns of surface air temperature change over the southern African region, simulating temperature increases which range from 4°C to 6°C under doubled CO_2 conditions. This range exceeds the IPCC "Business as Usual" scenario for globally-averaged warming (Mitchell *et al.*, 1990), but is in good agreement with predicted warming for the Australian region (Whetton and Pittock, 1991). Overall, simulated warming is greatest for the UKMO model. This model has a higher sensitivity to CO_2 doubling and therefore simulates larger temperature increases than the GISS and CSIRO9 models (Mitchell *et al.*,

1989). The GISS and CSIRO9 predictions of surface air temperature change are therefore likely to be more reliable estimates of future conditions.

In the tropics, predicted warming is lower than both the global and regional average, and does not vary greatly with the season. The lower estimate of temperature increase results from the fact that the saturation vapour pressure of water increases non-linearly with temperature, so that, at higher temperature, proportionally more of the increase in radiative heating of the surface is used to increase evaporation than to raise the surface temperature (Mitchell *et al.*, 1990). Surface warming is thus reduced relative to both regional and global averages because of enhanced evaporative cooling. The variation of simulated warming in the tropics between the models may be attributed to differences in the treatment of convection (Schlesinger and Mitchell, 1987), the choice of cloud radiative properties (Cess and Potter, 1988) and also the vertical distribution of model layers (Wetherald and Manabe, 1988).

Over the drier areas of the western central subcontinent, warming in excess of 5°C occurs in all models. The increased warming over the desert areas may be expected as increased surface dryness restricts evaporation and hence evaporative cooling, leading to further increases in surface warming (Mitchell *et al.*, 1990). In addition, the reduced evaporation may lead to reduction in low cloud (Manabe and Wetherald, 1987) which leads to further enhanced surface warming. During the dry mid-winter, evaporative cooling is reduced as cloud formation is uncommon, resulting in larger temperature increases during this season.

The considerable warming at high latitudes observed in all three simulations results from errors in the specification of the effects of sea-ice-albedo feedback, and a strong temperature inversion which limits warming to the near-surface layer in winter (Mitchell, 1989). These errors are common to all equilibrium climate models linked to mixed-layer slab oceans (Mitchell *et al.*, 1990). In more recent transient simulations with coupled ocean-atmosphere models (for example Cubasch *et al.*, 1993; Manabe *et al.*, 1991, 1992; Washington and Meehl, 1989), this problem has been overcome

due to the formation of deep water in the ocean, resulting in considerably reduced warming at higher latitudes (Gates *et al.*, 1992). An important consequence of the high-latitude warming simulated by the mixed-layer slab-ocean models is the significant decrease in the meridional temperature gradient under doubled CO_2 conditions. The weaker latitudinal temperature gradient implies a weaker north-south pressure gradient and thus a weakening of the mid-latitude westerlies (Mitchell *et al.*, 1990).

Changes in the frequency of extreme events determined by changes in variability under doubled CO_2 conditions have potentially more serious implications than changes in mean climate (Katz and Brown, 1992; Katz, 1988; Mearns *et al.*, 1990; Mearns *et al.*, 1984). The CSIRO9 model simulates a decrease in both spatial and temporal surface air temperature variability at the interannual time scale, for a doubling of CO_2. Temperature variability may be expected to decrease as a result of the decreased latitudinal temperature gradient and the increased greenhouse inhibition of radiative cooling (Rind *et al.*, 1989). Comparison of predicted changes in surface air temperature variability over southern Africa with similar predictions for other regions of the globe is difficult as these are likely to be both regionally- and model-specific (Mearns *et al.*, 1990; Rind *et al.*, 1989).

It is necessary to interpret the results presented in this study in terms of the known current climate deficiencies of particular models. Important among such deficiencies is the fact that variability studies are generally performed using few (in this case, ten) model years (Rind *et al.*, 1989). More recent transient simulations with slowly-increasing CO_2 concentrations and over longer time-periods have facilitated a more accurate investigation of possible changes in variability. Recent studies have shown that the effect of low-frequency variability in fully coupled models may be to obscure the CO_2 transient climatic change signal. Using a transient simulation of a fully coupled ocean-atmosphere model, Meehl *et al.* (1993) have shown that patterns of temperature anomalies are time- and space-dependent. These anomalies become more evident with longer averaging intervals. Since the coupled climate system has many non-linear interacting processes, it is possible that a CO_2 -induced climatic change signal could itself be a slowly

varying function of time and space, displaying different characteristics in different time-periods (Meehl *et al.*, 1993). This type of low-frequency variability presents problems to policy-makers who require advice for policy-formation on shorter (for example, decadal) time scales (Meehl *et al.*, 1993).

Another limitation of the simulation of surface air temperature changes by the early-generation models considered here is that annual and diurnal cycles in solar radiation are specified as boundary conditions in the models, thereby inhibiting the ability of the models to adjust temperature variability in response to changes in radiative forcing due to increasing CO_2 concentration. More significantly, however, simulated surface air temperature variability changes by the CSIRO9 model must be interpreted with caution as no estimate of the ability of the model to simulate present-day surface air temperature variability correctly over the southern African region is available.

Other important uncertainties remain in the simulation of surface air temperature changes under doubled CO_2 conditions. Simulations of future regional climate conditions are strongly dependent on the manner in which physical processes are treated in the models. The treatment of convection has been shown to be inadequate in the present-climate validation presented in Chapter 3. The models all hold cloud optical properties fixed in both their present-day and doubled CO_2 simulations. This effectively prevents cloud radiative feedbacks from reacting to changes in cloud microphysics and radiative forcing as a result of increasing CO_2 concentrations (Harrison *et al.*, 1990; Mitchell, *et al.*, 1990). The sensitivity of regional climatic change simulations to the treatment of physical processes may be illustrated with reference to a recent UKMO run with an improved cloud formulation (using a variable cloud water scheme) and cloud radiative properties over those used in the version of the model considered in this chapter (Mitchell *et al.*, 1989). Globally-averaged warming by the modified UKMO model was considerably reduced. The use of differing parameterisation schemes to simulate convection and cloud radiative forcing of temperature therefore represents a major area of uncertainty in simulations of future conditions.

The CSIRO9 model predicts a weakening of the both subtropical anticyclones and the mid-latitude circulation under doubled CO_2 conditions. The resulting southward migration of the subtropical high pressure belt and associated trade winds and mid-latitude westerlies predicted by the model occurs in response to the large high-latitude warming and consequently decreased meridional temperature gradient (Pittock and Salinger, 1982). These results closely resemble doubled CO_2 changes predicted by the CSIRO4 model for the Australian region (Whetton and Pittock, 1991) and are consistent with expected changes for the entire southern hemisphere (Mitchell *et al.*, 1990). More recent equilibrium climate simulations also using mixed-layer slab-ocean models, which similarly include increased horizontal resolution and a gravity wave drag term, estimate doubled CO_2 conditions which are similar to the CSIRO9 model (Mitchell, *et al.*, 1989). In addition, whilst transient simulations with fully coupled ocean atmosphere models simulate less high latitude warming and therefore an improved meridional pressure gradient, simulated changes in time-averaged mean sea level pressure as well as interannual pressure variability are generally similar to the estimates considered here (Gates *et al.*, 1992).

The approach adopted in this dissertation has been to examine grid-point changes in pressure. An alternative approach is to use the present-day mean sea level pressure field to develop empirically-derived relationships between the synoptic circulation and climate (Hewitson and Crane, 1992). Accurate transfer functions which describe the circulation-temperature relationship over North America in the GISS 4° x 5° GCM have been developed (Hewitson and Crane, 1992). Attempts to describe similar circulation-temperature and circulation-precipitation relationships for the southern African region have proved more difficult due to the poor simulation of mean sea level pressure by the GISS model in this region (Hewitson, personal communication). However, the application of observed circulation-climate relationships to the doubled CO_2 circulation does not rely directly on accurate grid-point simulation of present mean sea level pressure conditions and may prove more successful in the development of reliable regional-scale climatic change predictions as a whole.

Predicted changes in seasonal rainfall patterns are generally consistent with predicted circulation changes over southern Africa by all the models. The southward shift of the tropical rainbelt observed in, for example, the GISS model (Hansen *et al.*, 1984), leads to rainfall increases over tropical southern Africa. Rainfall increases during the late summer over the central subcontinent due to increased moisture availability from the tropics. In addition, possible drier conditions during winter over the south-western Cape may be associated with the southward shift of the mid-latitude storm track. This pattern of precipitation change is consistent with predictions by this generation of models for the Australian region (Whetton and Pittock, 1991) and for the southern hemisphere as whole (Mitchell *et al.*, 1990).

On a theoretical basis, increased precipitation in the tropics may be expected as a consequence of the generally moister tropical atmosphere predicted under doubled CO_2 conditions (Mitchell *et al.*, 1990). Warming of the lower atmosphere within the tropics results in an increased moisture-holding capacity of the atmosphere. The increased moisture leads to an increased moisture flux into regions of low level convergence (like the ITC) and therefore increased precipitation. The markedly increased tropical rainfall in mid-winter predicted by the UKMO model is related to the increased strength of the Asian monsoon under doubled CO_2 conditions. Decreased cloud cover over Eurasia leads to strong positive cloud feedback, thereby enhancing surface heating and increasing the land-sea temperature contrast which drives the monsoonal circulation (Wilson and Mitchell, 1987).

The use of four different precipitation simulations has allowed intercomparison of a range of predictions. Considerably less inter-model agreement exists concerning changes in precipitation over the subcontinent than for changes in surface air temperature. Gates *et al.* (1990) suggest there are two reasons for the large inter-model disagreement over regional precipitation change predictions. Firstly, precipitation changes are the indirect result of several different processes in the models, many of which are not resolved on the model's grid, whereas temperature changes are primarily a direct response to increased radiative heating. Secondly, changes in

precipitation represent fairly small deviations from the natural variations and are therefore more difficult to detect given the short sampling period available.

Predictions over much of southern Africa south of 10°S have been shown to be grid-point specific, suggesting that the accuracy of such predictions is adversely affected by the coarse horizontal resolution of the models. Given the coarse horizontal resolution and simplistic parameterisation of precipitation mechanisms (particularly cumulus convection) used in this generation of models, changes in precipitation of convective origin (predominant over the central subcontinent during summer) cannot be accurately simulated for specific regions (Gates *et al.*, 1990; 1992). In summary, therefore, little certainty can be expressed in predictions of precipitation change for southern Africa by the models considered in this study.

A more valuable approach to predicting changes in rainfall may be to examine changes in rainfall intensity and not total rainfall (Gordon *et al.*, 1992). Two studies using both the 4-level and 9-level CSIRO models indicate that changes in rainfall intensity provide more spatially homogeneous signals than do changes in total rainfall (Gordon *et al.*, 1992; Whetton *et al.*, 1993). Both of these investigations indicate that an increase in the frequency of extreme rainfall events combined with a shorter return period for extreme events, as well as decrease in the frequency of low-rainfall events may be expected with a doubling of CO_2. Similar studies remain to be done for southern Africa.

While the early-generation general circulation models considered in this analysis exhibit considerable agreement concerning possible changes in surface air temperature and mean sea level pressure under doubled CO_2 conditions, predictions of regional precipitation change have been shown to be less reliable. However, the analysis has successfully identified uncertainties associated with the parameterisation of physical processes which are important for climatic change over southern Africa.

More recent general circulation model simulations with improved spatial resolution and parameterisations of physical processes have resulted in more

accurate representation of *global* climate and *global* climatic change. Greater reality has been achieved in the simulation of the global climate system and of the processes responsible for climatic change. The most notable development of this kind has been the use of transient simulations with gradually-increasing CO_2 concentrations, linked to fully coupled ocean-atmosphere general circulation models (Cubasch *et al.*, 1993; Manabe *et al.*, 1991, 1992; Meehl *et al.*, 1993; Stouffer *et al.*, 1989; Washington and Meehl, 1989). These more sophisticated simulations generally confirm the predictions of global change of the early-generation equilibrium climate models (Gates *et al.*, 1992). Predictions of globally-averaged warming fall within the range of the IPCC "Business as Usual" scenario based on the earlier simulations. and the large-scale patterns of change predicted by the fully coupled models are similar to those of the equilibrium experiments presented here (Gates *et al.*, 1992). As there is a need to make predictions of global climatic change specific to the southern African region, further studies such that presented here, but based on the newer generation of models, need to be performed in order to develop more reliable predictions of southern African regional climatic change.

****

Predictions of future regional climate under doubled CO_2 conditions have been interpreted for several early-generation general circulation models which accurately simulate present-day climates. The models considered here predict temperature increases of between 4°C and 6°C throughout the year. Over the subcontinent, temperature increases may be expected to be least within the tropics and largest over the dry western subcontinent during mid-winter. Changes in mean sea level pressure indicate a southward shift in the subtropical high pressure belt and associated tropical easterlies and mid-latitude westerlies in response to a reduced meridional temperature gradient. Predicted changes in seasonal rainfall totals are in accordance with predicted circulation changes. Rainfall north of 10°S may be expected to increase throughout the year. South of 10°C precipitation may generally be expected to increase in January-March. Precipitation during July-September may be expected to decrease over the winter rainfall region of the south-western Cape, reflecting the southward migration of the mid-latitude storm track. However,

considerable disagreement exists between regional patterns of precipitation change over much of the subcontinent, with changes being strongly grid-point specific. Predictions of regional precipitation change are therefore not considered reliable for much of the subcontinent south of 10°S. Further development of regional climatic change predictions depends on the extension of the analysis performed in this chapter to the newer generation of general circulation models, including transient simulations using fully coupled ocean-atmosphere models.

CHAPTER 5

SUMMARY AND CONCLUSIONS

General circulation model predictions of *global* climatic change as a consequence of global warming are considered reliable. Much of the confidence in predictions of future conditions is based on the broad-scale agreement between the models on the features of present-day climate for the globe as a whole. Similarly, the reliability of climatic change predictions for specific *regions* depends on the ability of the models to simulate present conditions for those regions accurately. In contrast to predictions of globally-averaged change, little inter-model agreement exists for predictions of regional climatic change.

For the southern African region, previous studies presenting general circulation model estimates of possible future conditions have not been based on an assessment of the present-climate performance of the models. The initial aim of this dissertation was to assess the present-climate performance of six early-generation general circulation models for the southern African region. On the basis of this assessment, only those models which simulate present conditions accurately were used to develop more reliable estimates of possible future conditions over southern Africa which may occur as a consequence of CO_2 doubling. Such analyses have been undertaken and a number of important findings have emerged from the study. These are summarised below:

A. Simulations of Present Climate

1. The 1984 GISS, 1987 UKMO and 1992 CSIRO 9-level models simulate the pattern and magnitude of both *surface land and marine air temperatures*

most accurately. All three models combine relatively fine vertical resolution with adequate parameterisations of convection appropriate to the strong vertical uplift and latent heat release associated with cumulus convection in the region.

2. In January, however, the *pattern* and *magnitude* of surface air temperatures are poorly simulated by all the models, reflecting a failure to capture the effects of strong summer-season convection over the subcontinent. During July, the simulated pattern of winter temperatures improves markedly, when convective activity and cloud formation is diminished. There is no corresponding improvement in the *magnitude* of simulated temperatures, possibly related to errors in the specification of the annual cycle in solar radiation.

3. The generally accurate simulation of *marine air temperatures* in both January and July reflects the use of a Q-flux procedure in all except the 1987 GFDL model. The high latitude simulation errors demonstrated by each of the models are characteristic of all GCMs linked to mixed-layer slab oceans and are related to errors in the specification of sea-ice albedo feedbacks.

4. The major features of the *mean sea level pressure* distribution are correctly simulated. However, the strength of both the subtropical high pressure belt and mid-latitude westerlies is generally under-estimated and the Antarctic trough is poorly represented. Overall, the poor simulation of the equator-to-pole pressure gradient by the GISS, GFDL, GFDLQ and UKMO models is related to the inadequate parameterisation of surface stress in the momentum equations of the models. The parameterisation of surface stress by means of a gravity wave drag term (included in the CSIRO4 and CSIRO9 models only) may be considered essential for an accurate mean sea level pressure simulation by mixed-slab ocean models.

5. The CSIRO9 model simulates a markedly better mean sea level pressure distribution than any of the other models, owing to its relatively fine

horizontal and vertical resolution and incorporation of a gravity wave drag term in its momentum equations. For this reason, only this simulation of the observed mean sea level pressure distribution is considered adequate.

6. Grid-point simulation of *precipitation* over the subcontinent is poor. However, the pattern of *rainfall seasonality* over the subcontinent is accurately simulated and all models replicate a summer rainfall maximum over the central subtropical subcontinent as well as a semi-annual rainfall cycle over the tropical regions and a winter rainfall maximum over the south-western Cape.

7. All models generally fail to simulate average monthly precipitation rates accurately and perform inconsistently over the tropical, summer and winter rainfall regions. While *daily precipitation rates* and the *amplitude* of the semi-annual rainfall cycle are generally not accurately simulated for the tropical and winter rainfall regions, these are well simulated for the summer rainfall region of the central subcontinent. Inter-model disagreement concerning simulations of regional precipitation may be related to parameterisations of precipitation processes, particularly that of convection, which are specific to individual models.

8. In view of this, reliable predictions of regional precipitation are more likely from a range of models than from one particular model. For this reason, the accurate simulations of rainfall seasonality by the GISS, GFDL, UKMO and CSIRO9 were considered adequate.

9. With respect to all three variables assessed, the CSIRO9 model gives the best overall simulation of present-day southern African climate of all the models considered in this dissertation.

B. Model Uncertainties

1. The accurate parameterisation of sub-grid-scale processes is an important component of accurate regional climate simulations by general

circulation models. The inadequate parameterisation of such processes at model grid scales results in inaccurate simulations of regional climate and causes uncertainty in the predictions of future regional climates. The limitations imposed by these parameterisations must be considered when assessing simulations of both present and future climates by early-generation of general circulation models.

2. The parameterisation of cumulus convection has been shown to be critical to simulation of both surface air temperatures and precipitation. Unfortunately, due to the coarse horizontal and vertical resolution of the models considered here, the finer detailed structure of individual convective events cannot be accurately represented at model grid scales. The penetrative convection and modified moist convective adjustment (generating a mass flux) schemes used by the GISS, UKMO and CSIRO9 models respectively achieve relative success in the parameterisation of convective events because they capture the effect of strong vertical uplift and latent heat release associated with convection.

3. A large area of uncertainty in the present-day and future climate simulations from the early-generation general circulation models is the treatment of clouds and cloud radiative feedback processes. The early-generation models used here all diagnose clouds directly from the relative humidity of the atmosphere and hold cloud optical properties fixed for both present-day and future climate simulations. This imposes limits on cloud radiative forcing of temperature and hence directly on the ability of the models to react to radiative changes associated with CO_2 doubling. A more realistic treatment of clouds has been incorporated in more recent simulations which allows variable cloud optical properties based on cloud water content.

4. The mixed-layer slab-ocean general circulation models considered here provide a simplistic treatment of oceans an ocean circulation. The oceans simulated here are no more than 100 m deep. Sea-surface temperatures are prescribed and ocean currents are not simulated. The

absence of currents is accounted for using a Q-flux correction which calculates the additional heat flux at the ocean surface required to simulate present-day sea surface temperature patterns and their seasonal variation, in all except the GFDL model. However, this correction prevents ocean temperature and sea ice from responding in climatic change (doubled CO_2) experiments and thus a crucial feedback mechanism is excluded from the simulations. More recent fully coupled ocean-atmosphere models provide higher-resolution oceans which can form deep water and are allowed to interact more freely with the atmosphere.

C. *Predictions of Climatic Change*

1. *Surface air temperature* changes predicted by the GISS, UKMO and CSIRO9 models over the southern African region are considered. Each of the models predicts widespread temperature increases over the region, with a 4°C to 6°C warming predicted for the region as a whole in both January and July.

2. Within the tropics, temperature increases of 2°C to 4°C are predicted. Predicted temperature changes within the tropics are lower than for the rest of the subcontinent and vary little with the season. Warming is expected to be larger (greater than 5°C) over the drier central and western regions of the subcontinent, with largest increases expected during winter. Over the oceanic regions to the south of the subcontinent, temperature increases in excess of 10°C are predicted, although the large warming is related to errors in the specification of sea-ice albedo feedbacks in the models.

3. The CSIRO9 model predicts a decrease in both temporal and spatial surface air temperature *variability* for southern Africa under doubled CO_2 conditions.

4. The prediction of *mean sea level pressure* change by the CSIRO9 model indicates a southward shift and weakening of the subtropical high

pressure belt and mid-latitude westerlies in response to a weaker meridional temperature gradient. Associated poleward shifts in tropical easterlies and the mid-latitude storm-track have important implications for precipitation patterns over the southern part of the subcontinent.

5. No clearly-defined trend in mean sea level pressure *variability* changes is evident for the southern African region. Small increases and decreases in both temporal and spatial variability are predicted by the CSIRO9 model.

6. The GISS, GFDL, UKMO and CSIRO9 models predict broad-scale changes in *precipitation* patterns in accordance with expected circulation changes over the subcontinent. The southward shift of the tropical easterlies and ITC are expected to result in increased tropical rainfall throughout the region. Increased influx of moist air from the tropics during the January-March season may lead to increased rainfall over the summer rainfall region. During winter, the UKMO and CSIRO9 models suggest a decrease in rainfall over the winter rainfall region of the south-western Cape which may result from a southward migration of the mid-latitude storm track.

7. Over much of the subcontinent however, little inter-model agreement exists concerning seasonal rainfall changes for specific regions. The pattern of change in seasonal rainfall is patchy, suggesting that simulated precipitation change is grid-point specific. Predictions from the early-generation models considered in this analysis can therefore not be considered reliable and must be interpreted with caution.

In conclusion, a framework for interpreting general circulation model predictions of regional climatic change based on their simulation of present-day conditions has been established. From the six equilibrium models linked to mixed-layer slab oceans, general agreement exists concerning possible changes in surface air temperature and mean sea level pressure for the southern African region. There is a general consensus among the models that the entire region will become warmer and that tropical,

subtropical and mid-latitude circulation systems will shift southward. Considerably less certainty exists concerning possible changes in precipitation. It is encouraging that the broad-scale features of predicted changes are apparently in agreement with predicted circulation changes. Accordingly, northern tropical areas may be expected to become wetter, with wetter summers predicted for the summer rainfall region and possibly drier conditions for the winter rainfall region of the south-western Cape. However, several uncertainties in the predictions of precipitation changes may be related to the coarse horizontal resolution and simplistic parameterisation of convective precipitation mechanisms over the subcontinent used by the early-generation general circulation models considered here.

More recent general circulation models incorporating improved physical parameterisations, increased spatial resolution and more realistic simulations of the process of climatic change may be expected to predict future conditions with greater reliability than was hitherto the case. In particular, transient simulations with gradually-increasing CO_2 concentrations, linked to fully coupled ocean-atmosphere models, represent a significant advance in the modelling of climatic change. The development of reliable predictions of climatic change for the southern African region will benefit by extending the analytical framework presented in this dissertation to the more recent generation of general circulation models.

APPENDIX A

UNIVARIATE AND MULTIVARIATE SIGNIFICANCE TESTING

Spatial fields are compared here in terms of their means, variances and spatial patterns, using the suite of statistics recommended by Wigley and Santer (1990). Numerous other methods of statistical testing other than those utilised by Wigley and Santer (1990) exist for this type of analysis. However, the statistics used here are designed specifically to account for problems inherent in determining the statistical significance of results.

Differences between means and variances may be assessed using conventional t-tests and F-tests. However these univariate tests assume an *a priori* knowledge of the sampling distribution. In most cases involving GCM output, this assumption is not valid. Furthermore, in multivariate analyses there is a need to account for multiplicity (the possibility that where many tests are performed, a certain number may be passed, at a particular significance level, purely by chance) in the test results (Livezey and Chen, 1983). Test results may also be affected by temporal and spatial autocorrelation. Significance may then be assessed by generating a sampling distribution from the available data using a permutation or Monte Carlo method (Livezey and Chen, 1983; Preisendorfer and Barnett, 1983). The pooled permutation procedure suggested by Preisendorfer and Barnett (1983) is used to assess significance in all the statistics suggested by Wigley and Santer (1990).

The technique requires data of equivalent temporal extent (usually ten years) in which the correspondence in spatial ordering between the two fields compared is not disturbed. Data for the CSIRO4 and CSIRO9 GCMs is suitable for these purposes. In the case of the GISS, GFDL and UKMO models, only long-term means are available and hence these tests cannot be applied. For

this reason significance testing for differences between spatial fields of these models is incomplete in comparison to the Wigley and Santer techniques described below. Wigley and Santer (1990) define two space-time fields to be compared as D and M, of the multivariate form $[D1(x,t), D2(x,t), ...]$, comprising three-dimensional spatial arrays of a set of variables $D1, D2$, etc., at various times t. Considering D and M as corresponding two-dimensional (x,t) arrays, their elements can be written as d_{xt} and m_{xt}, where x and t are independent discrete variables representing space and time ($x = 1, n_x$; $t = 1, n_t$). The main quantities used in the analysis (means and variances over space and time, various sums of squares) are defined in Table A.1.

Comparison of Means

Grid-point by grid-point analysis. Time means are compared at each grid-point using a local t test for the difference in means. The local test is two-tailed. Assuming that the d and m variances do not differ significantly, the test statistic is,

$$t = (\overline{d}_x - \overline{m}_x)/S_x \tag{A.1}$$

where

$$S_x^2 = (s_{d,x}^2 + s_{m,x}^2)/(n_x - 1) \tag{A.2}$$

Local significance is assessed using a Student's distribution with $2n_t - 2$ degrees of freedom. Assessment of field significance is accomplished by using the fractional number of successes,

$$NT = n_s/n_x \tag{A.3}$$

where n_s refers to the number of locally significant results at a prescribed local significance level and n_x defines the total number of tests performed. The

Table A.1: Definitions of statistical quantities (after Wigley and Santer, 1990).

Quantity	Description
d_{xt}	value of d at point and time $t (x = 1, n_x;\ t = 1, n_t)$
$\bar{d}_t$	spatial average of d at time $t = \sum_x d_{xt}/n_x$
$\bar{d}_x$	time average of d at point $x = \sum_t d_{xt}/n_t$
$s^2_{d,t}$	spatial variance of d at time $t = \sum_x (d_{xt} - \bar{d}_t)^2/n_x$
$s^2_{d,x}$	time variance of d at point $x = \sum_t (d_{xt} - \bar{d}_x)^2/n_t$
$[d]$	grand mean $= \sum_x \sum_t d_{xt}/n_x n_t$
$GSSD$	total (grand) sum of squares $= \sum_x \sum_t (d_{xt} - [d])^2$ $= (\sum_x \sum_t d^2_{xt}) - n_x n_t [d]^2$
$SSTD$	within-x sum of squares $= n_x \sum_t (\bar{d}_t - [d])^2$ $= n_x (\sum_t \bar{d}^2_t) - n_x n_t [d]^2$
$SSXD$	within-x sum of squares $= n_t \sum_x (\bar{d}_x - [d])^2$ $= n_t (\sum_x \bar{d}^2_x) - n_x n_t [d]^2$
$V(\bar{d}_x)$	spatial variance of $\bar{d}_x = \sum_x (\bar{d}_x - [d])^2/n_x$ $= SSXD/n_{xt}$
$V(\bar{d}_t)$	time variance of $\bar{d}_t = \sum_t (\bar{d}_t - [d])^2/n_t$ $= SSTD/n_{xt}$
$\overline{s^2_{d,t}}$	time average of $s^2_{d,t} = GSSD - SSTD/n_x n_t$
$\overline{s^2_{d,x}}$	spatial average of $s^2_{d,x} = GSSD - SSXD/n_x n_t$
σ^2_b	$n_x n_t s^2_{d,x} = \sum_x \sum_t (d_{xt} - \bar{d}_x)^2$ $= (GSSD - SSXD)$ (As defined by Preisendorfer and Barnett, 1983)

variables *NT1* and *NT5* are used to define the fraction of locally significant results at the 1% and 5% significance levels respectively. Field significance is assessed using the pooled permutation procedure.

Comparison of Temporal Variances

The SPRET1 statistic. *SPRET*1 is defined as the ratio of the spatial means of the time variances,

$$SPRET1 = \overline{s^2_{d,x}} / \overline{s^2_{m,x}} = \sigma^2_D / \sigma^2_M \qquad (A.4)$$

where σ^2_D is defined by Preisendorffer and Barnett (1983). This can be written in terms of sums of squares as

$$SPRET1 = (GSSD - SSXD)/(GSSM - SSXM) \qquad (A.5)$$

*SPRET*1 is tested for significance using a one-tailed test in order to define a directional difference in variances.

Grid-point by grid-point analysis The time variances $s^2_{d,x}$ and $s^2_{m,x}$ are compared grid-point by grid-point using the test statistic

$$F = s^2_{d,x} / s^2_{m,x} \qquad (A.6)$$

and judging local significance using an F-distribution with $n_t - 1, n_t - 1$ degrees of freedom. A two-tailed test is used to assess significance and field significance is again calculated using the fractional number of locally significant tests, defined as *NF*1 and *NF*5 for the 1% and 5% significance levels respectively.

Comparison of Spatial Variances

The SPREX1 statistic. *SPREX*1 is defined as the ratio of the time-mean spatial variances such that

$$SPREX1 = \overline{s^2_{d,t}} / \overline{s^2_{m,t}} = (GSSD - SSTD)/(GSSM - SSTM) \qquad (A.7)$$

Comparison of Spatial Patterns

Correlating the time-mean fields The correlation coefficient between the time-mean fields is defined by

$$r = \left[\sum_{x} (\bar{d}_x - [d])(\bar{m}_x - [m]) \right] / \left[n_x \sqrt{V(\bar{d}_x) V(\bar{m}_x)} \right] \qquad (A.8)$$

As $V(\bar{d}_x)$ and $V(\bar{m}_x)$ are spatial variances of the time mean fields, r can be defined as

$$r = \left[\sum_{x} \bar{d}_x \bar{m}_x - n_x [d][m] \right] / \sqrt{SSXDSSXM} \qquad (A.9)$$

The conventional test for a correlation coefficient would be distorted by the presence of spatial autocorrelation. As not all tests are independent, the effective number of independent tests would be less than n_x, thereby reducing the effective degrees of freedom. As such, standard tests which assume a specific sampling distribution are invalid. Using a Monte Carlo simulation, this test differs from the standard test which determines whether the correlation coefficient differs significantly from zero or some *apriori* value, by testing whether the observed correlation differs significantly from the unknown value near 1 which would arise if D and M were drawn from the same population.

In the case of the grand-mean spatial fields available for the GISS,GFDL UKMO models, no estimate of the spatial variance is available. Hence statistical significance is tested without accounting for spatial autocorrelation at the 5% level. These tests are therefore weaker than those where significance is assessed using the pooled permutation procedure. However, a technique to account for spatial autocorrelation structure of the fields explicitly has been developed (Galpin, personal communication). By correlating the grid-point simulation error (simulated - observed) at several

spatial lags, the degree of spatial autocorrelation between adjacent grid-points can then be investigated. If these autocorrelations are low, then it can be assumed that the spatial autocorrelation found in the observed field is well accounted for by the simulated field as is also well described by the original correlation coefficient.

The Pooled Permutation Procedure

The pooled permutation procedure is designed specifically to account for significance of differences between data sets of small temporal extent (often, as here, only ten years). The procedure also accounts for such problems as multiplicity, unknown reference distributions of the test statistics, accounting for field significance and spatial autocorrelation.

Because the spatial autocorrelation is present in most meteorological data, the assumptions on which the theoretical sampling distributions are based are violated. Spatial autocorrelation will reduce the number of independent observations in a spatial field, thereby reducing the effective degrees of freedom. There is a further need to account for multiplicity (the probability that if a number of local significance tests are performed, then a certain number would be passed as significant at a prescribed significance level by chance). The sampling distribution of the test statistic is effectively unknown. By generating the sampling distribution from the available data using a permutation method such as the pooled permutation procedure, these problems can be overcome. Provided that the autocorrelation structure of the original data set is preserved in the permutation (by holding the spatial ordering of the grid-points constant) the pooled permutation procedure will automatically account for spatial, but not temporal autocorrelation (Wigley and Santer, 1990). The autocorrelation in the temporal structure of the data has not been assessed but is assumed to be minimal. It is recognised that the choice of observed reference decade is essentially arbitrary and controlled by data quality and availability. Assessing temporal autocorrelation over a single ten year period is unlikely to deliver significant results.

In the pooled permutation procedure the two samples are first combined to give $2n_t$ years each containing the same number of spatial grid-points (it is essential that the spatial ordering of these grid-points remain identical). The larger subset of years (20 years here) is then split randomly into two new samples of size n_t. The test values are then re-calculated in a series of randomisations. By performing a sufficiently large number of randomisations, it is possible to construct a null sampling distribution against which the original test statistic can be compared. Although Preisendorfer and Barnett (1983) recommended 500 randomisations, this dissertation will follow Wigley and Santer (1990) in performing 1000 permutations.

APPENDIX B

PREDICTED CHANGES IN SURFACE AIR TEMPERATURE

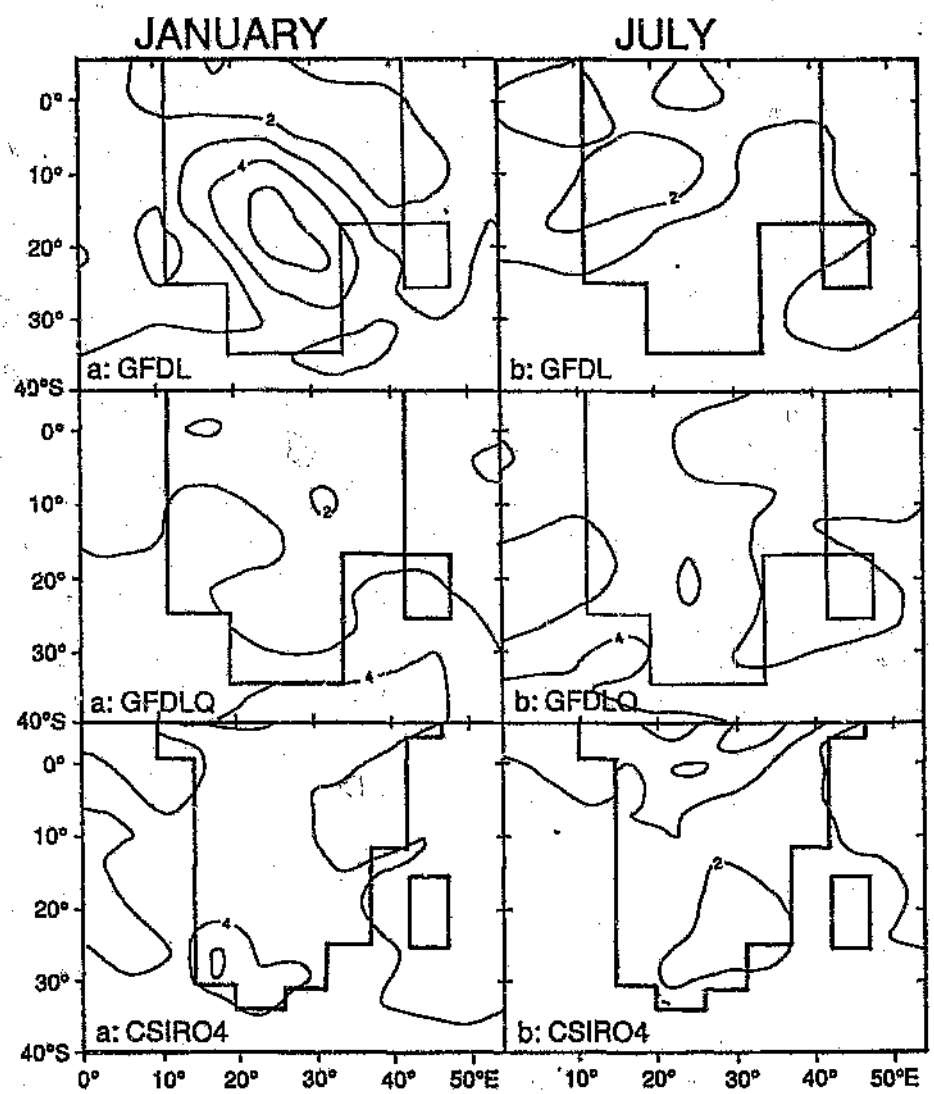

Figure B.1: Calculated surface air temperature differences (2 x CO_2 minus 1 x CO_2) in January and July for the GFDL (a,b), GFDLQ (c,d) and CSIRO4 (e,f) models, respectively (in °C). Temperatures differences for the CSIRO4 model are highly significant (above the 99 percent confidence level) throughout the region and are therefore not shaded.

APPENDIX C

PREDICTED CHANGES IN MEAN SEA LEVEL PRESSURE

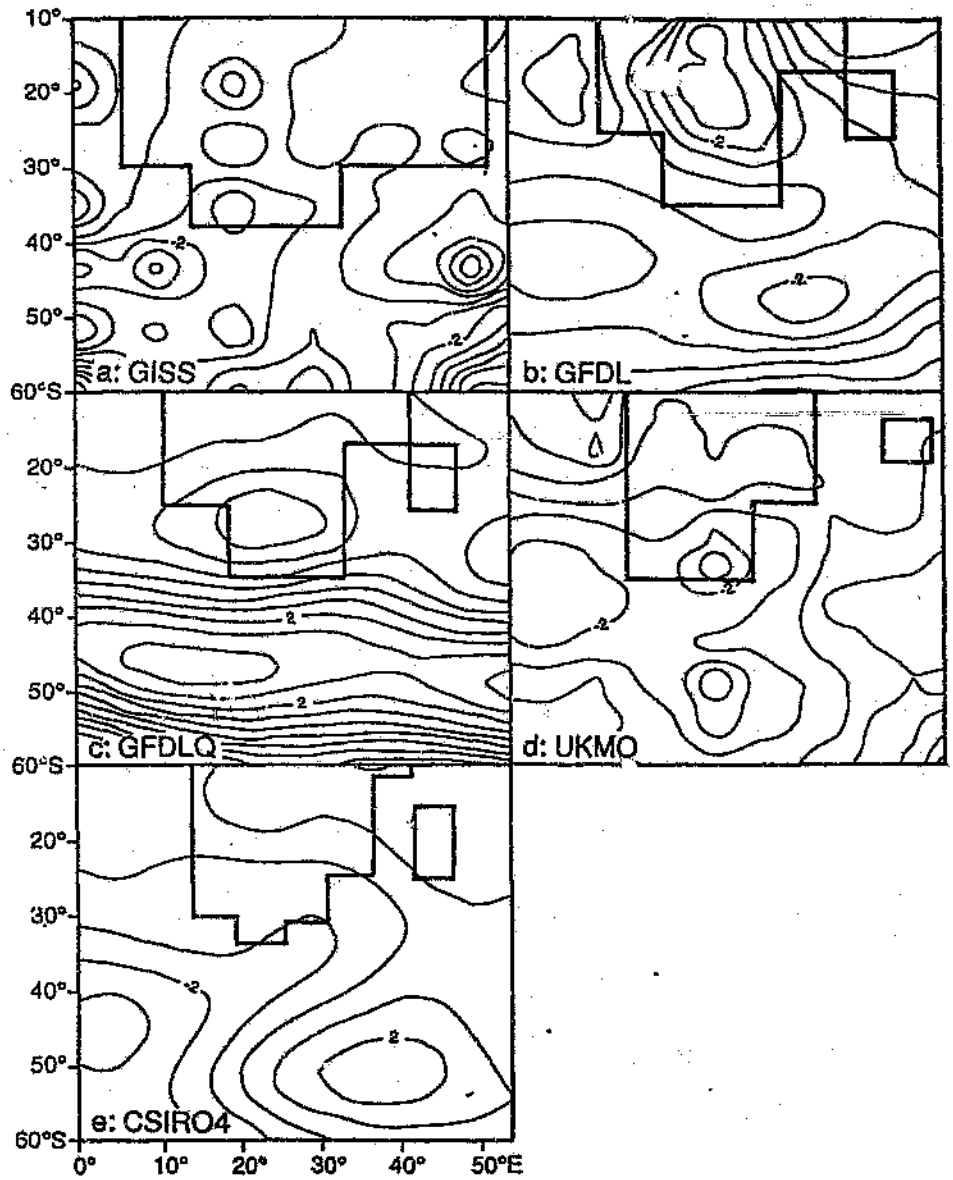

Figure C.1: Changes in mean sea level pressure (2 x CO_2 minus 1 x CO_2) in January for the GISS (a), GFDL (b), GFDLQ (c), UKMO (d) and CSIRO4 (e) models.

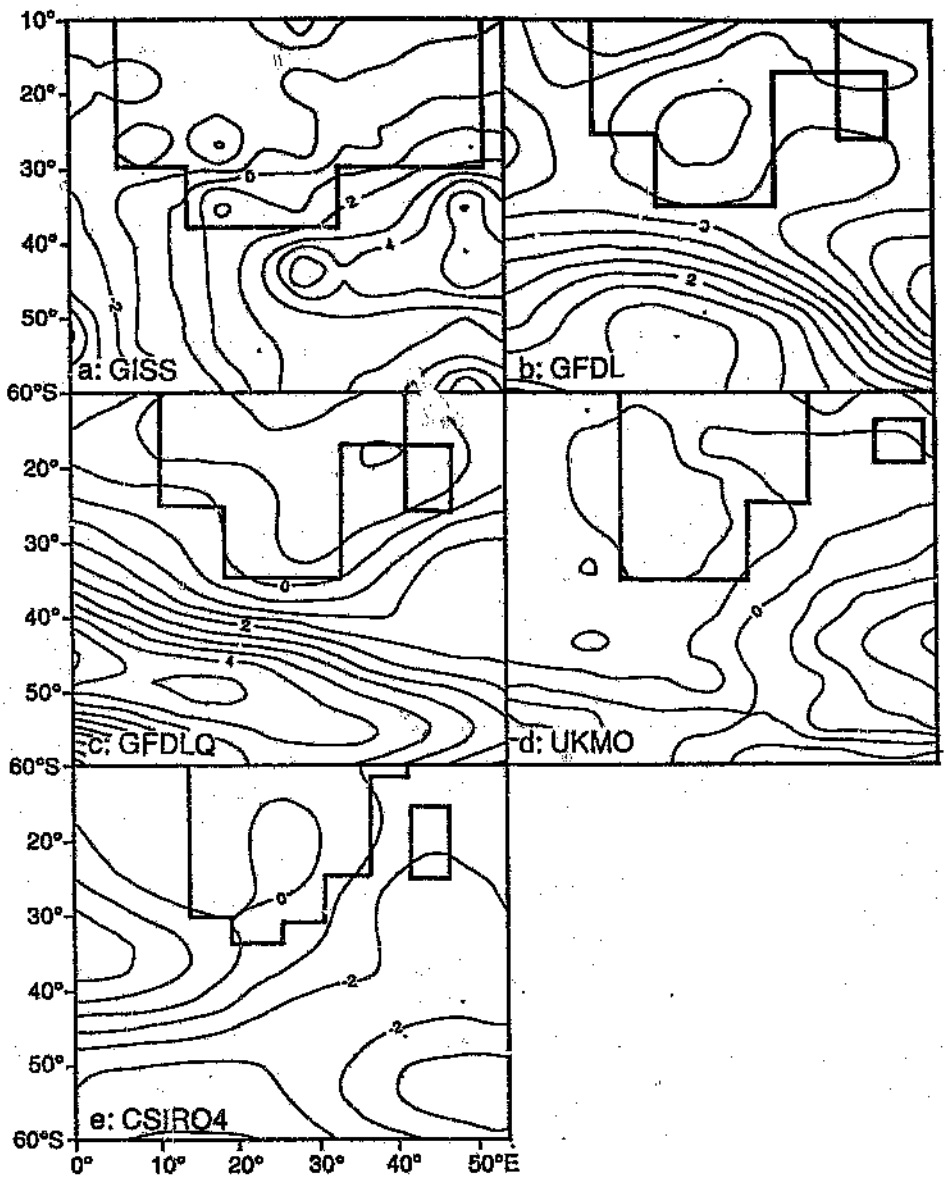

Figure C.2: Changes in mean sea level pressure (2 x CO_2 minus 1 x CO_2) in July for the GISS (a), GFDL (b), GFDLQ (c), UKMO (d) and CSIRO4 (e) models.

APPENDIX D

PREDICTED CHANGES IN PRECIPITATION

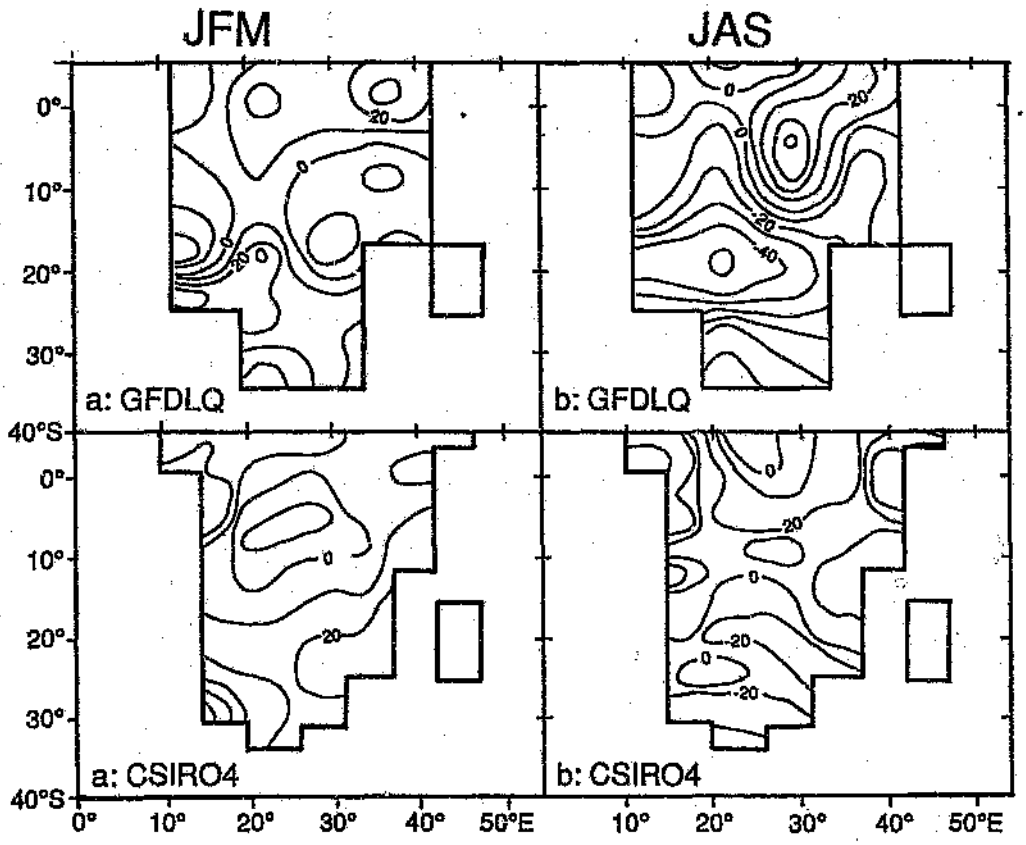

Figure D.1: January-March (JFM) and July-September (JAS) seasonal changes in rainfall (doubled CO_2 minus present-day) for the GFDLQ (a,b), and CSIRO4 (c,d) models, expressed as a percentage. shaded.

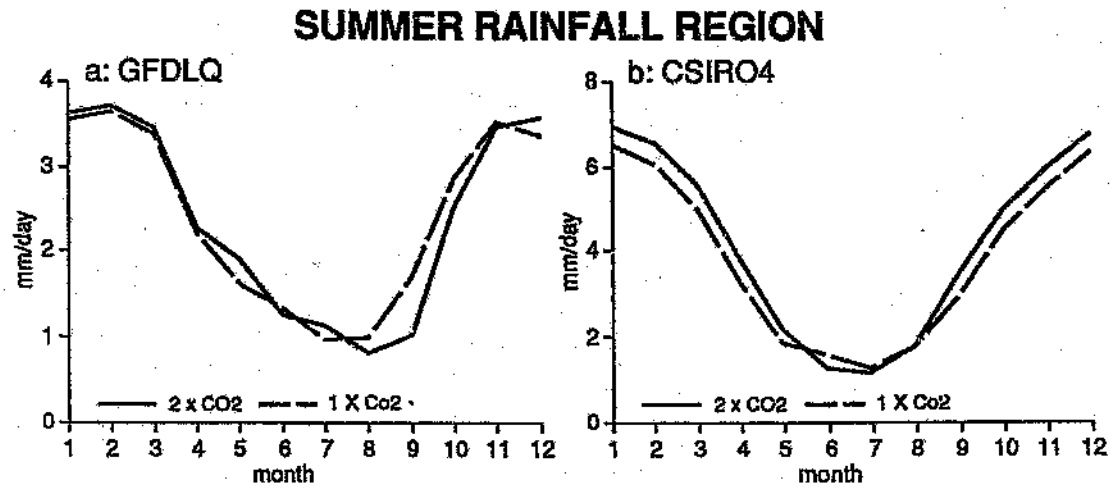

Figure D.2: Simulated present-day and doubled CO_2 precipitation rates (in mm/day) for the GFDLQ (a), CSIRO4 (b) models over the summer rainfall region defined in Figure 3.10.

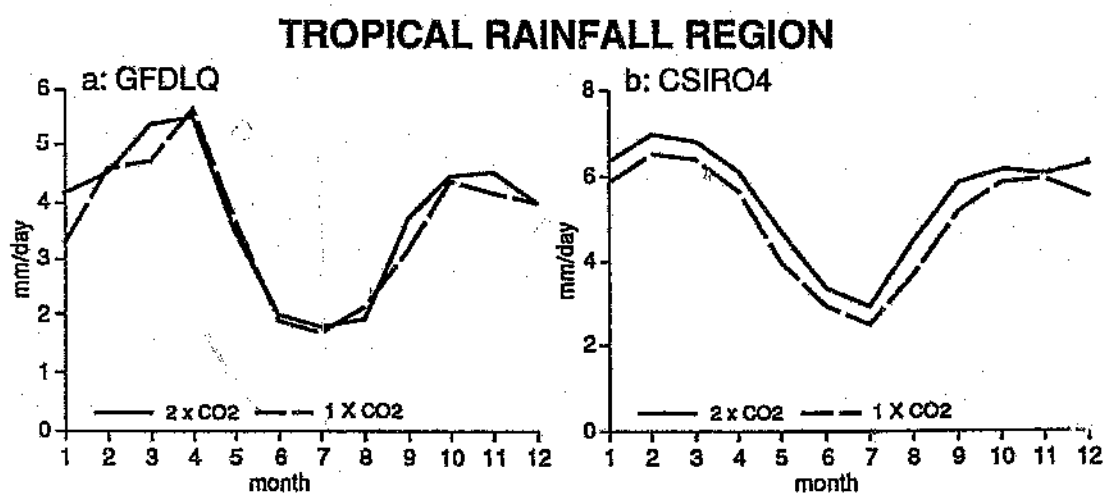

Figure D.3: Simulated present-day and doubled CO_2 precipitation rates (in mm/day) for the GFDLQ (a), CSIRO4 (b) models over the tropical rainfall region defined in Figure 3.10.

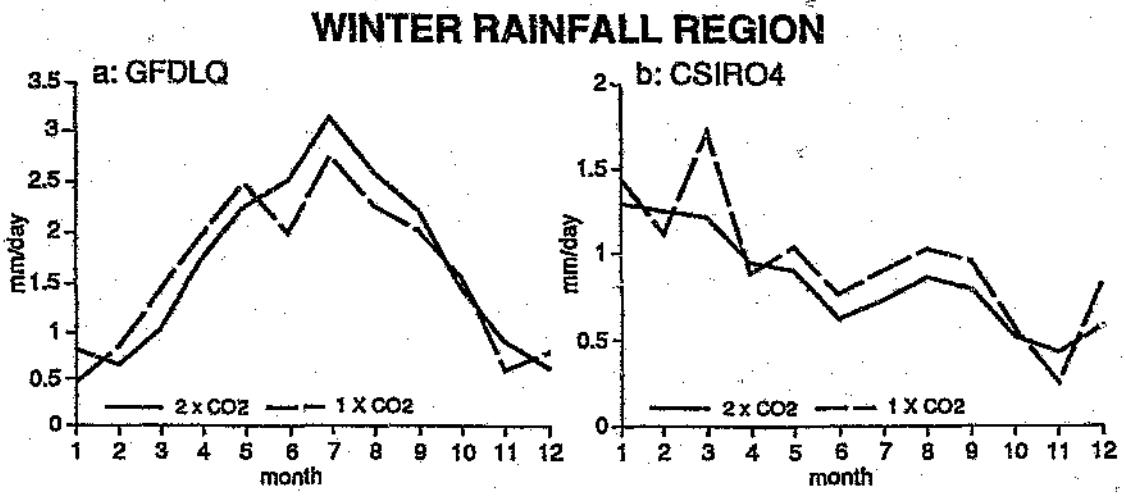

Figure D.4: Simulated present-day and doubled CO_2 precipitation rates (in mm/day) for the GFDLQ (a), CSIRO4 (b) models over the winter rainfall region defined in Figure 3.10.

REFERENCES

Arakawa, A., 1972: Design of the UCLA general circulation model. Numerical simulation of weather and climate, *Dept. of meteorology, University of California, Los Angeles, Technical Paper*, No. 7, 116pp.

Boer, G.J., Arpe, K., Blackburn, M., Déque, M., Gates, W.L., Hart, T.L., Le Treut, H., Roeckner, E., Sheinan, D.A., Simmonds, I., Smith, R.N.B., Tokioka, T., Wetherald, R.T. and Williamson, D., 1991: *An intercomparison of the climates simulated by 14 atmospheric general circulation models*, CAS/JSC Working Group on Numerical Experimentation Report No. 15, WMO/TD - No. 425, WMO, Geneva, 37pp.

Boer, G.J., Arpe, K., Blackburn, M., Déque, M., Gates, W.L., Hart, T.L., Le Treut, H., Roeckner, E., Sheinan, D.A., Simmonds, I., Smith, R.N.B., Tokioka, T., Wetherald, R.T. and Williamson, D., 1992: Some results from an intercomparison of the climates simulated by 14 atmospheric general circulation models, *Journal of Geophysical Research*, 97 (D12), 12771-12786.

Budyko, M.I., 1969: The effects of solar radiation variations on the climate of the Earth, *Tellus*, 21, 611-619.

Cess, R.D. and Potter, G.L., 1988: A methodology for understanding and intercomparing atmospheric climate feedback processes in general circulation models, *Journal of Geophysical Research*, 93 (D8), 8305-8314.

Cess, R.D., Potter, G.L., Blanchet, J.P., Boer, G.J., Del Genio, A.D., Déque, M., Dymnikov, V., Galin, V., Gates, W.L., Ghan, S.J., Kiehl, J.T., Lacis, A.A., Le Treut, H., Li, Z.-X., Liang, X.-Z., McAvaney, B.J., Meleshko, V.P., Mitchell, J.F.B., Morcrette, J.-J., Randall, D.A., Rikus, L., Roeckner, E., Royer, J.F., Schlese, U., Sheinin, D.A., Slingo, A., Sokolov, A.P., Taylor, K.E., Washington, W.M., Wetherald, R.T., Yagai, I. and Zhang, M.-H., 1990: Intercomparison and interpretation of climate feedback processes in 19 atmospheric general circulation models, *Journal of Geophysical Research*, 95 (D10), 16601-16615.

Conover, W.J., 1980: *Practical non-parametric statistics*, John Wiley and Sons, 2nd Edition, 462pp.

Cubasch, U. and Cess, R.D., 1990: Processes and Modelling, in *Climate Change, The IPCC Scientific Assessment*, Eds Houghton, J.T., Jenkins, G.J. and Ephraums, J.J., Cambridge University Press, 69-92.

Cubasch, U., Hasselmann, K., Höck, H., Maier-Reimer, E., Mikolajewicz, U., Santer, B.D. and Sausen, R., 1993: Time-dependent greenhouse warming computations with a coupled ocean-atmosphere model, *Climate Dynamics*, 8, 55-69.

D'Abreton, P.C., 1992: The dynamics and energetics of tropical-temperate troughs over southern Africa, Unpublished PhD Thesis, University of the Witwatersrand, 231pp.

Gates, W.L., Rowntree, P.R. and Zheng, Q-C., 1990: Validation of climate models, in *Climate Change, The IPCC Scientific Assessment*, Eds Houghton, J.T., Jenkins, G.J. and Ephraums, J.J., Cambridge University Press, 93-130.

Gates, W.L., Mitchell, J.F.B., Boer, G.J., Cubasch, U. and Meleshko, V.P., 1992: Climate modelling, climate prediction and model validation, in *Climate Change, The Supplementary Report to the IPCC Scientific Assessment*, Eds Houghton, J.T., Callander, B.A. and Varney, S.K., Cambridge University Press, 97-135.

Giorgi, F., Marinucci, M.R. and Visconti, G., 1990: Use of a limited-area model nested in a general circulation model for regional climate simulation over Europe, *Journal of Geophysical Research*, 95 (D10), 18413-18431.

Gordon, H.B. and Hunt, B.G., 1987: Interannual variability of the simulated hydrology in a climatic model - implications for drought, *Climate Dynamics*, 1, 113-130.

Gordon, H.B. and Hunt, B.G., 1991: Droughts, floods and sea surface temperature anomalies: a modelling approach, *International Journal of Climatology*, 4, 347-365.

Gordon, H.B., Whetton, P.H., Pittock, A.B., Fowler, A.M. and Haylock, M.R., 1992: Simulated changes in daily rainfall intensity due to the enhanced greenhouse effect: implications for extreme rainfall events, *Climate Dynamics*, 8, 83-102.

Grotch, S.L. and MacCracken, M.C., 1991: The use of general circulation models to predict regional climate change, *Journal of Climate*, 4, 286-303.

Hansen, J., Russell, G., Rind, D., Stone, P., Lacis, A., Lebedeff, S., Ruedy, R. and Travis, L., 1983: Efficient three-dimensional global models for climate studies: Models I and II, *Monthly Weather Review*, 111, 609-662.

Hansen, J., Lacis, A., Rind, D., Russell, G., Stone, P., Fund, I., Ruedy, R. and Lerner, J., 1984: Climate sensitivity: analysis of feedback mechanisms, in *Climate Processes and Climate Sensitivity, Geophysical Monograph Series No. 29*, Eds Hansen, J.E. and Takahashi, T., American Geophysical Union, Washington D.C., 130-163.

Hansen, J., Fung, I., Lacis, A., Rind, D., Lebedeff, S., Ruedy, R. and Russell, G., 1988: Global climatic changes as forecast by the Goddard Institute for

Space Studies three-dimensional model, *Journal of Geophysical Research*, 93 (D8), 9341-9364.

Harangozo, S.A., 1989: Circulation characteristics of some South African rainfall systems, Unpublished MSc Dissertation, University of the Witwatersrand, 123pp.

Harangozo, S. and Harrison, M.S.J., 1983: On the use of synoptic data in indicating the presence of cloud bands over southern Africa, *South African Journal of Science*, 79, 413-414.

Harrison, E.F., Minnis, P., Barkstrom, B.R., Ramanathan, V., Cess, R.D. and Gibson, G.G., 1990: Seasonal variation of cloud radiative forcing derived from the Earth Radiation Budget Experiment, *Journal of Geophysical Research*, 95 (D10), 18687-18703.

Harrison, M.S.J., 1983: Rain day frequency and mean daily rainfall intensity as determinants of total rainfall over the eastern Orange Free State, *Journal of Climatology*, 3, 35-45.

Harrison, M.S.J., 1984a: A generalised classification of South African summer rain-bearing synoptic systems, *Journal of Climatology*, 4, 547-560.

Harrison, M.S.J., 1984b: The annual rainfall cycle over the central interior of South Africa, *South African Geographical Journal*, 66, 47-64.

Harrison, M.S.J., 1986a: A synoptic climatology of South African rainfall variations, Unpublished PhD Thesis, University of the Witwatersrand, 341pp.

Harrison, M.S.J., 1986b: Circulation variations on a semi-annual cycle over southern Africa, Second International Conference on Southern Hemisphere Meteorology, American Meteorological Society, Wellington, 1-5 December 1986.

Harrison, M.S.J., 1993: Elevated inversions over southern Africa: climatological properties, formation processes and relationships with rainfall, *South African Geographical Journal*, 75, 1-8.

Hastenrath, S., 1985: *Climate and Circulation of the Tropics*, D. Reidel, Dordrecht, 455pp.

Henderson-Sellers, A. and McGuffie, K., 1987: *A Climate Modelling Primer*, John Wiley & Sons, Chichester, 217pp.

Hewitson, B. and Crane, R.G., 1992: Regional climates in the GISS global circulation model: synoptic-scale circulation, *Journal of Climate*, 5, 1002-1011.

Hsu, C-P.F. and Wallace, J.M., 1976: The global distribution of the annual and semiannual cycles in precipitation, *Monthly Weather Review*, 104, 1093-1101.

Hulme, M., 1992: A 1951-80 global land precipitation climatology for the evaluation of general circulation models, *Climate Dynamics*, 7, 57-72.

Jackson, I.J., 1989: *Climate, Water and Agriculture in the Tropics (2nd Edition)*, Longman Group Limited, London, 384pp.

Jones, P.D., 1991: Southern hemisphere sea level pressure data: An analysis and reconstruction back to 1951 and 1911, *International Journal of Climatology*, 6, 585-607.

Katz, R.W., 1988: Statistical procedures for making inferences about climate variability, *Journal of Climate*, 1, 1057-1064.

Katz, R.W. and Brown, B.G., 1992: Extreme events in a changing climate: variability is more important than averages, *Climatic Change*, 21, 289-302.

Karl, T.R., Wang, W.-C., Schlesinger, M.E., Knight, R.W. and Portman, D., 1990: A method of relating general circulation model simulated climate to the observed local climate. Part I: Seasonal statistics, *Journal of Climate*, 3, 1053-1079.

Keen, C.S. and Tyson, P.D., 1973: Seasonality of South African rainfall: a note on its seasonal delimitation using spectral analysis, *Archiv fur Meteorologie, Geophysik und Bioklimatologie, Ser B.*, 21, 207-214.

Lindesay, J.A., 1988a: The Southern Oscillation and atmospheric circulation changes over southern Africa, Unpublished PhD Thesis, University of the Witwatersrand, 284pp.

Lindesay, J.A., 1988b: Southern African rainfall, the Southern Oscillation and a Southern Hemisphere semi-annual cycle, *Journal of Climatology*, 8, 17-30.

Lindesay, J.A., 1994: Present climates of southern Africa, in *Southern Hemisphere Climates: Present, Past and Future*, Ed. Hobbs, J.E., Belhaven Press, London, in preparation.

Lindesay, J.A. and Jury, M.R., 1991: Atmospheric circulation controls and characteristics of a flood event in central South Africa, *International Journal of Climatology*, 11, 609-627.

Livezey, R.E. and Chen, W.Y., 1983: Statistical field significance and its determination by Monte Carlo techniques, *Monthly Weather Review*, 111, 46-59.

McFarlane, N.A., Boer, G.J., Blanchet, J.-P. and Lazare, M., 1992: The Canadian Climate Centre second-generation general circulation model and its equilibrium climate, *Journal of Climate*, 5, 1013-1044.

McGee, O.S. and Hasten[illegible], S.L., 1986: Harmonic analysis of the rainfall over South Africa, *Notos*, [illegible] 79-90.

McGregor, J.L., Gordon, H.B., Watterson, I.G. and Dix, M.R., 1993: The CSIRO 9-level atmospheric general circulation model, *CSIRO Division of Atmospheric Research Technical Paper*, No.26, CSIRO DAR, Mordialloc, 55pp.

Manabe, S. and Möller, F., 1961: On the radiative equilibrium and heat balance of the atmosphere, *Monthly Weather Review*, 89, 503-532.

Manabe, S. and Strickler, R.F., 1964: Thermal equilibrium of the atmosphere with a convective adjustment, *Journal of the Atmospheric Sciences*, 21, 361-385.

Manabe, S. and Stouffer, R.J., 1980: Sensitivity of a global climate model to an increase in CO_2 concentration in the atmosphere, *Journal of Geophysical Research*, 89 (D4), 5529-5554.

Manabe, S. and Wetherald, R.T., 1967: Thermal equilibrium of the atmosphere with a given distribution of relative humidity, *Journal of the Atmospheric Sciences*, 24, 241-259.

Manabe, S. and Wetherald, R.T., 1987: Large-scale changes of soil wetness induced by an increase in atmospheric carbon dioxide, *Journal of the Atmospheric Sciences*, 44, 1211-1235.

Manabe, S. Smagorinsky, J. and Strickler, R.F., 1965: Simulated climatology of a general circulation model with a hydrological cycle, *Monthly Weather Review*, 93, 769-798.

Manabe, S., Stouffer, R.J., Spelman, M.J. and Bryan, K., 1991: Transient responses of a coupled ocean-atmosphere model to gradual changes of atmospheric CO_2 Part I: annual mean response, *Journal of Climate*, 4, 785-818.

Manabe, S., Spelman, M.J. and Stouffer, R.J., 1992: Transient responses of a coupled ocean-atmosphere model to gradual changes of atmospheric CO_2 Part II: seasonal response, *Journal of Climate*, 5, 105-126.

Mearns, L.O., Katz, R.W. and Schneider, S.H., 1984: Extreme high-temperature events: changes in their probabilities with changes in mean temperature, *Journal of Applied Meteorology*, 23, 1601-1613.

Mearns, L.O., Schneider, S.H., Thompson, S.L. and McDaniel, L.R., 1990: Analysis of climate variability in general circulation models: comparison with observations and changes in variability in 2 x CO_2 experiments, *Journal of Geophysical Research*, 95 (D10), 20469-20490.

Meehl, G.A., Washington, W.M. and Karl, T.R., 1993: Low-frequency variability and CO_2 transient climate change, *Climate Dynamics*, 8, 117-133.

Miron, O. and Tyson, P.D., 1984: Wet and dry conditions and pressure anomaly fields over South Africa and the adjacent oceans, 1963-1979, *Monthly Weather Review*, 112, 2127-2132.

Mitchell, J.F.B., 1989: The "greenhouse" effect and climate change, *Reviews of Geophysics*, 27, 115-139.

Mitchell, J.F.B., Wilson, C.A. and Cunnington, W.M., 1987: On CO_2 climate sensitivity and model dependence of results, *Quarterly Journal of the Royal Meteorological Society*, 113, 293-322.

Mitchell, J.F.B., Senior, C.A. and Ingram, W.J., 1989: CO_2 and climate: a missing feedback?, *Nature*, 341, 132-134.

Mitchell, J.F.B., Manabe, S., Tokioka, T. and Meleshko, V., 1990: Equilibrium climate change, in *Climate Change, The IPCC Scientific Assessment*, Eds Houghton, J.T., Jenkins, G.J. and Ephraums, J.J., Cambridge University Press, 131-173.

Nicholson, S.E., Kim, J. and Hoopingarner, J., 1988: *Atlas of African Rainfall and its Interannual Variability*, Department of Meteorology, The Florida State University, Tallahassee, FL, 237pp.

Nieuwolt, S., 1977: *Tropical Climatology*, John Wiley & Sons, London, 207pp.

Portman, D.A., Wang, W.-C. and Karl, T.R., 1992: Comparison of general circulation model and observed regional climates: Daily and seasonal variability, *Journal of Climate*, 5, 343-353.

Pittock, A.B. and Salinger, M.J., 1982: Towards regional scenarios for a CO_2 -warmed earth, *Climatic Change*, 4, 23-40.

Preisendorfer, R.W. and Barnett, T.P., 1983: Numerical model-reality intercomparison tests using small-sample statistics, *Journal of the Atmospheric Sciences*, 40, 1884-1896.

Riehl, H., 1979: *Climate and Weather in the Tropics*, Academic Press, London, 611pp.

Rind, D., Goldberg, R. and Ruedy, R., 1989: Changes in climate variability in the 21st century, *Climatic Change*, 14, 5-37.

Santer, B.D. and Wigley, T.M.L., 1990: Regional validation of means, variances and spatial patterns in general circulation model control runs, *Journal of Geophysical Research*, 95 (D1), 829-850.

Schlesinger, M.E. and Mitchell, J.F.B., 1987: Climate model simulations of the equilibrium climatic response to increased carbon dioxide, *Reviews of Geophysics*, 25, 760-798.

Schlesinger, M.E. and Zhao, Z.-C., 1989: Seasonal climatic change induced by doubled CO_2 as simulated by the OSU atmospheric GCM/mixed layer ocean model, *Journal of Climate*, 2, 459-495.

Shine, K.P. and Henderson-Sellers, A., 1983: Modelling climate and the nature of climate models: A review, *Journal of Climatology*, 3, 81-94.

Sellers, W.D., 1969: A global climate model based on the energy balance of the earth-atmosphere system, *Journal of Applied Meteorology*, 8, 392-400.

Sellers, W.D., 1973: A new global climate model, *Journal of Applied Meteorology*, 12, 241-254.

Sellers, W.D., 1976: A two dimensional global climate model, *Monthly Weather Review*, 194, 233-248.

Siegel, S., 1956: *Non-parametric Statistics for the Behavioural Sciences*, McGraw-Hill Book Company, Tokyo, 312pp.

Stouffer, R.J., Manabe, S. and Bryan, K., 1989: Interhemispheric asymmetry in climate response to a gradual increase of atmospheric CO_2 ,*Nature*, 342, 660-662.

Streten, N.A., 1980: Some synoptic indices of the southern hemisphere mean sea level circulation 1972-77, *Monthly Weather Review*, 108, 18-36.

Taljaard, J.J., 1953: The mean circulation in the lower troposphere over southern Africa, *South African Geographical Journal*, 35, 33-45.

Taljaard, J.J., 1958: South African air-masses: their properties, movement and associated weather, Unpublished PhD Thesis, University of the Witwatersrand, 221pp.

Taljaard, J.J., 1967: Development, distribution and movement of cyclones and anticyclones in the Southern Hemisphere during the IGY, *Journal of Applied Meteorology*, 6, 973-987.

Taljaard, J.J., 1972: Synoptic meteorology of the Southern Hemisphere, In *Meteorology of the Southern Hemisphere*, Ed. Newton, C.W., Meteorological Monographs 35, American Meteorological Society, Boston, 139-213.

Taljaard, J.J., 1982: The March maximum of the rainfall over the western plateau of southern Africa, *South African Weather Bureau Newsletter*, 397, 51-53.

Taljaard, J.J., van Loon, H., Crutcher, H.L. and Jenne, R.L., 1969: Climate of the upper air: Part I - Southern Hemisphere. Vol. I Temperatures, dew points, and heights at selected pressure levels, *NAVAIR 50-1C-55*, Chief Naval Operations, Washington, D.C., 135pp.

Trenberth, K.E., 1981: Observed Southern Hemisphere eddy statistics at 500 mb: frequency and spatial distribution, *Journal of the Atmospheric Sciences*, 38, 2585-2605.

Tyson, P.D., 1981: Atmospheric circulation variations and the occurrence of extended wet and dry spells over southern Africa, *Journal of Climatology*, 1, 115-130.

Tyson, P.D., 1984: The atmospheric modulation of extended wet and dry spells over South Africa, 1958-1978, *Journal of Climatology*, 4, 621-635.

Tyson, P.D., 1986: *Climatic Change and Variability in southern Africa*, Oxford University Press, Cape Town, 220pp.

Tyson, P.D., 1990: Modelling climatic change in southern Africa: a review of available methods, *South African Journal of Science*, 86, 318-330.

Tyson, P.D., 1991: Climatic change in southern Africa: past and present conditions and possible future scenarios, *Climatic Change*, 18, 241-258.

Tyson, P.D., 1993: Recent developments in the modelling of the future climate of southern Africa, *South African Journal of Science*, 89, 494-505.

Tyson, P.D. and Dyer, T.G.J., 1978: The predicted above-normal rainfall of the seventies and the likelihood of droughts in the eighties in South Africa, *South African Journal of Science*, 74, 372-377.

Tyson, P.D. and Dyer, T.G.J., 1980: The likelihood of droughts in the eighties in South Africa, *South African Journal of Science*, 76, 340-341.

Tyson, P.D., Dyer, T.G.J. and Mametse, M.N., 1975: Secular changes in South African rainfall: 1880 to 1972, *Quarterly Journal of the Royal Meteorological Society*, 101, 817-833.

van Loon, H., 1972: Pressure in the Southern Hemisphere, in *Meteorology of the Southern Hemisphere*, Ed. Newton, C.W., Meteorological Monographs 35, American Meteorological Society, Boston, 59-86.

van Loon, H., Taljaard, J.J., Jenne, R.L. and Crutcher, H.L., 1971: Climate of the upper air: Southern Hemisphere Vol. II Zonal geostrophic winds, *NCAR TN/STR-57 and NAVAIR 50-1C-56*, NCAR, Boulder, Colorado, 43pp.

Vowinckel, E., 1956: Ein Beitrag zur Witterungsklimatologie des suedlichen Mozambiquekanals. Miscelanea Geofisica Publicada Pelo Servico Meteorologico de Angola em Comemoracao do X Aniversario do Servico Meteorologico Nacional, Luanda, 63-86.

Wang, W.-C., Dudek, M.P. and Liang, X.-Z., 1991: Inadequacy of effective CO_2 as a proxy in simulating the greenhouse effect of other radiatively active gases, *Nature*, 350, 573-577.

Warren, S.G. and Schneider, S.H., 1979: Seasonal simulation as a test for uncertainties in the parameterisation of a Budyko-Sellers zonal climate model, *Journal of the Atmospheric Sciences*, 36, 1377-1391.

Washington, W.M. and Meehl, G.A., 1984: Seasonal cycle experiment on the climate sensitivity due to a doubling of CO_2 with an atmospheric general circulation model coupled to a simple mixed-layer ocean model, *Journal of Geophysical Research*, 89 (D6), 9475-9503.

Washington, W.M. and Meehl, G.A., 1989: Climate sensitivity due to increased CO_2 : experiments with a coupled atmosphere and ocean general circulation model, *Climate Dynamics*, 4, 1-38.

Washington, W.M. and Meehl, G.A., 1991: Characteristics of coupled atmosphere-ocean CO_2 sensitivity experiments with different ocean formulations, in *Greenhouse-Gas-Induced Climatic Change: A Critical Appraisal of Simulations and Observations*, Ed. Schlesinger, M.E., Elsevier, Amsterdam, 79-110.

Watson, R.T., Rodhe, H., Oescher, H. and Siegenthaler, U., 1990: Greenhouse gases and aerosols, in *Climate Change, The IPCC Scientific Assessment*, Eds Houghton, J.T., Jenkins, G.J. and Ephraums, J.J., Cambridge University Press, 1-41.

Webster, P.J., 1983: Large-scale structure of the tropical atmosphere, in *Large-Scale Dynamical Processes in the Atmosphere*, Eds Hoskins, B.J. and Pearce, R.P., Academic Press, London, 235-275.

Wetherald, R.T. and Manabe, S., 1986: An investigation of cloud cover change in response to thermal forcing, *Climatic Change*, 8, 5-23.

Wetherald, R.T. and Manabe, S., 1988: Cloud feedback processes in a general circulation model, *Journal of the Atmospheric Sciences*, 45, 1397-1415.

Whetton, P. and Pittock, A.B., 1991: Australian region intercomparison of the results of some general circulation models used in enhanced greenhouse experiments, *CSIRO Division of Atmospheric Research Technical Paper*, No. 21, CSIRO, DAR, Mordialloc, 73pp.

Whetton, P.H., Fowler, A.M., Haylock, M.R. and Pittock, A.B., 1993: Implications of climate change due to the enhanced greenhouse effect on floods and droughts in Australia, *Climatic Change*, 25, 289-318.

Wigley, T.M.L. and Santer, B.D., 1990: Statistical comparison of spatial fields in model validation, perturbation and predictability, *Journal of Geophysical Research*, 95 (D1), 851-865.

Wigley, T.M.L., Jones, P.D., Briffa, K.R. and Smith, G., 1990: Obtaining sub-gridscale information from coarse-resolution general circulation model output, *Journal of Geophysical Research*, 95(D2), 1943-1953.

Wilson, C.A. and Mitchell, J.F.B., 1987: A doubled CO_2 climate sensitivity experiment with a global climate model including a simple ocean, *Journal of Geophysical Research*, 92 (D12), 13315-13343.